Effects of Exercise on Factors Regulating Adipose Tissue Expandability

by

Alison Claire Ludzki

A dissertation submitted in partial fulfillment
of the requirements for the degree of
Doctor of Philosophy
(Kinesiology)
in the University of Michigan
2020

Dissertation Committee:

Professor Jeffrey F. Horowitz, Chair
Professor Gregory D. Cartee
Associate Professor Carey N. Lumeng
Professor Matthew J. Watt, University of Melbourne

Alison C. Ludzki

aludzki@umich.edu

ORCID iD: 0000-0002-6967-034X

DEDICATION

This dissertation is dedicated to my parents, for leading by example.

ACKNOWLEDGEMENTS

First and foremost, I owe many thanks to my advisor, Jeff Horowitz, for embodying kindness and scientific rigor, for being open and receptive to important and difficult conversations, for teaching me to prioritize my scope and efforts, and especially for always caring about my best interests.

Thanks to my exceptional advisory committee members: Greg Cartee for being an always available and careful mentor, Matt Watt for lending energy and insights to my exploration of lipid metabolism, and Carey Lumeng for modeling inclusion and intentional exploration. I deeply valued the opportunity to learn from the Lumeng/Singer labs on a weekly basis.

I am extremely grateful to each and every member of Substrate Metabolism Lab with whom I interacted, and thankful for the many hands involved in my dissertation projects. Thanks to Lisa Pitchford and Doug Van Pelt for being widely available and active in teaching me an arsenal of skills upon joining the lab. Thanks to Jenna Gillen for her generous mentorship throughout every stage of my scientific development. Thanks to Mike Schleh for being a good friend and closely involved in developing Project 1 of this dissertation. Thanks to Pallavi Varshney, Chiwoon Ahn, and to my undergraduate support team including Darby Middlebrook, Natalie Taylor, Toree Baldwin, Konstantinos Karabetsos, and Emily Krueger. Finally, thanks to Suzette Howton and Thomas Rode for their constant clinical and technical support.

There are many people at the School of Kinesiology who made my work possible, and I am particularly grateful for Charlene Ruloff, Dianne Van Hoosear, and Jacquie Niven.

I would not have completed my PhD without Ben Ryan and Mark Pataky. Thanks to Mark for being a true friend and colleague, being there for every challenge I had, and teaching me lots with humility. Thanks to Ben for creating a culture of excellence and improvement, respect and professionalism, and for knowing when to prop me up.

I am lucky to have unbelievably giving mentors and talented scientists to learn from in Graham Holloway, David Wright, Martin Gibala, Lawrence Spriet, and George Heigenhauser. I am thankful for their additional guidance in my development as a student and scientist.

Not a day went by through my PhD that I wasn't cared for by friends in Ann Arbor and back home (eh). I have too many meaningful friends to thank within these pages, and every one has taught me something different that has contributed to my success. Thanks for every phone call, care package, card, text, visit, run, meal, beer, and joke.

Finally, all the thanks in the world to my supportive family! Thanks to my cousins, aunts, and uncles for cheering me on and intermittently housing and feeding me. Thanks to my sharp siblings Jenn, Nicole, Sean, and my brother-in-law Jeff for having my back no questions asked, and proving that laughter is the best medicine. Thanks to my awesome nieces Katie and Teagan for reminding me that the impact of science crosses generations. And thanks to my parents Laurienne and Paul for making me who I am today, accompanying my journey step for step, and living lives of reflection and activism that I try to follow myself.

TABLE OF CONTENTS

LIST OF FIGURES

Figure

LIST OF TABLES

Table

LIST OF APPENDICES

ABSTRACT

Obesity is tightly linked with the development of insulin resistance and associated metabolic diseases, including type 2 diabetes. Many of the health complications in obesity can be attributed to abnormalities associated with the excessive storage of fat within subcutaneous adipose tissue (SAT), such as hypertrophic adipocytes, tissue hypoxia, fibrosis, and inflammation. Therefore, given the continued alarming increase in the prevalence of obesity, identifying strategies to modify SAT structure and metabolic function in ways to more "healthfully" store body fat has very high clinical impact. Exercise is a powerful tool to reduce cardio-metabolic disease risk, but the effects of exercise on SAT are poorly understood. The overall purpose of this dissertation was to assess the effects of exercise on factors regulating SAT structural remodeling, metabolic function, and inflammation. In Project 1, RNA sequencing was performed on abdominal SAT samples collected from obese adults before and 1 hour after a session of exercise at either high-intensity (10x1min ~90% HR_{peak}; n=14) or moderate-intensity (45min ~70% HR_{peak}; n=15). Interestingly, gene set responses were not different between the high- and moderate-intensity exercise protocols, and gene sets involved in inflammation were up-regulated after exercise (IL6-JAK-STAT3 signaling, allograft rejection, TNFA signaling via NFKB, and inflammatory response; FDR q-value < 0.25), while gene sets related to adipogenesis and oxidative metabolism were down-regulated. These findings from Project 1 indicate that rapid responses to acute exercise at both moderate- and high-intensity feature *coordinated* changes in inflammatory signaling genes. In Project 2, we collected abdominal SAT from a separate cohort of obese adults (BMI 33±3kg/m^2, body fat 41±7%) the morning after a 1-hour session of moderate/vigorous intensity endurance-type exercise (80±3% HR_{peak}) versus sedentary control to establish whether these signals alter stromal vascular cell (SVC) proportions 12 hours after exercise. Exercise decreased preadipocyte number (38±7% vs. 30±13% SVC; P=0.04), which was driven exclusively by a reduction in $CD34^{hi}$ preadipocytes (18±5% vs. 13±6% SVC; P=0.002), a subset of preadipocytes that yield highly lipolytic fat cells. There was no change in the proportion of immune cells in SAT. Not only do these findings demonstrate exercise can rapidly remodel the

adipocyte progenitor pool, but these changes may also contribute to an important health benefit by modifying SAT metabolism. Finally, Project 3 was designed to examine the effects overeating on factors regulating adipose tissue remodeling in regular endurance exercisers (EX, n=11) compared with a cohort of non-exercisers (nonEX, n=11) who were matched for BMI (25±3kg/m^2). After 1 week of a standardized overeating protocol (30% energy surplus/day) all subjects gained ~1 kg ($P<0.01$), and insulin sensitivity (Matsuda ISI) declined by ~15% in both groups ($P=0.04$). Gene expression of factors involved in lipid metabolism (HSL, ATGL, DGAT, PPARγ) and angiogenesis (HIF1A, KDR) were increased ($P<0.05$). Interestingly, there was no difference in SAT responses between EX and nonEX. Findings from Project 3 indicate that overeating can rapidly impair insulin sensitivity, and modify gene expression for factors regulating angiogenesis and metabolism in SAT, but regular endurance-type exercise does not appear to alter these early adaptive responses to overeating. Overall, the projects in this dissertation demonstrate exercise can rapidly trigger signals involved in SAT remodeling, metabolic function, and inflammatory signaling. These outcomes have important health implications by revealing new metabolic pathways that could impact SAT structure and function that may help reduce obesity-related insulin resistance, and/or other obesity-related health complications.

Chapter I. Statement of the Problem

Over one third of American adults are obese (1). This alarming public health problem confers an increased risk of all-cause mortality (2), as well as a host of cardio-metabolic diseases including cardiovascular disease and type 2 diabetes (3,4). Beyond the impact of these health complications on quality of life of many obese adults, obesity-related disorders also place an enormous burden on the health care system, costing nearly $2 trillion per year in the US, according to recent estimates (5). Research aimed at better understanding key factors underlying the cardio-metabolic health complications in obesity is essential for optimizing therapies (e.g., exercise, nutritional, pharmacological) for the prevention and treatment of obesity-related diseases.

Excessive adipose tissue mass is a hallmark of obesity, and increasing evidence implicates associated factors such as high rates of fatty acid release from adipose tissue, adipose tissue hypoxia, and macrophage/immune cell infiltration within expanded adipose tissue depots as central to the development of many metabolic abnormalities (6–8). During periods of weight gain, adipose tissue expands primarily via adipocyte (i.e., fat cell) hypertrophy; but adipocytes can also undergo hyperplasia (i.e., adipogenesis), resulting in new and smaller fat cells. The degree of hypertrophy vs. hyperplasia, as well as accompanying structural adaptations to the extracellular matrix (ECM) and adipose tissue vasculature that occur during weight gain can vary greatly between people (9,10). These variations in adipose tissue phenotypes (e.g., differences in ECM structure and composition, capillarization, adipogenic capacity) may help dictate the severity of weight-gain-related metabolic complications. Consistent with this notion, the "adipose expandability hypothesis," posits that adipose tissue that can more readily expand during periods of weight-gain can more effectively store excess energy as neutral lipid (i.e., triacylglycerol). This is thought to reduce ectopic lipid deposition and adipose tissue inflammation, thereby protecting against the metabolic dysfunction that typically accompanies weight gain and obesity (11–13). Therefore, strategies aimed at modifying adipose tissue extracellular matrix, angiogenic capacity (formation of new blood vessels), adipogenic capacity

(formation of new fat cells), and immune cell infiltration could greatly improve metabolic health in obesity.

Regular exercise is known to improve metabolic health, and is often prescribed as part of the first-line approach for treating obesity-related diseases, such as type 2 diabetes. However, the mechanisms responsible for the metabolic health benefits of exercise are incompletely understood. The vast majority of research in this area has focused on exercise-induced adaptations within skeletal muscle, while adaptations within adipose tissue in response to exercise are not yet well characterized. Certainly, adipose tissue plays a key role in exercise. Adipose tissue lipolytic rate and blood flow rapidly increase during each exercise session to supply fatty acids to meet the energy demand of contracting muscle (14). In turn, these processes are known to trigger important adaptive responses, such as the upregulation of angiogenesis and adipogenesis (15–17). However, there is a paucity of data on the potential for exercise to alter adipose tissue vascularity, adipocyte hyperplasia, ECM composition/structure, and adipose tissue triglyceride storage capacity. Because long-term adaptations to exercise training are often a consequence of an accumulation of acute responses that occur during or soon after each session of exercise, there is a need to characterize the signaling events that could lead to modifications to adipose tissue structure and function in response to acute exercise. Moreover, because the intensity of exercise can have profound influence on the magnitude of metabolic adaptations (18), examining the acute effects of exercise intensity on markers of cellular signaling events in adipose tissue is essential at this stage in understanding adipose tissue adaptations to exercise. Such experiments will greatly enhance our understanding of the potential cumulative effects of exercise-related signals on adaptive metabolic and morphologic responses in adipose tissue, as well as provide valuable information for optimizing exercise prescriptions. ***The Specific Aims for project 1 of my dissertation were*** *(1) to determine the effects of acute moderate-intensity steady state exercise on the adipose tissue transcriptome in adipose tissue; and (2) to compare the adipose tissue transcriptional response to a single session of moderate-intensity exercise versus high-intensity interval exercise.*

Adipose tissue is a complex of many cell types (e.g., adipocytes, immune cells, endothelial cells, adipocyte precursor cells,) each of which can communicate and contribute to the metabolic "health" and function of adipose tissue. Therefore, to truly understand how exercise affects adipose tissue function, it is essential to understand how exercise affects the

individual cell populations in human adipose tissue. Some recent evidence suggests that exercise may induce anti-inflammatory effects on adipose tissue (19,20). However, the regulation of individual adipose tissue immune cell populations by exercise is largely unexplored, especially in humans. There is also evidence that acute exercise increases the expression of factors related to angiogenesis and adipogenesis in adipose tissue. Yet, there is no work directly assessing endothelial cell or adipocyte precursor cell responses to exercise. ***The Specific Aim for project 2 of my dissertation was*** *to determine the effects of acute moderate-intensity endurance exercise on macrophage, endothelial cell, and preadipocyte number in human subcutaneous adipose tissue from obese adults.* These potential exercise-induced modifications in adipose tissue constituents can directly impact metabolism, but may also remodel adipose tissue structure to increase its capacity for expansion. These changes could therefore represent key mechanisms to help accommodate storage of extra energy (triglycerides) during periods of overeating.

It is important to emphasize that an enhanced *capacity* for adipose tissue expansion does not lead to a greater body fat mass, because gaining body weight and body fat can only be achieved by a positive energy balance (i.e., when energy intake exceeds energy expenditure). Based on recent work from our lab (6), an important underlying premise of my dissertation studies is that when matched for total body fat mass, individuals with an enhanced capacity for their adipose tissue to effectively store excess energy may actually be somewhat *protected* against the negative health effects of overeating and weight gain. With this in mind, the benefits of having (or acquiring) an enhanced capacity to expand adipose tissue may not be clinically relevant until a person experiences meaningful weight gain; which unfortunately is the norm for the vast majority of adults living in developed countries. Along these lines, the prospect that some of the metabolic health benefits of exercise may be due to adipose tissue responses that foster effective fat storage and therefore reduced inflammation during periods of energy surplus is very intriguing and opens the door to the development of new "adipo-centric" strategies to improve metabolic health. ***The Specific Aims for project 3 of my dissertation were*** *(1) to determine the effects of one week of overeating (30% increase in energy intake above that estimated to maintain body weight) on factors involved in regulating adipose tissue metabolism (i.e. lipolytic rate); storage capcity (i.e. adipogenesis, angiogenesis, and ECM remodeling; inflammation) in human subcutaneous adipose tissue; and (2) to determine the effects of exercise on overeating-induced changes in factors involved in regulating adipose tissue metabolism (i.e.*

lipolytic rate); storage capacity (i.e. adipogenesis, angiogenesis, and ECM remodeling; inflammation) in human subcutaneous adipose tissue.

In summary, these projects address the following specific aims:

PROJECT 1:

Specific Aim 1: Determine the effects of acute moderate-intensity steady state exercise on the adipose tissue transcriptome in adipose tissue.

Specific Aim 2 Compare the adipose tissue transcriptional response to a single session of moderate-intensity exercise versus high-intensity interval exercise.

PROJECT 2:

Specific Aim: Determine the effects of acute moderate-intensity endurance exercise on macrophage, endothelial cell, and preadipocyte number in human subcutaneous adipose tissue.

PROJECT 3:

Specific Aim 1: Determine the effects of one week of overeating (30% increase in energy intake above that estimated to maintain body weight) on factors involved in regulating adipose tissue metabolism (i.e. lipolytic rate); storage capcity (i.e. adipogenesis, angiogenesis, and ECM remodeling; inflammation) in human subcutaneous adipose tissue.

Specific Aim 2: Determine the effects of exercise on overeating-induced changes in factors involved in regulating adipose tissue metabolism (i.e. lipolytic rate); storage capcity (i.e. adipogenesis, angiogenesis, and ECM remodeling; inflammation) in human subcutaneous adipose tissue.

These proposed dissertation projects were designed to test the overall hypothesis that exercise induces signals for adipose tissue remodeling that may prime adipose tissue to be a more effective storage site when exposed to episodes of energy surplus (i.e., overeating), thereby reducing inflammatory pathway activation, pro-inflammatory cytokine release, and weight-gain related insulin resistance. The proposed experiments will generate novel information on mechanisms underlying adipose tissue dysfunction in humans that will contribute to lifestyle and pharmacological interventions aimed to reduce tissue-specific and systemic inflammation and insulin resistance in humans.

Chapter II. Review of Literature

Introduction

Obesity is an epidemic associated with increased mortality, disease risk, reduced quality of life, and stigmatization, and it afflicts over one third of adults in America (1–4). Obesity confers a high risk of cardio-metabolic diseases, especially insulin resistance and Type 2 Diabetes (3,21). Together, this places an enormous burden on the health care system currently worth ~$2 trillion USD per year (5). The Surgeon General's Report has identified overweight and obesity as one of the most pressing national health problems and there is a profound need for interventions that can prevent and treat the metabolic complications associated with excessive weight gain (22,23).

Adipose tissue is the primary storage site for the excess energy when energy consumption exceeds energy expenditure (24). While "healthy" adipose tissue is exquisitely effective at storing and releasing fatty acids according to metabolic need, excessive expansion of this depot can result in structural changes and dysfunction (25). There is strong evidence that adipose tissue dysfunction and the consequent ectopic lipid deposition (i.e. excessive lipid storage in other tissues such as liver and skeletal muscle) are central to the development of obesity-related insulin resistance (26). Even among obese adults, there is a range of insulin sensitivity, and up to one third of obese adults have been found to remain insulin sensitive (27). Understanding the factors within the adipose tissue that could preserve metabolic health during the periods of weight gain that seem inevitable in the Western world could provide a major breakthrough towards developing therapies that can reduce the public health burden of obesity.

Cross-sectional data identify some important structural features of adipose tissue from obese adults that may impact normal function, which may in turn underlie the corresponding ectopic lipid deposition and metabolic abnormalities. Chief among these structural features that can impact adipose tissue function are: insufficient vascularization/hypoxia (7,28), fibrotic extracellular matrix (ECM) (6,29), and excessive pro-inflammatory immune cell infiltration

(30,31). Structural changes within adipose tissue have been coined adipose tissue "remodeling", and collectively these changes can influence the ability of adipose tissue to effectively sequester fat as neutral lipid, thereby minimizing its deleterious effects on insulin sensitivity and cardio-metabolic health (32). While the mechanisms conferring "healthier expansion" of adipose tisse are not well understood, the common phenotype among obese adults who remain insulin sensitive appears to be more effective storage within the adipose tissue (6,33,34). Given the complexity of adipose tissue remodeling in obesogenic expansion, no pharmacological treatment to effectively mitigate the adipose tissue dysfunction that often accompanies obesity exists as of yet.

Regular exercise improves whole body insulin sensitivity and metabolic health (35,36), but the underlying mechanisms are incompletely understood. In particular, the acute and chronic effects of exercise on adipose tissue structure and function are grossly understudied, especially in humans. Since the discovery of the protein irisin, which has been suggested to be released during exercise to trigger white adipose tissue "browning" (37), there has been considerable attention on the potential for exercise to increase thermogenesis and mitochondrial uncoupling within adipose tissue (38–41). While the possibility that exercise might modify adipose tissue thermogenesis is intriguing, the role of exercise-induced irisin on adipose tissue remodeling in humans is heavily debated. In addition to any potential effects of exercise on adipose tissue thermogenesis, exercise may also modify adipose structure and function in ways to allow it to store fat more effectively (thereby reducing ectopic lipid deposition). For example, some evidence suggests exercise training can increase adipose tissue capillarization and decrease inflammation (42–44); but no work to our knowledge has comprehensively assessed the exercise stimulus or signals that might achieve meaningful changes in adipose tissue structure. Certainly, there is unexplored potential for the signaling changes induced by each session of exercise to alter adipose tissue structure and function in the hours and days after exercise to make it a more effective storage depot during periods of nutrient excess.

This review will provide background on the importance of effective fat storage in subcutaneous adipose tissue, and the regulation of fatty acid storage and release. It will then outline the regulation of adipose tissue expansion in response to energy surplus/overeating (e.g. adipocyte hypertrophy and hyperplasia), along with the structural changes that accompany adipose tissue remodeling (e.g. angiogenesis, ECM remodeling, and immune cell infiltration).

Throughout, I will propose pathways through which we hypothesize that regular exercise might increase adipose tissue expandability and storage capacity to reduce ectopic lipid deposition and the ensuing insulin resistance.

Fatty Acid Metabolism in Adipose Tissue

Effective fat storage in subcutaneous adipose tissue is important for insulin sensitivity

The importance of adipose tissue in preserving whole body insulin sensitivity is canonically illustrated by studies of lipodystrophy. Lipodystrophy is a group of genetic diseases characterized by impaired fat storage/adipose tissue mass and often associated with diabetes (45). Work showing that the transplantation of adipose tissue explants into lipodystrophic rats reduces ectopic lipid deposition and improves glycemic control led to a frameshift in thinking, revealing the importance of adipose tissue for metabolic health (46). Santomauro et al. (47) supported the importance of fatty acid storage in humans by showing that the administration of acipimox (an anti-lipolytic drug that lowered plasma fatty acids 60-70%) improved insulin sensitivity with a hyperinsulinemic euglycemic clamp and oral glucose tolerance test.

Our group has recently reported that fatty acid mobilization from adipose tissue dictates the degree of insulin resistance among obese adults (33). Strikingly, among obese adults matched for adiposity, those with relatively low rates of basal fatty acid mobilization from adipose tissue (i.e. *in vivo* rate of release of fatty acids from adipose tissue into the systemic circulation) were largely protected from developing insulin resistance (6,33). However, the factors (genetic or environmental) conferring more or less effective fatty acid storage in the adipose tissue are not clear. Given that the subcutaneous adipose tissue is responsible for ~80-90% of systemic fatty acid release (48), discussion of therapies to improve fatty acid storage in this review will focus on the subcutaneous adipose tissue. Identifying mechanisms for improving fatty acid storage in adipose tissue requires an understanding of the regulation of lipolysis and esterification; as well as a strong grasp of the processes involved in adipose tissue expansion, and how these can be modified to maximize adipose tissue storage capacity. The remainder of this section will outline the regulation of fatty acid metabolism in adipose tissue focusing on the adipocyte.

Regulation of esterification in adipose tissue

Adipose tissue is heterogeneous, containing adipocytes, preadipocytes, endothelial cells, ECM components, and immune cells among other stromal cells (49). Adipocytes are the biggest constituent of adipose tissue by volume, and are the site for most of the body's energy stores (50). Nearly all of the energy stored in adipocytes is delivered to adipose tissue in the form of TGs in VLDL and chylomicrons, as well as a small amount of albumin-bound fatty acids (51). Fatty acid uptake into adipose tissue relies on the enzyme lipoprotein lipase (LPL), which is synthesized by adipocytes and acts at the capillary lumen (endothelial cells) to bind circulating triglycerides and hydrolyze their fatty acids for subsequent diffusion or active transport (via fatty acid transport proteins) into adipocytes (52,53). Similarly, albumin-bound fatty acids are directly taken up at the adipocyte plasma membrane by diffusion or via fatty acid transport proteins. Within the adipocyte, fatty acids are esterified with glycerol-3-phosphate (G3P) into triglyceride for storage in the lipid droplet. G3P is predominantly derived from glyceroneogenesis by phosphoenolpyruvate carboxykinase (PEPCK) decarboxylation of oxaloacetate to form phosphoenolpyruvate; for which PDK4 inhibition of the PDH complex is a key regulator of pyruvate availability (54). Fatty acids are then acylated (energy-dependent) by key enzymes DGAT and GPAT for re-esterification with G3P (55). Insulin is a key regulator of re-esterification, and the increase in insulin following a meal increases both LPL activation and re-esterification enzymes (51). Fat storage within the adipocyte is also regulated by lipid droplet proteins (in particular the PLIN family of proteins), whose regulation is not well understood but will be briefly discussed in the section "Regulation of adipose tissue lipolysis," below. Altogether, these factors regulating fatty acid re-esterification within adipose tissue are key contributors to the rate of fatty acid mobilization. Importantly, healthy or excessive fatty acid mobilization by adipose tissue depends on the balance of rates of re-esterification and lipolysis.

Regulation of adipose tissue lipolysis

Adipose tissue lipolysis involves the sequential hydrolysis of fatty acids from glycerol by lipolytic enzymes adipose triglyceride lipase (ATGL), hormone-sensitivite lipase (HSL), and monoglyceride lipase (MGL) (56). This occurs within the lipid droplet in the adipocyte, which is coated with surface proteins of the PLIN family (57). Phosphorylation of PLIN1 has been shown

to be essential for maximal adipose tissue lipolysis by facilitating access of lipases to the lipid droplet (58). While HSL can also release the first FA from triglycerides, ATGL is now known to be essential for this stage of adipose tissue lipolysis (59). There is some activation of ATGL by phosphorylation (by protein kinase-A; PKA), but the majority of increased ATGL activity is related to PKA phosphorylation of CGI-58, signaling its localization to ATGL and thereby increasing ATGL activity (60). There are other fat interacting proteins important for the regulation of lipolysis, which are reviewed by Tsiloulis et al. (61). HSL is rate-limiting in lipolysis, and its Serine phosphorylation by PKA increases its localization to the lipid droplet as well as its activity (there is also inhibitory regulation on HSL by different phosphorylation site(s)) (62). Evidently, the control of lipolysis requires coordination of these processes as well as other players beyond the scope of this review.

Lipolysis, like re-esterification, is regulated primarily at the hormonal level by insulin (inhibitory), and catecholamines (stimulatory); though our knowledge of other hormonal regulators is growing. Resting lipolytic rate is maintained mostly by α-adrenergic-inhibition (63). With increasing energy demand (e.g. exercise), there is a rapid increase in catecholamines that increase β-adrenergic stimulation, and decrease α-adrenergic-inhibition of lipolysis (63). Catecholamine binding to β-adrenergic receptors increases lipolysis by G-protein-coupled increase in PKA (64), which phosphorylates lipolytic rate-limiting enzyme HSL (65), as well as PLIN proteins, CGI-58, and ATGL (66). Adipose tissue is very sensitive to small increases in epinephrine, and the largest increase in lipolysis occurs with the onset of low-intensity exercise. Insulin inhibits lipolysis by stimulating PDE-3B, which lowers cAMP and thereby PKA activity (67). Insulin therefore regulates both re-esterification and lipolysis, as the reduction in insulin during exercise facilitates the increase in lipolysis and this reciprocal control of supply versus storage is a suitable system. There are a variety of other hormonal regulators of lipolysis, including cortisol (increases lipolysis), and ANP (increases lipolysis) (61). Adipose tissue vasculature is also important in the regulation of fatty acid uptake and release, as fatty acids and triglycerides are hydrophobic, so transport is a key process controlled by the capillaries (14). The increase in adipose tissue blood flow during exercise is required for the increase in lipolysis (68). Adipose tissue blood flow decreases immediately after exercise, but increases above baseline by ~30 minutes post-exercise (14). An endurance exercise training effect on adipose tissue sensitivity to adrenergic stimulation and/or major lipolytic proteins remains equivocal (61).

The section above outlines the regulation of fatty acid uptake and release in response to normal fluctuations in food intake and energy demand within an individual. Importantly, a higher basal lipolytic rate is seen in obese versus lean persons (69,70). However; within obese adults matched for BMI and fat mass, there is a range of basal lipolytic rates, and higher lipolytic rate correlates with worse insulin sensitivity (6,33). This suggests that there are different responses to weight gain that could exacerbate or attenuate the phenotype of excessive fatty acid mobilization among obese individuals. Importantly, this reduction in fatty acid mobilization might reduce ectopic lipid deposition and protect against obesity-related insulin resistance.

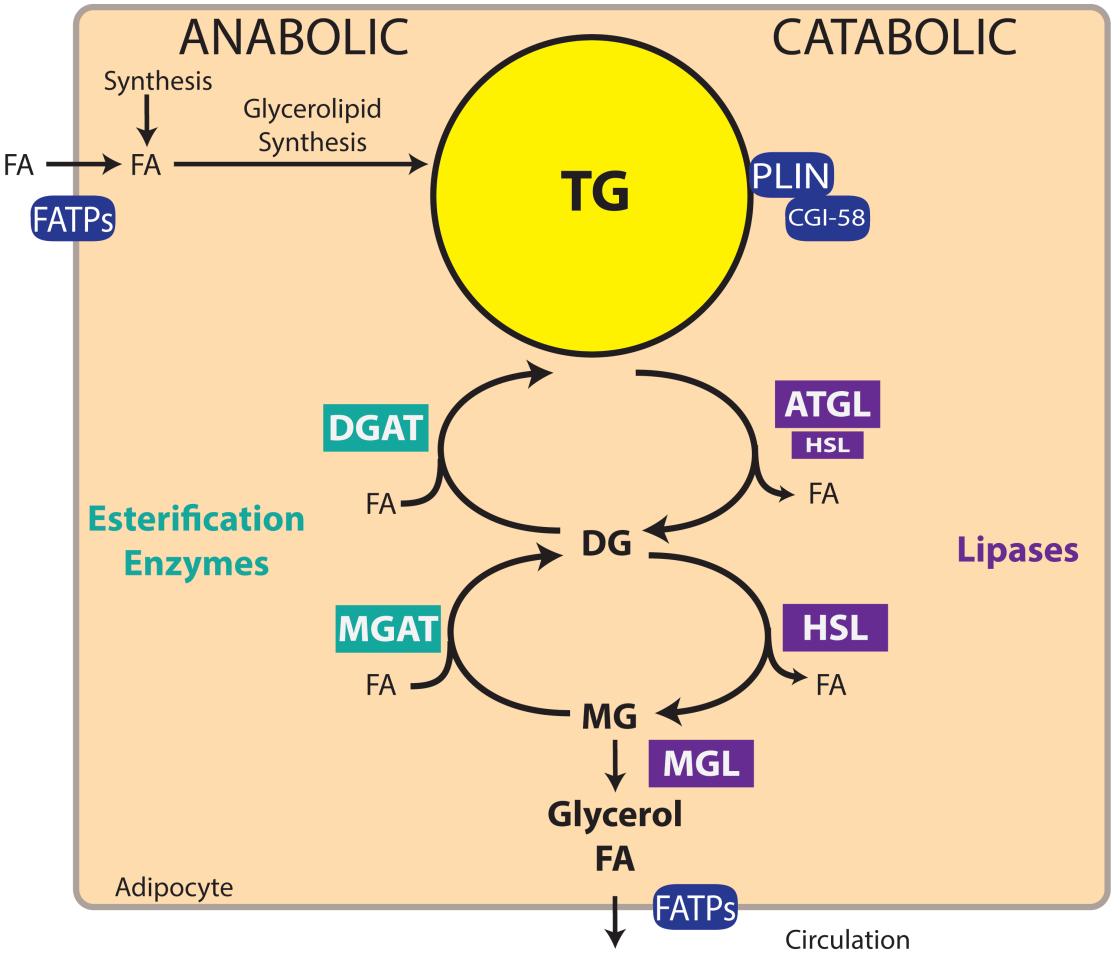

Figure II-1 Simplified representation of major regulators of fat storage in the adipocyte.

Triglyceride (TG) storage in the lipid droplet within the adipocyte is regulated by the balance between fatty acid (FA) esterification and lipolysis. Key players include (i) esterification proteins acyl-CoA:monoacylglycerol acyltransferase (MGAT) and acyl-CoA:diacylglycerol acyltransferase (DGAT); (ii) lipases adipose triglyceride lipase (ATGL), hormone-sensitive lipase (HSL), and monoglyceride lipase (MGL); (iii) fatty acid transport proteins (FATPs); and lipid droplet protein Perilipin. Figure redrawn from Yen et al (71).

Adipose Tissue Remodeling

Adipose Tissue Expandability Hypothesis

Adipose tissue storage capacity is heavily influenced by the structural accommodation of the expanding fat mass. Differences in adipose tissue mass at the onset of diabetes has led to the hypothesis that each individual has a maximal threshold for adipose tissue expansion; depicted in Figure II-2 below (12). Commonly referred to as the "adipose expandability hypothesis," there is support that individuals with a better capacity for healthy adipose tissue expansion may be protected from insulin resistance by sequestering fatty acids as neutral lipids within the adipose tissue and out of other important insulin-responsive tissues (liver, skeletal muscle, pancreas, etc.) (26). Kim et al. (72) directly increased adipose tissue expansion capacity in *ob/ob* mice with a leptin knockout/adiponectin overexpression model and found that despite greater body mass and fat mass, these animals had comparable glucose tolerance to wild-type animals (i.e. the genotype prevented the glucose intolerance that was observed in the *ob/ob* counterparts that represented a model of exhausted adipose tissue expansion). Adipose tissue expansion capacity is likely to depend on a variety of structural features of adipose tissue that have been linked with metabolic function. Hypertrophy, adipogenesis, angiogenesis, and ECM remodeling are key players in adipose tissue expandability (11). The sections following here will explain our current understanding of these processes. Each section will highlight the potential for exercise to impact adipose tissue health in humans.

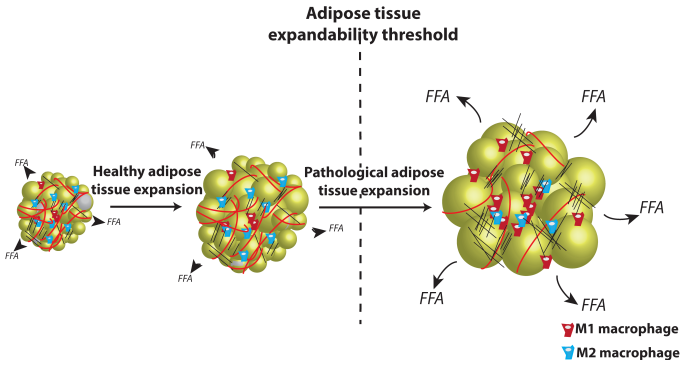

Figure II-2 Adipose tissue expandability threshold.

Differences in adipose tissue mass at the onset of diabetes led to the hypothesis that each individual has a maximal threshold for adipose tissue expansion before excess free fatty acid (FFA) mobilization from adipose tissue results in ectopic lipid accumulation and insulin resistance. Modified from Gray & Vidal-Puig (12).

Adipocyte Hypertrophy

Adipose tissue can expand by hypertrophy (enlargement of existing adipocytes), and/or hyperplasia (production of new adipocytes from precursor cells; adipogenesis) (73). Adipocyte hypertrophy is largely regulated by the balance of fatty acid lipolysis and esterification, which increase triglyceride content within the lipid droplet in the adipocyte in conditions of caloric surplus (outlined in the "Fatty Acid Metabolism in Adipose Tissue" section above). However, the cellular and structural surroundings of the adipocyte also impact its ability to expand. In particular, sufficient vasculature and "compliant" (versus fibrotic) ECM are important features to support healthy adipocyte hypertrophy. In other words; adipocyte hypertrophy might be limited by insufficient vasculature resulting in adipocyte hypoxia and insufficient nutrient exchange (7,74). Similarly, dense, fibrotic ECM is thought to physically limit adipocyte hypertrophy (75,76). Adipose tissue vascularization and extracellular matrix remodeling are also required for adipogenesis (77,78), and altogether the balance of adipogenesis, angiogenesis, and ECM remodeling are likely to represent important targets for improving adipose tissue expandability.

Adipogenesis

While the majority of adipose tissue expansion occurs by hypertrophy, adipose tissue mass also expands by hyperplasia. Though few, direct assessments of adipogenesis in humans demonstrate a small contribution to the mature adipocyte population. $^{2}H_2O$/deuterium incorporation into adipocyte DNA has been used to assess adipocyte replacement rates (from fraction of new adipocytes) in lean and obese, weight-stable humans (79,80). Marc Hellerstein's group has contributed these seminal assessments using $^{2}H_2O$/deuterium incorporation into triglyceride glycerol, triglyceride palmitate, and DNA to determine total triglyceride synthesis, *de novo* lipogenesis, and cell proliferation *in vivo* over several weeks. This technique has allowed the determination of adipocyte replacement rates (from fraction of new adipocytes) as 0.16-0.29% per year in healthy, weight-stable humans (79). Allister et al. (80) subsequently applied this technique in BMI-matched insulin sensitive versus insulin-resistant humans to measure adipocyte "proliferation" rates of 0.6% and 0.7% per day respectively. However, to truly assess the regulation of adipogenesis it seems logical to examine this process under conditions where there is a stimulus for adipose tissue expansion, as is the case during periods of overeating.

Unfortunately, to our knowledge no study has assessed the rate of adipogenesis during weight gain in humans.

Cross-sectional comparisons of adipocyte size have been used to assess differences in adipogenesis (i.e., adipose tissue with more, smaller fat cells considered to have higher adipogenic rates) and also to infer the contribution of adipogenesis to metabolic health. While the rationale for this approach is reasonable, these findings are limited. These cross-sectional comparisons do not capture information on the *rate* of adipogenesis, and therefore cannot ascertain whether the smaller adipocyte size really was a consequence of elevated adipogenesis. In other words, more smaller adipocytes could represent increased adipogenesis; but a person may have more smaller adipocytes for other reasons, such as structural limitations preventing further hypertrophy It is therefore not surprising that there is no consensus on the relationship between adipocyte size and metabolic health from such comparisons (9,75,81,82). However, studies examining the regulation of adipogenesis in mice on a high-fat diet suggest that adipogenic capacity is affected by the local environment. Jeffrey et al. (83) reported that high-fat feeding induces adipogenesis more in visceral adipose tissue in male mice, and subcutaneous adipose tissue in female mice; and transplantation in the male mice (of preadipocytes if visceral origin to subcutaneous fat pads and vice versa) has suggested that the these adipogenic rates are regulated by the microenvironment, not the source (because this phenotype did not persist after transplantation, i.e. transplanted preadipocytes differentiated according to the environment into which they were). Similarly, the local inflammatory environment can regulate adipocyte differentiation. Macrophage-secreted factors, (such as TNF-α and IL-1β) have been shown to decrease differentiation of 3T3-L1 cells and primary human preadipocytes, partly through activation of Wnt-signaling (84–86). Many of these experiments use rodent-derived cell populations that are quite different from human adipocyte precursor cells; but these findings provide intriguing support that the environment can be manipulated to influence adipogenic capacity *in vivo*.

The regulation of adipogenesis involves complex transcriptional regulation on several potential precursor populations that has not been elucidated especially in adult humans. A comprehensive account of our understanding of the factors involved in adipocyte differentiation is reviewed in detail elsewhere (87,88). In short, peroxisome proliferator-activated receptor-γ (PPARγ) was identified as a master regulator of adipogenesis over 20 years ago (89,90). Since

then, CCAAT/enhancer-binding proteins (C/EBPs; α, β, and δ) have also proven important for adipocyte differentiation using among other regulators. There are many circulating factors that can influence the adipogenic pathway, including fatty acids, insulin, cortisol, catecholamines, IL-6, and lactate (91). Intriguingly, many of these factors are released during and/or after a session of exercise. In fact, preliminary data from our lab demonstrates that human adipocyte precursor cells differentiate faster when exposed to serum collected from subjects after a session of exercise compared with incubation in serum collected without prior exercise (unpublished data). Importantly, an increase in adipogenic capacity may only manifest into a meaningful increase in the production of new fat cells under conditions when adipose tissue is stimulated to expand (i.e. during episodes of overeating and weight gain). Therefore, assessing the effects of regular exercise (versus inactivity) on markers of adipogenesis during periods of overeating may be important for determining whether exercise can enhance adipose expandability through increasing adipogenesis (thereby relieving hypertrophy-related fibrosis and inflammation). The dynamics of hypertrophy and hyperplasia in adipose tissue of course are not independent of structural features of the adipose tissue including vasculature and ECM, whose dynamics must be considered in any assessment of adipose tissue expansion.

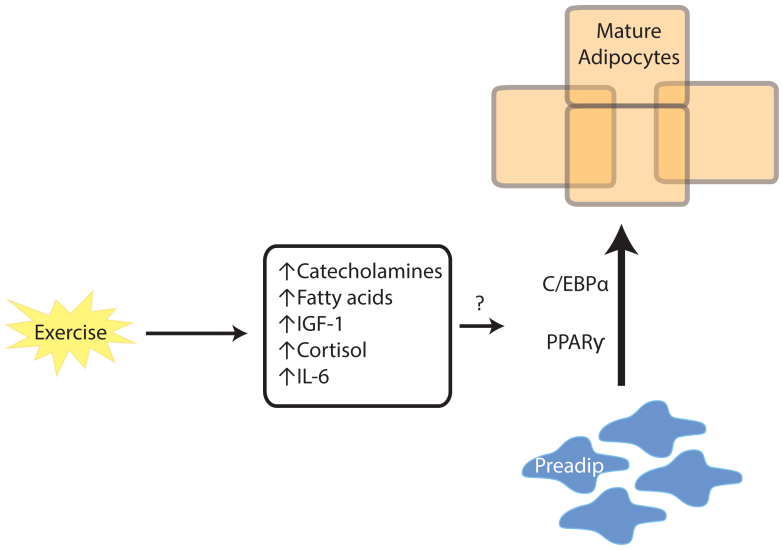

Figure II-3 Outline of key circulating factors released during exercise that have been linked to adipogenesis.

Exposure of preadipocytes in the adipose tissue to elevated levels of these factors (e.g. catecholamines, fatty acids, IGF-1, corticol, IL-6) could increase adipogenic rate and increase the contribution of new, small adipocytes to adipose tissue expansion. PPARγ, peroxisome proliferator-activated receptor-γ; C/EBPα, CCAAT/enhancer-binding protein-α): key transcriptional regulators of adipogenesis.

Adipose Tissue Angiogenesis

Adipose tissue is highly vascularized, allowing for effective exchange of nutrients and signaling molecules between adipose tissue cells and the rest of the body (92). Well-controlled perfusion is especially important in adipose tissue because fatty acids are water insoluble and so regulation of their exchange between the adipose tissue and vasculature must be facilitated (as outlined in the *Fatty Acid Storage in Adipose Tissue* section of this review). Adipose tissue also plays an important role in regulating metabolism by exchanging cytokines and hormones with the periphery (93), which also relies on an extensive vasculature. Dramatic increases in adipose tissue blood flow occur according to metabolic stimuli such as feeding and exercise, and sufficient adipose tissue vasculature is key in regulating these responses (94–96). The adipose tissue vasculature can expand in response to metabolic signals through the process of angiogenesis: the development of new vessels from existing vasculature.

Angiogenesis is required for adipose tissue remodeling and expansion, and precedes adipogenesis (97); therefore, improving angiogenic capacity could improve adipose tissue expandability. While the adipose tissue vasculature expands with obesity (98), it has been suggested that adipocyte hypertrophy often exceeds the expansion of adipose tissue vasculature, which is thought to be a major cause of the often-observed hypoxia in obese adipose tissue (28). There remains some debate over whether increasing adipose tissue angiogenesis improves adipose tissue health; but recent genetic rodent models suggest it can attenuate high-fat diet-related metabolic dysfunction (99,100). In particular, multiple groups found that overexpressing vascular endothelial growth factor (VEGFα; considered the master regulator of angiogenesis) attenuates glucose intolerance, crown-like structures (a marker of immune cell infiltration), and markers of hypoxia during the early stages of weight gain, while adipose-specific ablation or inhibition (by Mcr84 antibody administration to decrease VEGF-receptor binding) of VEGF exacerbates these pathologies (99,100). Interestingly, adipose VEGF inhibition by Mcr84 in "established" obesity (9-week-old *ob/ob* mice) improved their metabolic phenotype, suggesting the role of angiogenesis could be different during "early" weight gain compared with animals who are already obese. Steps to ascertain whether pro-angiogenic therapies might have a place in treatments of human obesity-related diseases will require a direct assessment of angiogenic capacity in humans during weight gain along and establishing targeted approaches to manipulate it.

Valuable insights into the molecular regulation of angiogenesis have come from settings like tumor growth and exercise training in skeletal muscle (17,101,102). However, our understanding of adipose tissue angiogenesis is more limited, and whether the same molecular regulation occurs with obesogenic adipose tissue expansion is not known. The process of angiogenesis involves endothelial cell migration, proliferation, and tubulogenesis (103). It is initiated primarily by VEGF binding to the VEGF receptor (VEGF-R; with VEGF-R2 being most implicated in existing literature. The detailed regulation of adipose tissue angiogenesis is outside the scope of this review; Corvera et al. (104) review the regulation of adipose tissue angiogenesis in the context of obesity. In short, existing vasculature is maintained by basal inhibition of VEGF, which is overcome by pro-angiogenic stimuli (105). Hypoxia is a classic pro-angiogenic signal, but genetic manipulation of hypoxia-inducible factor-1 (HIF1, a key transcriptional regulator in the hypoxia response) suggest factors other than hypoxia are important regulators of angiogenesis during diet-induced adipose tissue expansion (106). As of now, the primary molecular signal(s) responsible for inducing *VEGF* expression during adipose tissue expansion remain unclear but inflammatory pathway activation is also known to activate VEGF (107). In fact, sustained inflammation is known to be a trigger for VEGF in several tissues, with NF-kB being a major promoter for this process by binding to a response element in VEGF (108). VEGF can also be secreted by macrophages, providing more potential for immune regulation of angiogenesis during adipose tissue expansion (109,110). In this context, chemokines may be important mediators of angiogenesis by altering macrophage secretion of VEGF with obesity (104) . Signals associated with energy stress and exercise (AMPK, *PGC1α,* and *PPARγ*) can also trigger angiogenesis; underscoring the complex regulation of this process (104).

There is very little work assessing the effects of exercise on adipose tissue angiogenesis. Walton et al. (42) found that exercise training increased capillarization in the adipose tissue of healthy, but not insulin-resistant subjects. However; there are no studies to our knowledge that have explored the ability of different exercise stimuli (e.g. varying intensity) to result in adipose tissue angiogenesis. Furthermore, there is no work assessing exercise-induced adipose tissue angiogenesis during a stimulus for weight gain/adipose tissue expansion in healthy (not yet insulin resistant) subjects. There is evidence that exercise activates AMPK, *PGC1α,* and *PPARγ* within adipose tissue; signals that have been described to upregulate VEGF in other tissues

(111). Our group has found that a single session of aerobic exercise increases adipose tissue VEGF expression in healthy, weight-stable humans (112) and in rats on a 2-week HFD (113). Consistent with the notion that angiogenesis could be an effective therapy to attenuate metabolic dysfunction during the early stages of weight gain; it is worth pursuing whether exercising during the periods of weight gain that precede insulin resistance could effectively reduce hypoxia and enhance adipose expandability by increasing adipose tissue vascularization. It will be important to assess this in a physiological setting given evidence that stromal cells (i.e. ECM, preadipocytes, and immune cells) are key sources of angiogenic signals, and that ECM remodeling (described in the next section) is essential to accommodate capillarization within adipose tissue (114).

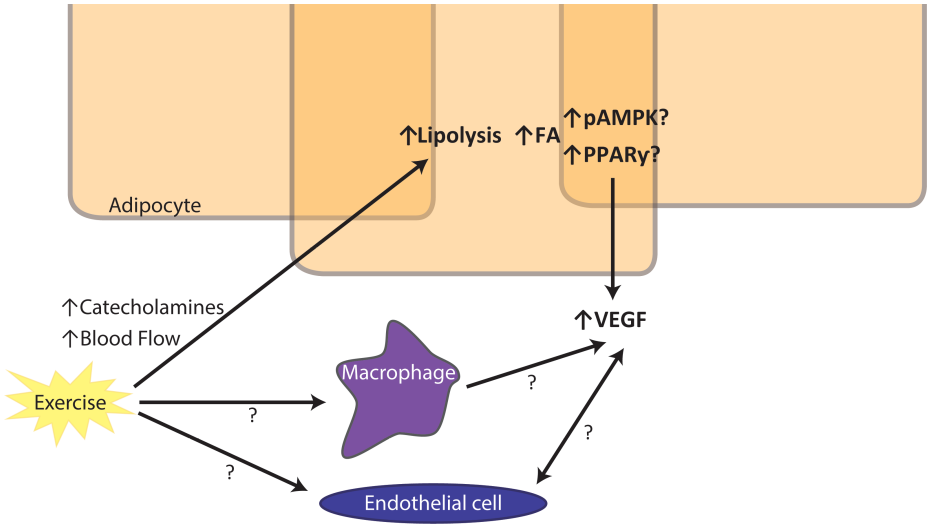

Figure II-4 Potential links between exercise and adipose tissue angiogenesis.

The increase in adipose tissue blood flow, catecholamines, and lipolysis in response to exercise could implicate several regulators of VEGF (e.g. *PPARγ,* and AMPK; these effects could be dependent or independent on the exercise-related increase in fatty acids (FA)). The specific cell types responsible for the upregulation of adipose tissue VEGF in response to exercise, and the potential to increase adipose tissue endothelial cell proliferation or capillarization have not yet been assessed. PGC1α, peroxisome proliferator-activated receptor gamma coactivator 1-alpha; PPARγ, peroxisome proliferator-activated receptor-γ; VEGF, vascular endothelial growth factor.

Adipose Tissue ECM Remodeling

Adipose tissue ECM provides a structural support for the adipose tissue as well as an important signaling role for adipocyte growth, differentiation, and continuing response to environmental changes (115). The major component of adipose ECM is collagen, though it is a complex network of a variety of proteins (e.g. osteopontin, hyaluronan, elastin) outside the scope of this

review; for a more detailed review, see Lin et al. (115). ECM forms a basement membrane of collagen IV, collagen VIII, heparin sulfate proteoglycans and laminins (116–119). The largest component of the pericellular ECM is collagen VI, which directly cross-links adipocytes to the basement membrane (76,120). The pericellular ECM is heterogeneous, containing also meaningful amounts of Collagens I, III, IV, VI, and VIII, among other proteins (121). The ECM communicates with the constantly changing environment within the adipose tissue via transmembrane receptors including integrins (with CD11b and CD11c receptors among the most abundant), CD44, and CD36, equipping them to regulate key aspects of inflammation and fatty acid metabolism – reviewed in (115,122). Therefore, ECM composition could play a unifying role in adipose tissue expandability and the signals in response to weight gain.

The observation of excess extracellular matrix deposition (fibrosis) is one of the most consistent findings in high fat diet studies and human obesity (29,123). Genetic ablation of Collagen VI in mice has revealed superior adipose tissue expansion (larger fat cells and fat pad size) in conjunction with improved glucose tolerance and decreased fibrosis on a high fat diet (76). These data support a causal role for ECM deposition in the insulin resistance that is commonly correlated with fibrosis in obese humans. It also provides direct support that the ECM might limit adipose tissue expansion in obesity, and that removing this limit could improve metabolic health. Based on these and other genetic studies in rodents, Lin et al. (115) propose a model whereby excessive ECM might physically limit adipocyte hypertrophy, leading to adipocyte death; might be part of a pathway distinct and counter to adipose tissue angiogenesis thereby inhibiting sufficient vascularization and nutrient exchange of obese adipose tissue; and might induce macrophage infiltration by signals downstream of integrin and CD44 receptors. Clearly, there is interplay between the structural changes involved in healthy or pathological adipose tissue expansion. Furthermore, depot differences (greater fibrosis in visceral versus subcutaneous adipose tissue) suggest there are environment-related factors that might prove useful for manipulating adipose tissue ECM expandability.

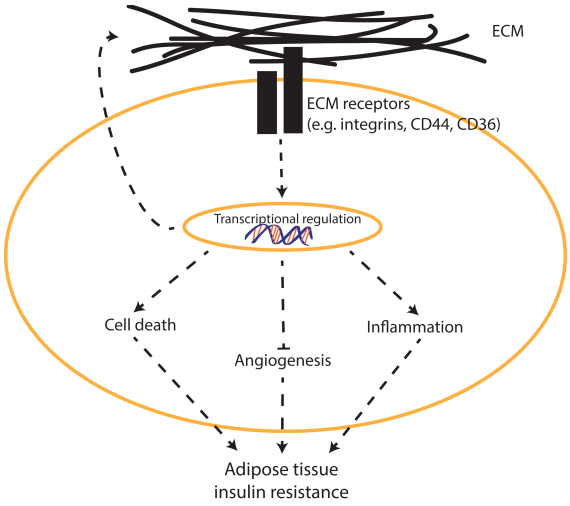

Figure II-5 ECM receptors regulate insulin resistance in adipose tissue.

Unified model through which excessive ECM might (i) physically limit adipocyte hypertrophy, leading to adipocyte death; (ii) be part of a pathway distinct and counter to adipose tissue angiogenesis thereby inhibiting sufficient vascularization and nutrient exchange of obese adipose tissue; and (iii) induce macrophage infiltration by signals downstream of integrin and CD44 receptors. Figure from Lin et al. (115).

Adipose tissue ECM is constantly being turned over and the balance of ECM degradation and deposition plays a major role in establishing "healthy" versus fibrotic adipose tissue (124). Key factors regulating ECM turnover include but are not limited to matrix metalloproteinases (MMPs; degradation); tissue inhibitors of MMPs (TIMPs; inhibit degradation); and secreted protein acidic and rich in cytoseine (SPARC; general organization) (32). Humans have 23 different MMPs whose expression is transcriptionally regulated by stimuli including inflammatory cytokines, growth factors, hormones, cell-cell, and cell-matrix interactions (reviewed in (125)). The major endogenous inhibitors of MMPs in adipose tissue are TIMPs, and activation of the MMPs is largely regulated by TIMP binding to MMPs (126). In general, models with higher TIMP or lower MMP expression present protection from disease phenotypes on a high-fat diet (127,128), but the complete regulation and function of ECM remodeling in obesity and insulin resistance remains unclear and understanding the complex interplay of these processes could enhance our understanding of adipose tissue health and expansion.

There are very few data on the role of exercise in adipose ECM remodeling in humans, but Kawanishi et al. (44) provide compelling evidence that exercise training (treadmill exercise 5d/week) while on a 16 week high-fat diet can attenuate adipose tissue fibrosis (lower Col1a, Col3a, TIMP-1 mRNA) in mice compared with mice that did not exercise. The authors linked this to an exercise-induced reduction in TGFβ; which is among other anti-inflammatory effects

of exercise that can influence adipose tissue expandability (to be discussed in the Adipose Tissue Inflammation section of this review). However, the protective role of exercise in weight-gain-related adipose tissue fibrosis was not corroborated by Pincu et al. (129), who measured adipose tissue stromal cell number and ECM gene expression in eWAT from mice that consumed a HFD for 8 weeks before and then throughout a 16-week treadmill training protocol. The authors found that the HFD and associated weight gain increased adipose stem cell number and expression of ECM remodeling genes MMP2, Timp1, Timp2, and Col1a1; but found no difference in this gene expression profile (or fibrosis by Sirius red staining) compared with animals that completed exercise training. Clearly, we have much to learn about the effects of exercise training on adipose tissue structure, especially during episodes of weight gain. Given the potential for exercise to alter key components of adipose tissue expandability (i.e. adipogenesis, angiogenesis, and ECM remodeling), it could be incredibly informative to directly assess factors regulating these processes in response to a controlled exercise stimulus in humans; especially during a period of caloric surplus, when adipose tissue is expanding to accommodate the excess energy. Importantly, all of these processes have been connected to adipose tissue inflammation; so assessing the role of the immune system in conjunction with the structural features of adipose tissue remodeling outlined in this section will be fundamental to successfully implementing adipose tissue-centric therapies for obesity-related diseases.

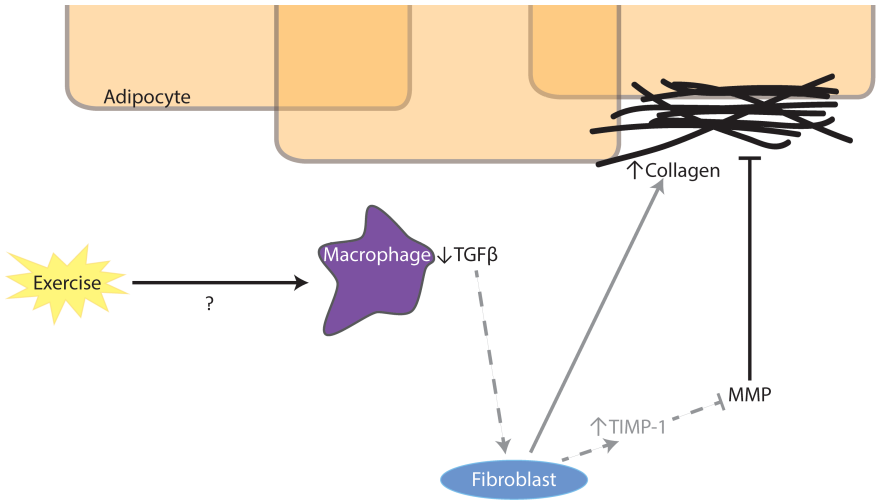

Figure II-6 Proposed model linking exercise with reduced adipose tissue fibrosis.

Work by Kawanishi et al. (44) suggested a reduction in adipose tissue macrophage TGFβ could be responsible for the protection from adipose tissue fibrosis in exercise-trained mice on a high-fat diet. While there are many factors involved in ECM remodeling that could be implicated in the anti-fibrotic effects of exercise, reduced *TIMP-1* expression represents one potential player to indirectly decrease fibrotic collagen deposition (via reduced MMP inhibition).

Adipose Tissue Inflammation

Healthy (lean) adipose tissue has a variety of immune cells that maintain adipocyte health (i.e. normal sensitivity to hormonal regulators) (130). This is achieved by the generally anti-inflammatory/"Th2" state maintained by regulatory T cells and other immune cells (131). In this environment, M2 macrophages predominate and maintain adipocyte sensitivity through secretion of cytokines like interleukin-10 (132). With weight gain and obesity, there is a dramatic shift in immune cell number and phenotype in adipose tissue, which impacts all of adipose tissue fatty acid storage, expandability, and insulin sensitivity (13).

The relationship between obesity and systemic inflammation (133) has identified the immune response as a central piece in the obesity puzzle, giving rise to the field of "metainflammation"; the inflammatory response to a metabolic stimulus. The systemic inflammation observed with obesity has been largely attributed to the adipose tissue (30), where the infiltration of macrophages with a pro-inflammatory phenotype was observed over a decade ago (132,134,135). Other immune cell populations are increasingly implicated in this phenotypic shift, in particular CD4+ and CD8+ T cells (131). It is now accepted that the adipose tissue immune response with obesity is much more complex than a pro-inflammatory macrophage polarization, involving a combination of pro- and anti-inflammatory changes across a host of immune cells, altogether resulting in insulin resistance among other changes within the adipose tissue (86).

A key mechanism by which adipose tissue inflammation causes insulin resistance is through reducing adipocyte sensitivity to insulin; reviewed in (136). TNFα is one of the important pro-inflammatory cytokines elevated in adipose tissue from obese humans (30,137). TNFα results in serine phosphorylation of the insulin receptor substrate 1 (Irs1) in the adipocyte, which impairs insulin signaling (138). Given that insulin is the key hormone regulating the suppression of lipolysis, this local insulin resistance exacerbates the excessive adipose tissue lipolysis that is characteristic of "overloaded" (obese) adipose tissue. Importantly, there are many more pro-inflammatory signaling pathways that have been linked to insulin resistance. The Pattern Recognition Receptors (PRR) pathway is another key pro-inflammatory pathway through which pathogens (e.g. saturated fatty acids) bind to members of the PRR family, which induce transcription of inflammatory genes (e.g. toll-like receptor 4 (TLR4) activates nuclear factor

kappa-light-chain-enhancer of activated B cells (NFκB) transcription, which increases production of a variety of inflammatory genes) (139). The upstream signals for these immune changes in adipose tissue are unclear, but are thought to include a combination of systemic and local factors. Key candidate signals include the gut-derived antigen lipopolysaccharide (via TLR4 signaling); free fatty acids (via TLR4 or TLR2 signaling); dead adipocytes (via nod-like receptor (NLR) signaling); hypoxia; and mechanical adipocyte stress (140). Many of these signals have been linked to the adipose tissue expandability "threshold" as outlined in the former parts of this review. Given the complexity of these responses, there is a need for creative therapeutic approaches to improve adipose tissue expandability and to reduce adipose tissue inflammation during weight gain.

There is preliminary evidence that exercise can attenuate high-fat diet-induced adipose tissue inflammation in mice (19,20). Oliveira et al. (20) found the stromovascular fraction from epididymal fat pads from rats on a high-fat diet had a more Th1-like profile (more IL-10, less TNFα, etc.) after two three-hour swim bouts with a 45-minute break. Using a more feasible exercise stimulus, MacPherson et al. (19) found reduced macrophage content (by immunofluorescence) in inguinal adipose tissue from high-fat fed mice two hours after a single two-hour treadmill exercise session. The authors linked these findings to an increase in exercise-induced IL-6 and IL-10 expression in the adipose tissue (19). Certainly, the discovery of exercise-induced IL-6 secretion from skeletal muscle has yielded much excitement about the potential anti-inflammatory effects of exercise (e.g. reduced TNFα) (141,142). However, there remains limited understanding of the signals regulating the adipose tissue immune response to exercise. Furthermore, no work to-date has directly quantified (i.e. using flow cytometry) changes in immune (or other) cell populations in response to a single session of exercise in adipose tissue. Assessing the acute signals regulating adipose tissue cellular responses to exercise as well as their potential to enhance adipose tissue expandability during a stimulus for adipose tissue expansion (i.e. overeating) could reveal very effective targets for therapies for the treatment of obesity-related metabolic diseases.

Summary

Adipose tissue expands with weight gain by means of sequestering excess energy as triglyceride within the adipocyte. Eventually, the capacity for the adipose tissue to sequester fatty acids as neutral lipids is exceeded, characterized by excessive FA mobilization and ectopic lipid deposition (26,70). This ectopic lipid deposition causes systemic insulin resistance among other cardio-metabolic problems (26).

The physical "limit" to healthy expansion is often called the "adipose tissue expandability threshold," and this threshold is different between people. The expandability threshold depends on several key structural features including adipogenic capacity, angiogenic capacity, ECM remodeling, as well as interplay with immune cells. There is preliminary evidence that exercise might modify these factors, but this has not been directly assessed in human adipose tissue.

Each exercise session triggers changes that have been identified to modify these processes; namely increased adipose tissue blood flow, lipolysis, and IL-6; and the resultant increase in fatty acids, PPARγ, AMPK, and PGC1α (proposed model outlined in Figure II-7). The stimulus (i.e. exercise intensity and duration) required to elicit these signals in human adipose tissue remains unclear. Furthermore, the ability of these signals to result in structural changes (cell number, or cumulative remodeling with repeated exercise sessions) is also unknown. Importantly, these potential signaling effects of exercise might be most meaningful *during a stimulus for adipose tissue expansion* (i.e. weight gain). Therefore, studies should be designed to assess the effects of exercise on key factors regulating adipose tissue expandability during a caloric surplus.

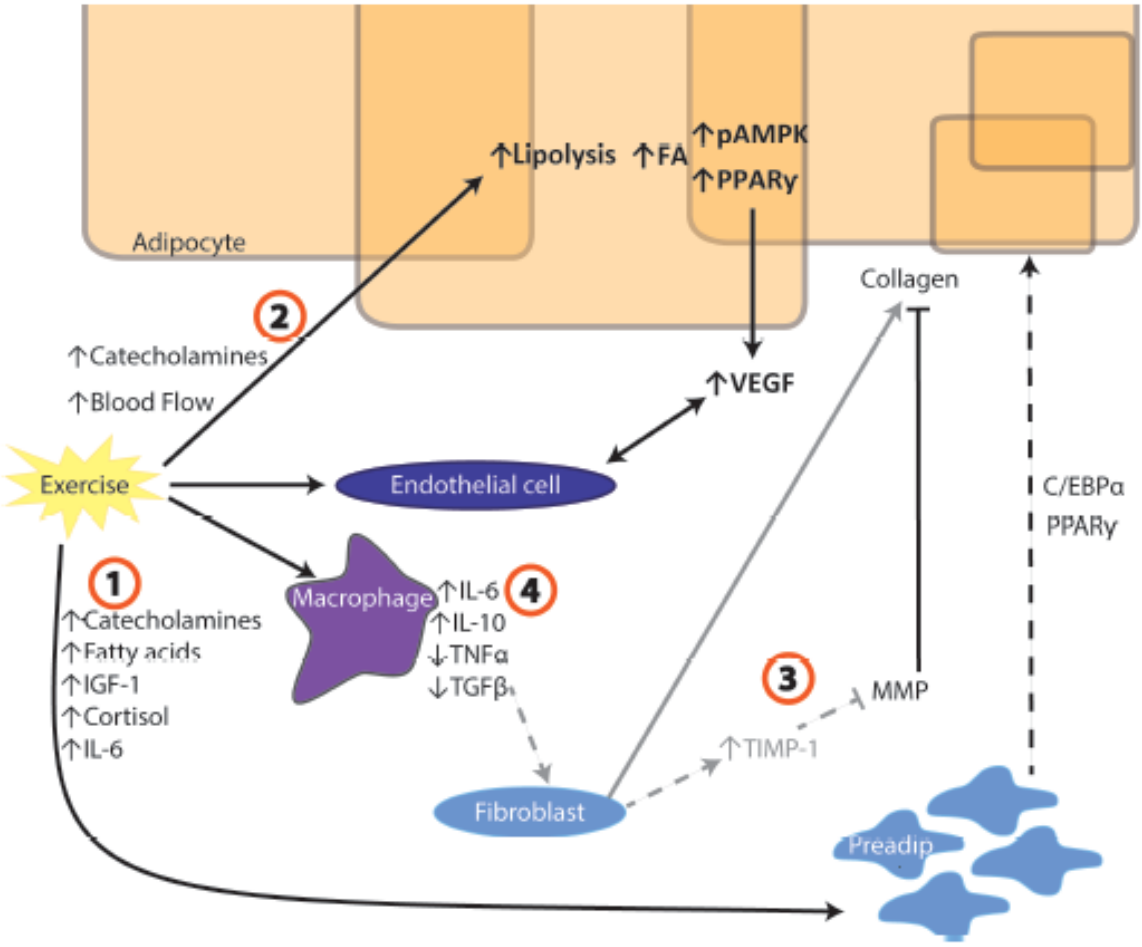

Figure II-7 Proposed model of exercise-related signals that might regulate adipose tissue expandability.

(1) Adipogenesis: exercise-induced increases in circulating factors including catecholamines, fatty acids, IGF-1, cortisol, and IL-6 could increase preadipocyte differentiation by enhancing transcriptional regulation by PPARγ and C/EBPα. **(2) Angiogenesis**: exercise-induced increases in catecholamines and blood flow result in increased adipocyte lipolysis, fatty acids, p-AMPK, and finally PPARγ; a key signal for VEGF, the master regulator of angiogenesis. **(3) ECM remodeling**: exercise-induced reduction in macrophage TGFβ attenuates TIMP-1 release from fibroblasts, decreasing adipose tissue fibrosis by indirectly increasing MMP levels. **(4) Inflammation**: The exercise-induced increase in IL-6 levels in adipose tissue might be related to an altered immune environment (reduced TNFα, increased IL-10), and a shift towards a Th2, anti-inflammatory profile within the adipose tissue.

Chapter III. Project 1
The Effects of a Single Session of Moderate-intensity and High-intensity Exercise on Factors Regulating Adipose Tissue Structure and Metabolic Function

ABSTRACT

Adipose tissue inflammation and dysfunction are among the primary drivers of insulin resistance and metabolic disease. Although very limited information is available regarding the direct effects of exercise on adipose tissue, some evidence suggests a session of exercise may upregulate factors related to adipose tissue inflammation and structural remodeling. However, the effects of exercise on factors regulating inflammation and remodeling in obese adipose tissue are poorly understood. The primary aims of this study were to perform an unbiased analysis of the subcutaneous adipose tissue transcriptomic response to acute exercise in obese adults, and to assess the effects of different exercise stimuli on this response. We recruited 29 obese adults who performed either high-intensity interval exercise (HI; 10x1 min at 90 ± 2 %HRpeak with 1 min recovery between intervals; n = 14) or moderate-intensity continuous exercise (MI; 45 min at 71 ± 1 %HRpeak; n = 15). Groups were matched for BMI (HI 33 ± 3 vs. MI 33 ± 4 kg/m^2) and there was no difference in their fasting blood metabolite or insulin levels at baseline. Adipose tissue was collected before and 1 hour after a single session of HI or MI, and samples were processed for RNA sequencing. We used Gene Set Enrichment Analysis (GSEA) to assess groups of genes that were associated with the response to exercise. Despite the vastly different exercise stimuli in HI vs. MI, transcriptional responses to exercise were surprisingly similar between groups (7 out of 21 enriched gene sets overlapping). Our major finding was that acute exercise upregulated gene sets involved in inflammation (IL6-JAK-STAT3 signaling, allograft rejection, TNFA signaling via NFKB, and inflammatory response; FDR q-value < 0.25) by GSEA. Exercise also downregulated adipogenic and oxidative metabolism gene sets. Overall, these data suggest genes involved in adipose tissue remodeling, and in particular inflammatory signaling, are an important part of the immediate response to a session of exercise.

INTRODUCTION

In obesity, adipose tissue is often associated with chronic, low-grade inflammation, featuring diverse immune cell populations, polarized towards a pro-inflammatory phenotype (1,2). Adipose tissue inflammation has been linked to systemic insulin resistance through direct action on the adipocyte, where pro-inflammatory cytokines (e.g. TNFα) impair insulin signaling at IRS1, which exacerbates the high rates of lipolysis in obesity (3). This in turn results in ectopic lipid deposition in metabolically active tissues, causing systemic insulin resistance (4). Therefore, interventions that can modify adipose tissue structure to reduce inflammation and better accommodate triglyceride storage are essential to improve metabolic health in obesity.

Participation in regular exercise is known to reduce cardiometabolic disease risk (5), but the impact of exercise on adipose tissue structure and function is poorly understood, especially in humans. While there is growing interest in the potential for exercise-induced browning of white adipose tissue by the release of myokines such as irisin (6), studies in humans have not found clear evidence for adipose tissue "browning" after exercise training (7,8). Interestingly, there is some evidence that exercise can alter structural components related to adipose tissue storage capacity, such as angiogenesis (the formation of new blood vessels), extracellular matrix, and inflammation (9–11). However, there has been very little work assessing the signals regulating these processes within adipose tissue, particularly in response to exercise in human subjects.

There is evidence that acute exercise reduces pro-inflammatory macrophage content in inguinal white adipose tissue from high-fat diet-fed mice, but there is no work assessing the inflammatory signaling response to acute exercise in obese human adipose tissue. Overall, there is quite limited work assessing the acute response to exercise in human adipose tissue. The majority of work assessing the immune response in the hours after exercise has measured circulating immune cells (1–3), with no clear consensus on whether acute exercise is pro- or anti-inflammatory (4). Despite the lack of clarity regarding the acute effects of exercise on inflammatory pathway activation, there is promise for longer-term adaptive responses to exercise that could reduce chronic inflammation (5,6). If exercise-induced adaptations to adipose tissue structure and vasculature could improve its ability to sequester fatty acids as neutral lipids during weight gain and obesity, this could be a mechanism to reduce adipose tissue inflammation and improve insulin sensitivity.

Adaptations to exercise typically accrue in response to repeated exposure to transient exercise-induced transcriptional responses after each exercise session (12). Therefore, establishing the signals that occur rapidly after exercise is an important step to understand the mechanisms for chronic adaptations to exercise training, and whether this can be manipulated to induce favorable adipose tissue remodeling. Furthermore, the intensity of the exercise stimulus is known to influence the magnitude of the metabolic adaptations to exercise (13). For example, classic work has established that exercise-induced muscle mitochondrial biogenesis is most robust in response to high-intensity exercise (7,8). Additionally, cellular stress, blood flow, substrate mobilization and fuel selection during/after exercise are also greatly impacted by the intensity, duration, and energy expenditure of the exercise session (9–11). Therefore, the purpose of this study was two-fold: (1) to perform an unbiased analysis of the subcutaneous adipose tissue transcriptomic response to a session of exercise in obese adults, and (2) to examine the effects of different exercise stimuli on the transcriptional response to exercise by comparing low-volume high-intensity interval exercise with more conventional steady-state endurance exercise. Expanding our understanding about the adipose tissue transcriptional response to exercise can help uncover new mechanisms for improving metabolic health in obesity.

METHODS

Subjects

Twenty-nine obese, non-diabetic, weight stable (±3kg for ≥ 6 months) men and women participated in this study. Subjects completed a medical history questionnaire, physical examination, and resting 12-lead electrocardiogram before entering the study and were excluded if they were taking medications that affect lipid or glucose metabolism, had EKG abnormalities, or were pregnant/smokers. The study protocol was approved by the University of Michigan Institutional Review Board.

Cardiorespiratory fitness testing

After enrolling in the study, we assessed cardiorespiratory fitness by measuring peak oxygen consumption (VO_{2peak}) using an incremental exercise test to exhaustion. The test began with a 4-min warm-up, followed by an increase in resistance every minute until volitional fatigue. This

exercise test was also used to establish heart rate targets during the experimental exercise sessions.

Exercise familiarization/short-term training protocol

Subjects were randomized into either a high-intensity (HI) or moderate-intensity (MI) exercise group. In order to avoid the influence of novelty of the exercise stimulus, we measured the response to acute exercise after subjects completed 6 weeks of 4 sessions of weekly exercise. For the first week, sessions were 25 min steady state exercise in both groups. In the second week, participants ramped up to the full experimental protocol shown in Figure III-1A. HI participants ramped from 2 to 10 one-minute intervals over the course of week 2, and MI participants completed 35 min steady state exercise during week 2. From weeks 3 to 6 (the week of the experimental trial), participants performed the full exercise protocol (Figure III-1A): 10x1 min at 90% HR_{peak}, with 3 min warmup and cooldown (HI – 25 min, ~150kcal); or steady-state exercise at 70% HR_{peak} for 45min (MI – 45 min, ~250 kcal). Subjects performed their last exercise training session 2 days before the experimental trial.

Experimental protocol

The experimental trial is shown in Figure III-1B. Subjects reported to the laboratory between 0700-1000h, after an overnight fast. Participants then rested for 20-30 minutes before the Pre-exercise (Pre) blood and subcutaneous abdominal adipose tissue samples were collected (details of the biopsy procedure are provided in Appendix A). Subjects then completed a supervised exercise session, identical to one of their typical training sessions (see Figure III-1A). Importantly, the two exercise protocols (HI and MI) differed by intensity, duration, and total work performed. Immediately post-exercise (IPEX), another blood sample was taken, and subjects rested quietly in the lab for one hour before 1h post-exercise (1hPost) blood and fat samples were collected from the opposite side of the umbilicus to the Pre biopsy.

Analytical Procedures

Approximately 200 mg whole adipose tissue was blotted clean with saline and partitioned for RNA sequencing and qPCR per below. In both cases, RNA was isolated from ~80 mg tissue using a Qiagen RNeasy Plus Universal Mini Kit (cat 73404), with Turbo DNAse treatment (cat

AM1907) after RNA isolation. Full RNA isolation and sequencing SOP is provided in Appendix B.

RNA-sequencing. Library preparation and sequencing were performed by the University of Michigan Advanced Genomics Core. The Lexogen QuantSeq 3' mRNA library prep (cat 015) was used on 100 ng total RNA to generate fragment lengths of ~100 nucleotides. Single-end sequencing was performed on the NovaSeq 6000 with 100 cycles and ~10 million reads per sample. Data was analyzed in collaboration with the University of Michigan Bioinformatics Core. Data passed FastQC analysis and samples had ~80% alignment to the reference genome. Differential Expression (DE) analysis was performed on log-CPM values calculated using Voom, which were further normalized by the trimmed mean of M-values technique through edgeR. Leading edge analysis was used to identify the key genes driving these gene set differences. The Limma software package of Bioconductor was used for DE analysis. Gene Set Enrichment Analysis (GSEA; Broad Institute) was used to identify gene sets from the Hallmark database (Liberzon) that were up- or down-regulated for the same comparisons. This was established by Normalized Enrichment Scores (NES), which reflect the degree to which the expression of genes from a given gene set are collectively increased or decreased one hour after exercise (1hPost) compared with all genes detected in the experiment.

qPCR. Real-time quantitative PCR was used to assess the mRNA expression levels of target genes of interest identified by RNA-sequencing. Because there was insufficient RNA remaining after library prep for QuantSeq, RNA was isolated from a separate ~80mg piece of adipose tissue for qPCR. Predesigned primer and probe sequences were purchased from IDT PrimeTime qPCR Assays and are shown in Table III-2. The qPCR data was normalized to the expression of 2 housekeeping genes (peptidylprolyl isomerase A (PPIA) and beta-2-microglobulin (B2M)) using the -ΔCt method (12) and expressed as fold induction ($2^{-\Delta\Delta Ct}$) of mRNA expression compared with Pre.

Blood measurements. Plasma was collected in an ice-cold EDTA tube, and serum was collected in a silica tube, left to clot for 30 min at room temperature before centrifugation. All samples were centrifuged at 2000G, 15min, 4°C and stored at -80°C until analysis. Plasma glucose

(Thermo Scientific, Waltham, MA, USA), non-esterified fatty acid (Wako Chemicals USA, Richmond, VA, USA), triacylglyceride (Triacylglyceride reagent; Sigma Aldrich), and total- and high-density lipoprotein (HDL; Cholesterol E and HDL-Cholesterol E;Wako Chemicals USA) concentrations were measured using commercially available colorimetric assay kits. Serum insulin concentration was measured by IMMULITE 1000 chemiluminescent assay (Siemens, Flanders NJ, USA). Epinephrine and norepinephrine (Abnova, Taipei City, Taiwan; KA1877), IL6 (R&D cat HS600C), and cortisol (R&D cat KGE008B) were measured by ELISA. Norepinephrine had several undetectable values (below the lowest standard) Pre and 1hPost, so statistics were run on the available data with N = 6-7 Pre, N = 13-14 IPEX (full available samples), and N = 9 IPEX by a linear mixed model.

Statistics

Paired student's t-tests (HI vs. MI) or linear mixed models (group vs. time) were used to analyze blood and anthropometric data. IL6, cortisol, NEFA, epinephrine, and norepinephrine concentrations were log-transformed to achieve normality prior to analysis. Sidak's multiple comparisons test was performed when an interaction effect was observed. RNA sequencing data was analyzed in collaboration with the University of Michigan Bioinformatics Core. DE of RNA-sequencing data was fit to a linear model per Smyth (13), and P values of <0.05 after multiple comparisons correction by false discovery rate (FDR) per Benjamini (14) were considered significant. For GSEA, gene sets found to be enriched with a false discovery rate (FDR) < 0.25 were considered significant. Two-way ANOVAs with one factor repetition (time; Prism 8.0) were used to assess differences between exercise conditions in qPCR data, following log-transformation where normality tests failed. One outlier was excluded from VEGF qPCR analysis, identified by Robust regression and Outlier removal (ROUT). Tukey's post-hoc test was used when required. Statistical significance was defined as $P<0.05$.

RESULTS

Subject Characteristics

A total of 29 subjects completed the study: 15 HI (9 women and 6 men) and 14 MI (10 women and 4 men). The groups were well matched for age, weight, BMI, and fasting plasma concentrations of glucose, insulin, triglycerides, and cholesterol (Table III-2). Samples were collected after 6 ± 1 weeks of HI or MI (4 sessions per week) in order to avoid the confounding effects of a novel exercise task on the inflammatory response to exercise.

Exercise Response to HI vs. MI Exercise

During the experimental exercise session, MI subjects exercised at an intensity eliciting 71 ± 1% of their HR_{peak} (132 ± 7 bpm) for 45 minutes, while HI subjects exercised at an intensity eliciting 90 ± 2% of their HR_{peak} (163 ± 8 bpm) during their 10 x 1 minute high-intensity intervals. After exercise, plasma concentrations of epinephrine, norepinephrine, cortisol, IL6, and NEFA were all elevated above pre-exercise levels in both MI and HI (main effect for exercise, all $P \leq 0.01$; Figure III-2). In addition, the increase in plasma cortisol concentration was significantly greater in HI vs. MI, while the increase in plasma NEFA concentrations was significantly greater in MI vs. HI (both P=0.03; Figure III-2).

Effects of Exercise on Adipose Tissue Gene Expression

Targeted analysis of gene expression for factors regulating adipose tissue remodeling. Based on previous findings from our lab (15,16) and others (6,17), we used qPCR to assess gene expression of 6 *a priori* targets related to adipose tissue remodeling. Consistent with our previous work, we found a trend for exercise to increase VEGFA gene expression ($P = 0.07$; Figure III-3). We also found an increase in TIMP1 mRNA after exercise (main effect $P < 0.01$; Figure III-3) and IL6 mRNA increased 2.5-fold after HI ($P < 0.01$), but not MI (Figure III-3).

Untargeted analysis of the effects of exercise on adipose tissue gene expression. Using QuantSeq RNA sequencing, 12077 total genes were detected in this experiment. We found 17 DE genes in adipose tissue collected one hour after HI compared with before exercise (10 upregulated, 7 downregulated – Table III-3, Figure III-4A), while in MI, there were 10 DE genes (8

upregulated, 2 downregulated – Table III-3, Figure III-4B). Surprisingly, there was no overlap in DE genes between HI and MI – the full list is provided in Table III-3.

We used qPCR to validate a total of 4 genes (ANGPTL4, MMP7, CXCL5, CISH) with among the highest log fold-change (logFC) after exercise, and three additional genes (CXCR2, NFKBIA, ADAMTS1) central to the regulation of adipose tissue remodeling that exhibited a trend for DE (adjusted $P < 0.1$, Figure III-5). Of this panel of seven genes (Figure III-5), we found small, yet significant main effects of exercise for only ANGPTL4 and MMP7 (both $P \leq 0.01$), but the increase in MMP7 mRNA after exercise by qPCR was actually in contrast to the reduction in MMP7 found with RNA sequencing. The relatively large mean increase in CXCR2 did not reach statistical significance ($P = 0.68$). Overall, our qPCR analysis did not corroborate our DE analysis.

Gene Set Enrichment Analysis. Given the inconsistencies between RNA-sequencing and qPCR analyses, we used GSEA for its power to identify gene set-level changes in cases where individual gene expression changes may not be robust (18). We identified 13 pathways that were affected by HI (5 increased, 8 decreased), and 15 pathways affected by MI (10 increased, 5 decreased; Figure III-6 and Table III-4). We found that 7 of these gene sets changed in the same direction between HI and MI (4 upregulated and 3 downregulated; Figure III-6B). Individual enrichment plots for these 7 gene sets are shown in Figure III-6C. Interestingly, the four pathways that were upregulated after exercise were all related to immune function (IL6-JAK-STAT3 signaling, allograft rejection, TNFA signaling via NFKB, and inflammatory response), whereas the three downregulated pathways were broadly related to metabolism (oxidative phosphorylation, adipogenesis, and peroxisome).

DISCUSSION

A key finding from this project was that acute exercise rapidly alters the adipose tissue transcriptome (i.e. 1 hour after exercise). In addition, despite HI and MI representing distinct exercise stimuli, we found similar gene sets were altered one hour after exercise in both groups. Specifically, pathways related to inflammation were upregulated after both HI and MI exercise, while pathways related to adipogenesis and oxidative metabolism were downregulated. These data suggest that gene set-level increases in inflammatory signaling pathways are likely an

important component of the early response in adipose tissue after a session exercise – while reductions in metabolic pathways may reflect downregulation during the early-phase recovery in response to exercise.

The intensity of exercise is known to have profound impact on the metabolic response during the exercise session (10,19) and for at least the few hours afterwards (20). Furthermore, there is now a large body of literature suggesting that high-intensity interval training (HIIT) can induce similar adaptations to more conventional moderate-intensity continuous training (MICT) despite a lower time commitment, which may certainly be attributed to the high intensity stimulus, but could also be due to other factors associated with the HIIT protocol such as the pulsatile nature of the stimulus (21). Much of this previous work examining the effects of HIIT vs. MICT has focused on whole-body responses and changes within skeletal muscle (19), with very little information available regarding effects on signaling responses within adipose tissue. In our study, the greater adrenergic/cortisol response after HI indicated that we did indeed achieve distinct metabolic stimuli between the two exercise protocols. However, despite robust differences in exercise intensity, as well as differences in exercise duration and energy expenditure between HI and MI, the gene expression responses were remarkably similar. Strikingly, all gene sets that were upregulated after exercise were inflammation-related, while most of the gene sets that were downregulated were related to metabolic control, in both HI and MI.

Our finding that acute exercise upregulated gene sets involved in inflammation just one hour after exercise suggests that inflammatory signaling may be an important early-phase post-exercise response within human subcutaneous abdominal adipose tissue. This is consistent with recent work in lean participants reporting that the top upregulated gene ontology (GO) pathways in subcutaneous adipose tissue collected four hours after exercise were inflammation-related (22). Acute exercise has mixed effects on immune cells in circulation and tissues including spleen and liver (4,23,24); but the effects of exercise on immune cells in obese human adipose tissue remain unclear. The gene sets enriched in our adipose tissue samples after exercise included several genes involved in chemoattraction (e.g. CCR2, CCL5), as well as genes encoding for cytokines and inflammatory signaling molecules (lists in full in Appendix D). This suggests there are signals for the recruitment of immune cells and/or immune cell activation within adipose tissue as quickly as only one hour after exercise, which is in agreement with the

hypothesis that exercise-induced inflammatory signaling within adipose tissue could result in a phenotypic shift in immune cell populations after exercise. Among the inflammatory gene sets upregulated by GSEA in this cohort, the IL6-JAK-STAT signaling pathway had the greatest normalized enrichment score (NES), indicating this pathway exhibited the most robust collective upregulation of genes within the overall transcriptome. This is consistent with the work by MacPherson et al. (17), who reported an increased IL6-signaling in inguinal adipose tissue samples collected two hours after exercise from high-fat diet mice (17), as well as the well-established role of IL6 as an exercise-induced myokine (25). Together, these data support a key role of immune signaling (including IL6 signaling) in the early adipose tissue response to exercise in obese humans. It is important to consider that IL6 is among inflammatory cytokines with potential pro- *and* anti-inflammatory effects (26). Therefore, these results should be considered in the context that immune signaling is complex, and assessment of specific signaling pathways over the several hours and even day(s) after a session of exercise or over days and weeks of repeated exercise is required to achieve a better understanding of the impact of this general regulation of immune signaling. Furthermore, because the magnitude of the inflammatory gene response to a session of exercise is quite modest (Appendix D), especially when compared with a classic inflammatory insult such as sepsis or even exercise-induced muscle damage, measurable changes at the protein-level and/or changes in biological function may only be evident after several weeks of repeated exercise.

The increased gene expression of TIMP1 and trend for elevated VEGFA we found only one hour after exercise supports the notion that exercise may quickly elicit signals capable of modifying key structural components in subcutaneous adipose tissue. VEGFA is the master regulator of angiogenesis, and we have previously reported increased VEGFA expression in subcutaneous adipose tissue one hour after a session of exercise (15), and immediately after exercise in rats (16). Exercise training has been found to increase adipose tissue capillarization (measured histologically) (27), and our recent finding of greater CD31 (an endothelial cell marker) in subcutaneous adipose tissue samples from regular exercisers compared with sedentary controls (15) further supports this finding that angiogenic signals in adipose tissue stemming from each exercise session may lead to increased vascularization after chronic exercise training.

A single session of exercise also may trigger signals related to ECM remodeling in adipose tissue. The fibrotic network of adipose tissue ECM is primarily modified by a family of matrix

metalloproteinases (MMPs), whose function of cleaving collagenous proteins is regulated transcriptionally, post-translationally, and by the tissue inhibitor of MMP (TIMP) protein family. TIMP 1, thereby, modifies the ECM in its role as an MMP inhibitor, and our finding that TIMP1 expression was increased after exercise suggests that exercise may upregulate factors involved in ECM remodeling. A better understanding of the factors involved in the remodeling of adipose tissue angiogenesis and ECM remodeling in response to exercise will require measurements over several hours after exercise, and assessment of related structural changes after weeks/months of exercise training. However, these qPCR data suggest that exercise can activate key players in these processes.

Our GSEA finding that the adipogenic gene set was downregulated after a session of exercise is consistent with previous work (28,29). This reduction in adipogenic signaling one hour after exercise is not surprising given that adipogenesis is usually triggered by conditions of energy *surplus*, and our participants had just expended ~200-300 kcals during the exercise session. Importantly, this finding does not preclude the possibility that factors released during and/or immediately after a session of exercise (e.g. catecholamines, IL6, growth factors, NEFA) may augment adipogenic *capacity* when energy availability is high; as suggested by some preliminary findings from our lab (30). Furthermore, our finding that several gene sets related to oxidative metabolism in adipose tissue were downregulated one hour after exercise may also reflect adipose tissue responses during the "recovery phase" after the exercise session. Specifically, this downregulation in oxidative metabolism genes within adipose tissue may be a compensatory response for the increased energy demands experienced during the exercise session. This acute down regulation of gene expression of oxidative metabolic pathways may be transient, because subcutaneous adipose tissue oxidative capacity and mitochondrial biogenesis have been suggested to remain stable with chronic exercise training in human subjects (31–33). Together, these data suggest the metabolic response to long-term exercise training is distinct from this rapid (1 hour) response. A thorough assessment of the time course of changes in gene expression and protein level responses will be required to elucidate the mechanisms for exercise-induced metabolic adaptations in adipose tissue.

There are several limitations to consider in interpreting these data. It is possible the very small number of differentially expressed genes after exercise was a consequence of the timing of our sample collection (i.e. 1 hour after exercise). Work by Fabre et al. (22) identified ~350 DE

genes in lean, trained subjects when measured 4h after exercise. Our decision to collect adipose tissue samples one hour after exercise was based on our interest in the rapid signals induced in adipose tissue after exercise. The use of GSEA allowed us to identify that this response, though mild at the individual gene level, is consistent at the gene set level. Furthermore, to detect individual gene expression changes in this complex tissue may require analysis in single cell populations, but the objective of this work was to perform exploratory analysis on whole tissue to provide some direction on which novel transcripts are impacted by acute exercise. While the adipose tissue immune response to weight gain is different between males and females (34), the analyses in this project reveal pathways that are up/downregulated with both sexes pooled, providing insight to consistent exercise-induced signals that are triggered in both sexes – which is important for practical exercise prescription. Finally, while the central focus of this project was to expand our understanding of exercise induced adaptations to *subcutaneous* adipose tissue that could improve its storage capacity, thereby reducing ectopic lipid deposition and inflammation in visceral adipose tissue during periods of weight gain, there are well known regional differences among adipose tissue depots. Therefore, the findings reported here may not translate to the response in visceral adipose tissue, or even gluteal/femoral subcutaneous adipose tissue.

In summary, our key findings indicate that one hour after a session of exercise there was an upregulation of gene sets involved in inflammation, and a downregulation of gene sets related to oxidative metabolism and adipogenesis in adipose tissue from obese adults. Furthermore, our findings support the notion that genes involved in adipose tissue structural remodeling are altered one hour after a session of exercise. These data suggest that an upregulation in inflammatory pathways is an important part of the immediate response to regular acute HI and MI exercise. This provides new evidence suggesting immune signaling in adipose tissue from obese subjects could be a key early trigger for the purported long-term adipose tissue adaptations to exercise training such as reduced pro-inflammatory macrophage content (17). Finally, our findings indicate that low-volume, high-intensity exercise evokes similar adipose tissue transcriptomic responses to more conventional moderate-intensity exercise (consistent with most standard exercise guidelines (36)), despite meaningful differences in energy expenditure and time commitment between these two exercise protocols.

ACKNOWLEDGEMENTS

This project was supported by NIH R01#DK077966 and CIHR DFS #0077000623. I am thankful to Michael Schleh, Emily Krueger, Natalie Taylor, Benjamin Ryan, and Toree Baldwin for their intellectual and technical contributions to these experiments. RNA sequencing was performed by the University of Michigan Advanced Genomics Core and analysis was performed in collaboration with the University of Michigan Bioinformatics Core. Additional thanks to Suzette Howton for subject recruitment and coordination, and Chiwoon Ahn, Pallavi Varshney, and Thomas Rode for additional support.

FIGURES

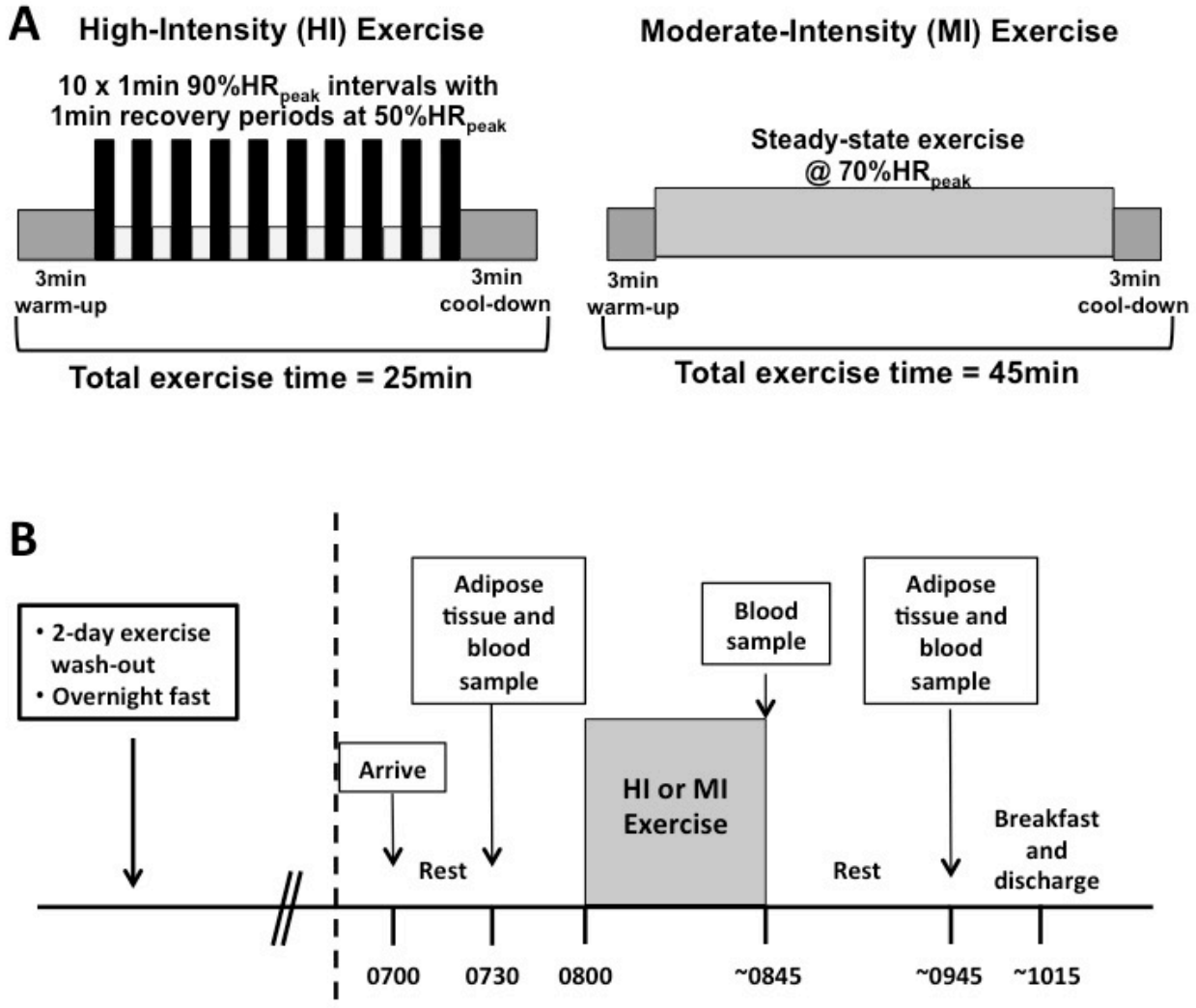

Figure III-1 Experimental Design.

(A) Subjects completed a single bout of MI (45 min at ~70% HRpeak) or HI (10x1 min at ~90% HRpeak with 1 min recovery in 25 min total). HI: high-intensity exercise; MI: moderate-intensity exercise. (B) Sample collection was performed 2 days after the last regular exercise training session, following a 12 h overnight fast.

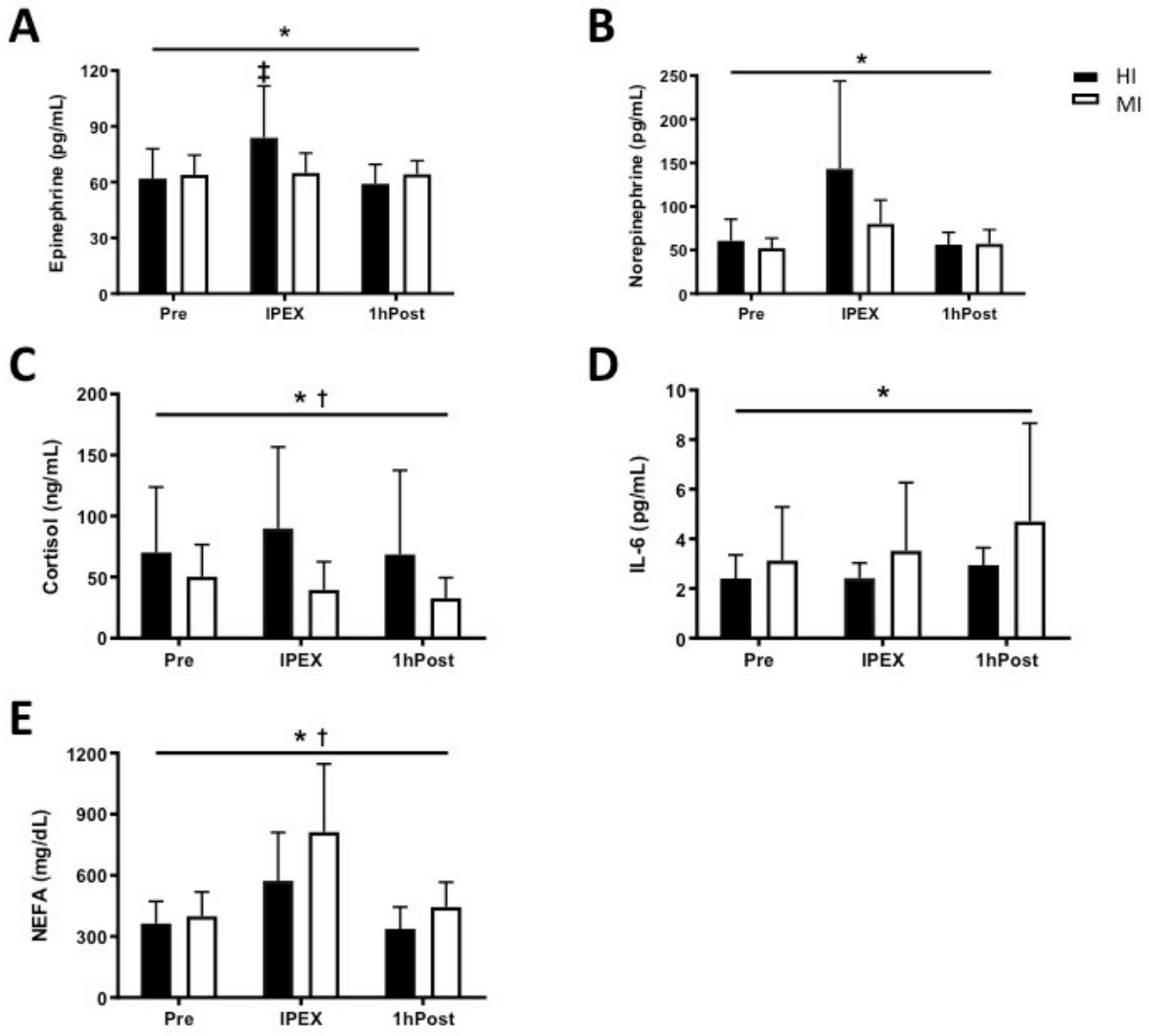

Figure III-2 Exercise Response of Circulating Factors.

Plasma samples were collected Pre, IPEX, and 1hPost for analysis of hormones/NEFA. (A) Epinephrine concentration - significantly greater IPEX v. Pre and 1hPost ($P < 0.01$); main effect for time ($P < 0.01$). N = 12-14. (B) Plasma norepinephrine concentration – main effect for time ($P < 0.01$). N = 6-14. (C) Cortisol concentration – main effect for time ($P = 0.01$), and main effect for group ($P = 0.03$). N = 13-15. (D) Plasma IL-6 concentration – main effect for time ($P < 0.01$). N = 13-15. (E) Plasma NEFA concentration: main effect for time ($P < 0.01$) and main effect for group ($P = 0.03$). N = 13-15. IPEX: immediate post-exercise; NEFA: non-esterified fatty acids. Data are Means ± SD. *$P < 0.05$ for time effect; †$P < 0.05$ for group effect. ‡$P < 0.05$ for Sidak's multiple comparison test.

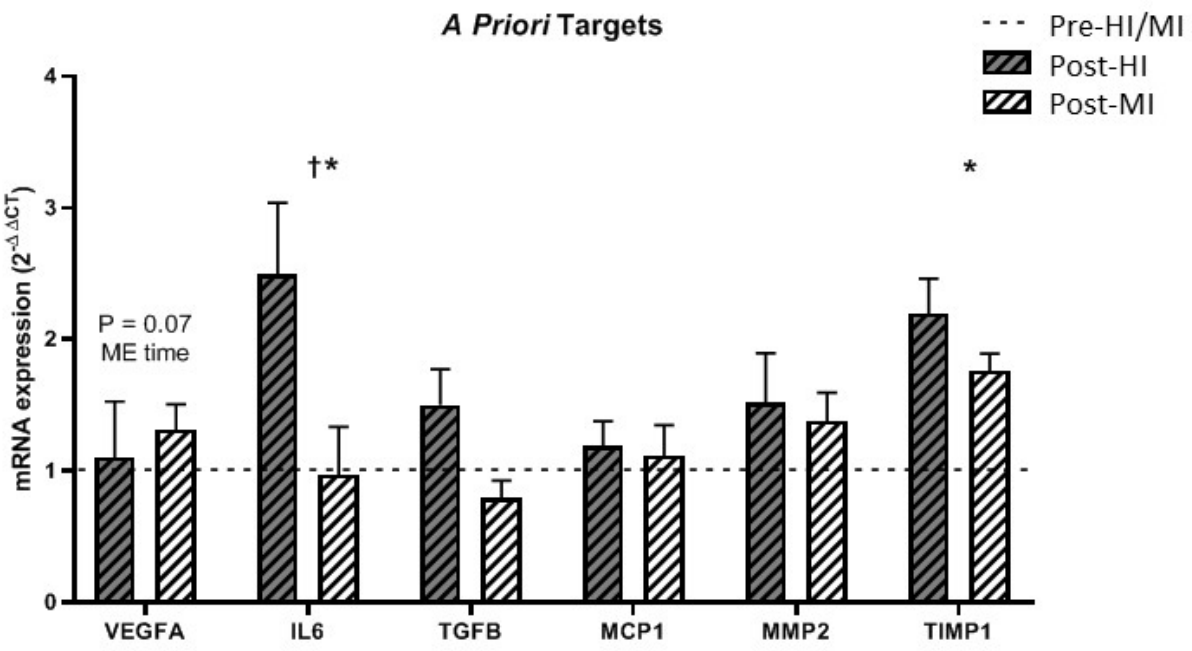

Figure III-3 Gene Expression for Factors Regulating Adipose Tissue Remodeling.

Fold-change of *a priori* transcripts related to adipose tissue remodeling in whole adipose tissue samples. There was a trend for exercise to increase VEGFA expression ($P = 0.07$). There was a main effect of group on IL6 expression ($P = 0.04$), wherein post-hoc analyses determined IL6 was increased in the HI group only ($P < 0.01$). There was a trend for a group effect on TGFB expression ($P = 0.06$), and there was an exercise effect on TIMP1 expression ($P < 0.01$). N = 9-15. Data are Mean ± SD. *$P < 0.05$ for exercise effect; †$P < 0.05$ for group effect. ME: main effect.

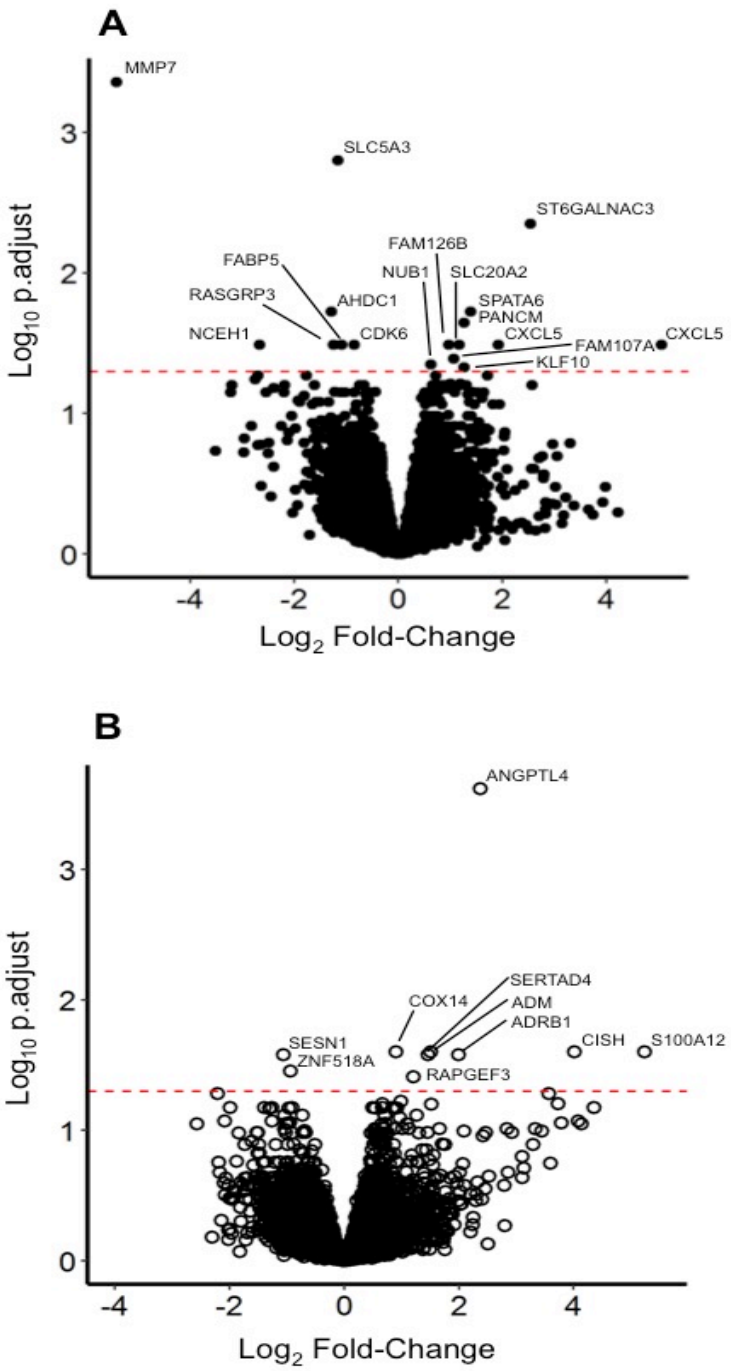

Figure III-4 Differentially Expressed Transcripts within HI and MI.

(A) Adjusted P-value vs. log2(Fold-Change) for transcripts from Pre-HI vs. 1hPost-HI. Positive Fold-Change represents an upregulation 1hPost. (B) Adjusted P-value vs. log2(Fold-Change) for transcripts from Pre-MI vs. 1hPost-MI. Points above the dashed lines were DE at an FDR adjusted $P < 0.05$. DE: differentially expressed; FDR: false discovery rate. N = 12 per group.

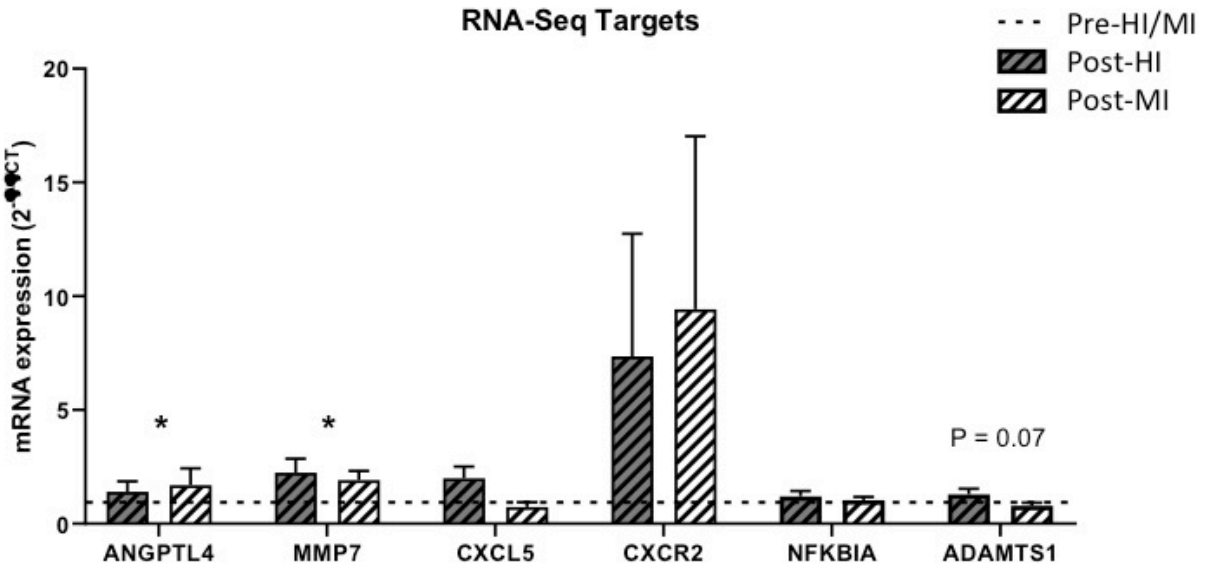

Figure III-5 qPCR Validation.

Fold-change of targets that were differentially expressed by RNA-sequencing in HI (dark) and MI (light). There was a main effect for exercise to increase ANGPTL4 and MMP7 gene expression ($P < 0.01$). N = 12-15. Data are Mean ± SD. *$P < 0.05$ for exercise effect.

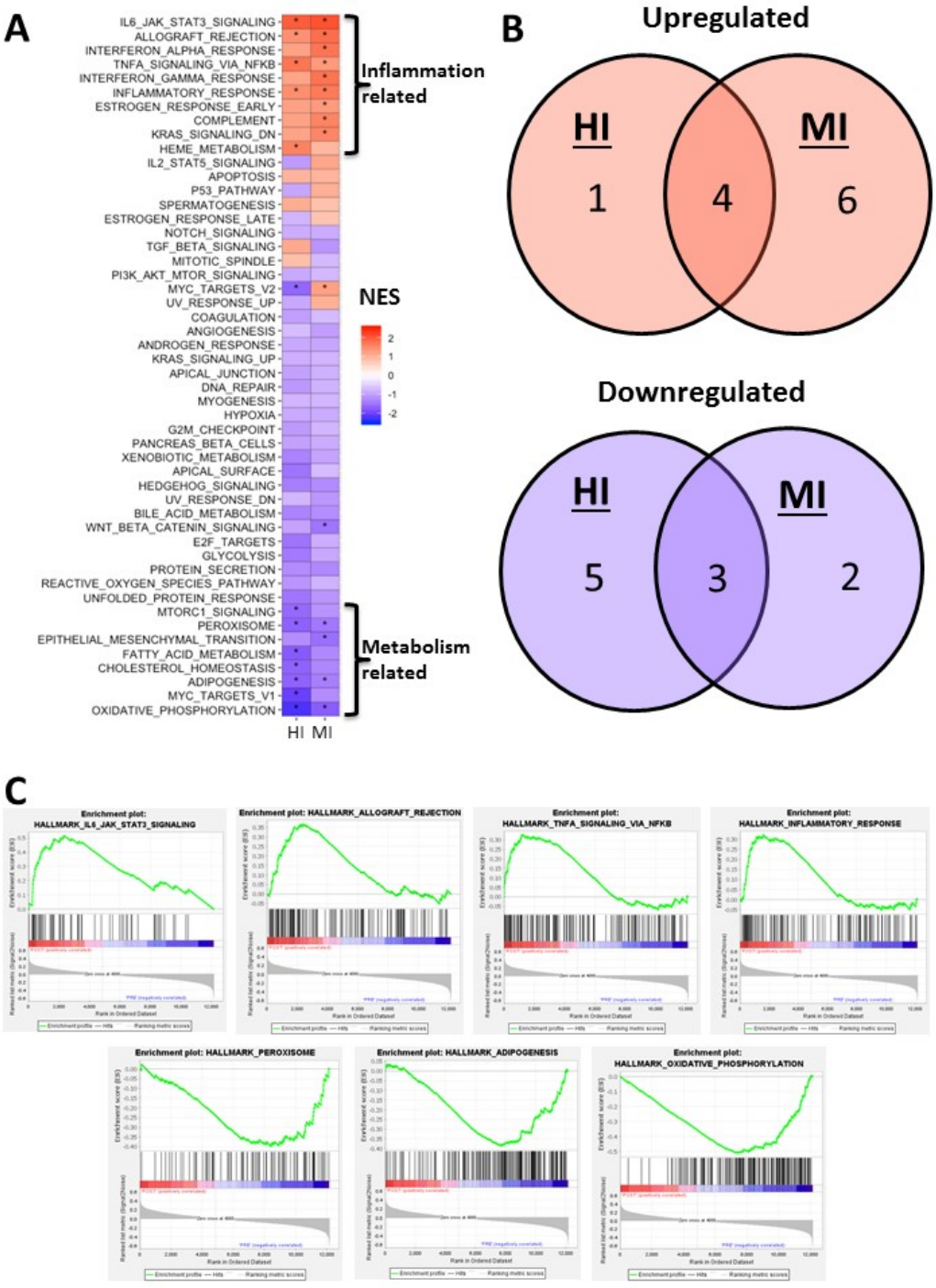

Figure III-6 Gene Set Enrichment Analysis.

(A) Heat map depicting the NES for gene sets from the Hallmark database. * denotes FDR q-val < 0.25. NES: normalized enrichment score; FDR: fase discovery rate. (B) Venn diagram presenting common gene set enrichment between HI and MI. Gene sets that were enriched 1hPost are shown in red; Gene sets that were enriched Pre (i.e. downregulated) are shown in blue. Seven pathways falling into immune or metabolic function were common between all comparisons. (C) Enrichment plots for these common immune (top) and metabolism (bottom) pathways. N = 12 per group.

TABLES

Table III-1 qPCR targets in the subcutaneous adipose tissue.

Gene symbol	Protein encoded
ANGPTL4	angiopoietin-like 4 (ANGPTL4)
MMP7	matrix metallopeptidase 7 (MMP7)
CISH	cytokine inducible SH2 containing protein (CISH)
CXCL5	C-X-C motif chemokine ligand 5 (CXCL5)
CXCR2	C-X-C motif chemokine receptor 2 (CXCR2)
NFKBIA	nuclear factor of kappa-B inhibitor alpha (IκBα)
ADAMTS1	A disintegrin and metalloproteinase with thrombospondin motifs 1 (ADAMTS1)
VEGFA	vascular endothelial growth factor (VEGF)
IL6	interleukin 6 (IL6)
TGFB	transforming growth factor beta 1 (TGF-β1)
CCL2	monocyte chemotactic protein 1 (MCP1)
TIMP1	tissue inhibitor of matrix metalloproteinases 1 (TIMP1)
MMP2	matrix metallopeptidase 2 (MMP2)

Table III-2 Physical characteristics of subjects

	HI	MI	P
Age (years)	32 ± 6	29 ± 5	0.13
Body mass (kg)	97.2 ± 13.7	96.5 ± 11.4	0.89
BMI (kg/m^2)	33.2 ± 2.9	33.4 ± 3.6	0.85
Fasting glucose (mg/dL)	84 ± 9	86 ± 9	0.46
Fasting insulin (uIU/mL)	18 ± 12	13 ± 6	0.29
Triglycerides (mg/dL)	104 ± 62	114 ± 61	0.65
Total Cholesterol (mg/dL)	149 ± 30	155 ± 33	0.61
HDL Cholesterol (mg/dL)	34 ± 7	34 ± 8	0.95
LDL Cholesterol (mg/dL)	116 ± 33	122 ± 37	0.64

BMI: body mass index, HDL: high density lipoprotein, LDL: low density lipoprotein. n = 14-15 per group. Data are Mean ± SD.

Table III-3 Differentially expressed genes in HI and MI

HI					MI				
Upregulated					Upregulated				
Gene	Expression		logFC	adj. P	Gene	Expression		logFC	adj. P
	Pre	Post				Pre	Post		
ST6GALNAC3	7.2	12.1	0.76	0.00	**ANGPTL4**	**159.2**	**254.5**	**0.71**	**0.00**
SPATA6	16.5	21.6	0.42	0.02	**CISH**	**13.6**	**31.8**	**1.21**	**0.03**
FANCM	16.0	20.0	0.38	0.02	S100A12	2.4	9.0	1.58	0.03
CXCL5	**6.1**	**40.4**	**1.52**	**0.03**	ADM	151.9	202.6	0.45	0.03
SLC20A2	5.1	7.5	0.58	0.03	COX14	161.1	196.5	0.27	0.03
FAM126B	70.8	90.4	0.29	0.03	SERTAD4	18.0	24.3	0.44	0.03
GALNT15	122.4	148.2	0.35	0.03	ADRB1	32.4	48.9	0.60	0.03
FAM107A	118.3	138.2	0.32	0.04	RAPGEF3	28.9	37.6	0.36	0.04
NUB1	107.8	121.3	0.19	0.04					
KLF10	36.4	45.1	0.38	0.05					
Downregulated						Downregulated			
Gene	Expression		logFC	adj. P	Gene	Expression		logFC	adj. P
	Pre	Post				Pre	Post		
MMP7	**7.2**	**1.9**	**-1.63**	**0.00**	SESN1	60.1	47.4	-0.32	0.03
SLC5A3	355.2	267.0	-0.35	0.00	ZNF518A	65.0	53.6	-0.28	0.04
AHDC1	30.0	22.6	-0.39	0.02					
NCEH1	28.5	14.2	-0.80	0.03					
FABP5	112.8	85.7	-0.33	0.03					
CDK6	96.4	80.0	-0.26	0.03					
RASGRP3	24.8	19.0	-0.38	0.03					

Genes are divided by upregulated (1hPost > Pre; top) and downregulated (1hPost < Pre; bottom). Expression represents mean normalized logCPM per group. Bolded genes were validated by qPCR. Expression represents the mean expression level for that group. logFC: log2(fold change); adj.P: adjusted P value for false discovery rate. N = 12 per group.

Table III-4 Gene Set Enrichment Analysis for samples collected before (Pre) vs. after (1hPost) exercise

	Gene Set Name	Size	ES	NES	FDR q-val.
HI: Pre vs. Post	HALLMARK_IL6_JAK_STAT3_SIGNALING	63	0.44	1.97	**0.001**
	HALLMARK_TNFA_SIGNALING_VIA_NFKB	158	0.33	1.72	**0.014**
	HALLMARK_HEME_METABOLISM	153	0.30	1.57	**0.035**
	HALLMARK_INFLAMMATORY_RESPONSE	134	0.28	1.44	**0.075**
	HALLMARK_ALLOGRAFT_REJECTION	140	0.27	1.41	**0.074**
	HALLMARK_OXIDATIVE_PHOSPHORYLATION	180	-0.51	-2.27	**0.000**
	HALLMARK_MYC_TARGETS_V1	190	-0.46	-2.04	**0.000**
	HALLMARK_FATTY_ACID_METABOLISM	132	-0.42	-1.78	**0.011**
	HALLMARK_ADIPOGENESIS	184	-0.38	-1.69	**0.056**
	HALLMARK_PEROXISOME	81	-0.43	-1.69	**0.057**
	HALLMARK_CHOLESTEROL_HOMEOSTASIS	62	-0.44	-1.69	**0.059**
	HALLMARK_MYC_TARGETS_V2	50	-0.45	-1.64	**0.102**
	HALLMARK_MTORC1_SIGNALING	185	-0.36	-1.61	**0.144**
MI: Pre vs. Post	HALLMARK_IL6_JAK_STAT3_SIGNALING	63	0.47	2.07	**0.000**
	HALLMARK_ALLOGRAFT_REJECTION	140	0.37	1.81	**0.005**
	HALLMARK_INTERFERON_GAMMA_RESPONSE	173	0.34	1.75	**0.006**
	HALLMARK_INTERFERON_ALPHA_RESPONSE	89	0.38	1.73	**0.005**
	HALLMARK_INFLAMMATORY_RESPONSE	134	0.34	1.66	**0.011**
	HALLMARK_COMPLEMENT	154	0.31	1.56	**0.020**
	HALLMARK_KRAS_SIGNALING_DN	63	0.35	1.53	**0.022**
	HALLMARK_TNFA_SIGNALING_VIA_NFKB	158	0.26	1.30	**0.130**
	HALLMARK_ESTROGEN_RESPONSE_EARLY	141	0.26	1.28	**0.129**
	HALLMARK_MYC_TARGETS_V2	50	0.30	1.22	**0.194**
	HALLMARK_OXIDATIVE_PHOSPHORYLATION	180	-0.39	-1.76	**0.022**
	HALLMARK_EPITHELIAL_MESENCHYMAL_TRANS	163	-0.35	-1.55	**0.120**
	HALLMARK_WNT_BETA_CATENIN_SIGNALING	36	-0.44	-1.49	**0.151**
	HALLMARK_PEROXISOME	81	-0.37	-1.46	**0.160**
	HALLMARK_ADIPOGENESIS	184	-0.31	-1.38	**0.247**

Only pathways with FDR q-val < 0.25 are shown. Size represents the number of genes in the listed gene set. A negative normalized enrichment score (NES) represents enrichment in the Pre condition. ES: enrichment score; NES: normalized enrichment score; FDR q-val: false-discovery rate-adjusted significance score. N = 12 per group.

Chapter IV. Project 2
The Effects of Acute Moderate-intensity Exercise on Adipose Tissue Cellular Composition and Function in Obese Humans

ABSTRACT

Adipose tissue pathology in obese patients often features impaired adipogenesis, angiogenesis, and chronic low-grade inflammation, all of which are processes that are regulated in large part by adipose tissue stromal vascular cells (SVC; i.e. non-adipocyte cells within adipose tissue including preadipocytes, endothelial cells, and immune cells). Exercise activates many processes in adipose tissue, such as lipolysis and adipokine secretion, but the impact of exercise on the individual adipose tissue SVCs has not been explored. The purpose of this study was to assess the effects of a session of exercise on changes in preadipocyte, endothelial cell, macrophage, and T cell content in human subcutaneous adipose tissue. We collected abdominal subcutaneous adipose tissue samples from ten obese regular exercisers (BMI 33 ± 3 kg/m^2, body fat 41 ± 7 %) the morning (12h) after 60 min endurance-type exercise (80 ± 3 %HR_{peak}) versus quiet rest in the laboratory. SVCs were isolated by collagenase digestion and stained for flow cytometry. We found exercise reduced preadipocyte content (38 ± 7 vs. 30 ± 13 %SVC; P = 0.04). The reduction was driven by an exercise-induced decrease in $CD34^{hi}$ preadipocytes (18 ± 5 vs. 13 ± 6 %SVC; P = 0.002), a subset of preadipocytes that generates high lipolytic rate adipocytes *ex vivo*. Exercise did not alter endothelial cell content, suggesting the exercise signal for endothelial cell migration may take longer to accrue. Exercise did not change total immune cell number, or macrophage or T cell content, and future work should assess subpopulations of these cells. We conclude that exercise may rapidly regulate the subcutaneous adipose tissue pre-adipocyte pool in ways that may help attenuate the high lipolytic rates that are commonly found in obesity.

INTRODUCTION

The ability of adipose tissue to expand and store excess energy during weight gain and obesity is important for maintaining tissue and systemic insulin sensitivity. While the adipocyte is the main site for fatty acid storage, the adipose tissue stromal vascular cell (SVC) composition is heterogeneous and includes adipocyte precursor cells (preadipocytes), immune cells (e.g. macrophages, T cells, dendritic cells), and endothelial cells – among others. These cells play a key role in regulating the overall "metabolic health" of adipose tissue. For example, impairments in the ability of these cells to (i) differentiate into new adipocytes; (ii) maintain an anti-inflammatory immune environment; and (iii) propagate angiogenesis to maintain sufficient tissue oxygenation and tissue crosstalk are some of the main maladaptive features commonly found in adipose tissue from obese, insulin resistant adults (1).

Preadipocytes are self-renewing SVCs that can differentiate into mature adipocytes. These cells can play a key role during periods of growth/weight gain by differentiating into new adipocytes in response to adipogenic stimuli including insulin, fatty acids, catecholamines, and cortisol (2). While the contribution of adipogenesis to mature adipocytes in obesity is relatively low (~8% new cells per year (3)), there is evidence that adipogenic rate can be altered/accelerated *in vivo*, which might enhance adipose tissue storage capacity by providing more small fat cells to sequester bioactive fatty acids as triglycerides (4). Furthermore, the recent identification of preadipocyte subtypes that differentiate into adipocytes with distinct metabolic phenotypes (5) highlights the potential for these cells to impact adipose tissue function.

Insufficient adipose tissue angiogenesis in expanding adipose tissue in obesity is thought to result in hypoxia of their hypertrophic adipocytes (6). Endothelial cells (EC) are the primary component of adipose tissue vasculature, and EC migration to the tip of capillary sprouts is a key step in angiogenesis (7). Therefore, signals that could improve endothelial cell migration and function during periods of weight gain could minimize adipose tissue hypoxia and the ensuing chronic low-grade inflammation.

While "healthy" adipose tissue function is maintained by a variety of anti-inflammatory immune cells (e.g., T regulatory cells and M2-like macrophages), adipose tissue hypoxia, pathogen-associated molecular patterns (e.g. LPS), and adipocyte death are among the triggers for a shift towards chronic low-grade inflammation in obesity. This pro-inflammatory environment impairs adipose tissue storage and insulin action by increasing pro-inflammatory

cytokine production (8). In turn, adipose tissue inflammation and insulin resistance can exacerbate the high rates of fatty acid release and cytokine production from obese adipose tissue, contributing to systemic insulin resistance.

Acute exercise increases signals in adipose tissue that impact adipogenesis, angiogenesis, and inflammation (9,10), suggesting unique potential for exercise to coordinately regulate the stromal cell composition of obese adipose tissue. Although visceral adipose tissue is often a predominant site of obesity-related inflammation, this is often a consequence of impairments in subcutaneous adipose tissue storage capacity that result in ectopic lipid deposition in visceral adipose tissue as well as other tissues such as the liver and skeletal muscle. Therefore, the goal of this study was to quantify changes in preadipocytes, ECs, macrophages, and T cells in abdominal subcutaneous adipose tissue in response to a single session of endurance-type exercise in obese adults.

METHODS

Subjects

Ten obese adults (3 men, 7 women) participated in the study. All participants were regular exercisers (≥ 3 days/wk of 30-60min moderate/vigorous endurance-type exercise) in order to avoid the confounding effect a novel exercise stress can impart on unaccustomed exercisers. Participants with elevated blood pressure (i.e., > 140/90 mmHg), history of cardiovascular or metabolic disease, and regular use of medications known to affect metabolism or inflammation were excluded. All women were pre-menopausal, with regularly occurring menses. The study protocol was approved by the University of Michigan Institutional Review Board.

Preliminary testing

Subjects were screened for physical activity status, cardiovascular disease risk, and medical history by questionnaires. Resting blood pressure, weight, height, body composition (DEXA; GE Lunar DPX) and peak oxygen consumption (VO_2peak) were also measured during screening. The VO_2peak test began with a warm up at a moderate running speed individualized for each subject, after which the incline of the treadmill was increased every 1-2 minute(s) until volitional fatigue. During a separate visit, we performed an oral glucose tolerance test (OGTT) after an overnight fast (12 h). Because all subjects were regular exercisers, to avoid the robust influence

of acute exercise, the OGTT was conducted exactly three days after their most recent exercise session.

Experimental trial

General study design. All subjects completed two separate experimental trials. The only difference between the two trials was whether they exercised (EX) or remained sedentary (SED) in the evening before adipose tissue samples were collected the next morning. Each trial required subjects to visit the laboratory in the evening for supervision of the study treatment (EX or SED), and again the next morning for blood and adipose tissue sample collection (see Figure IV1 and protocol details below). All participants were required to perform their last regular exercise session exactly 2 days before beginning their experimental trial (3 days before sample collection). On the day of their first evening visit, participants recorded everything they ate that day in order to replicate this diet on the day before their second experimental trial. The order of the EX and SED trials was randomized.

Evening before sample collection. Subjects arrived to the laboratory at approximately 1800h. After resting quietly for 30 min, participants either: 1) 60 min exercise (EX) at 80 ± 3% HR_{peak} (152 ± 8 bpm) – or 2) remained sedentary (SED) by resting quietly in the laboratory (in randomized order). EX was completed on a treadmill, except for one participant who used a cycle ergometer. Fifteen minutes after completing the hour of SED/EX, participants were provided with a standardized meal: 33% daily energy expenditure calculated by the Mifflin St. Jeor equation (11). The meal was composed of ~55% carbohydrate, 30% fat, and 15% protein. Participants then abstained from exercise, food and drink (other than water) overnight.

Morning of sample collection. Participants returned to the laboratory at approximately 0645h. After resting quietly for 30 minutes, we collected a baseline blood sample by venipuncture. We then collected the abdominal subcutaneous adipose tissue sample by needle aspiration (see details of adipose tissue biopsy procedure in Appendix A). After completion of all sample collection, subjects were provided with a meal, and they were discharged from the laboratory.

Analytical procedures

Adipose tissue stromal vascular cell isolation. Two grams of adipose tissue were collected into FACS buffer (Hank's Balanced Salt Solution (HBSS) with calcium and magnesium) and processed by collagenase digestion for isolation of the SVCs. Full SVC isolation protocol is available in Appendix D. In short, large pieces within the aspirated sample were minced by hand with sterile scissors before incubating the samples in 3 mg/mL Collagenase Type I (Worthington cat NC9633623) in FACS buffer (~30 mg/g tissue), while rocking at 37^{o}C for ~45 minutes until samples became slurry. This slurry was passed through a 300 μm filter to isolate the SVCs. Following centrifugation, this cell pellet was treated with a red blood cell lysis buffer (recipe in Appendix D), and SVCs were subsequently washed, pelleted, and counted with a hemocytometer. SVCs were then stained and fixed for flow cytometry.

Flow cytometry. SVCs were stained for flow cytometry as described previously (12) with minor modifications (detailed protocol in Appendix D). Briefly, ~1E6 cells were used for full stain and fluorescence minus one controls (FMO's; controls to identify the signal of a given fluorochrome in the context of the full remaining panel of fluorochromes), and ~0.2E6 cells were used for single stain/unstained controls. Details regarding cell surface markers and fluorophores used in this study are provided in Table IV-1. Sample tubes were incubated in Fc block (for nonspecific binding to Fc receptors of immune cells) for 5 minutes prior to staining. Cells were incubated in conjugated antibodies (Table IV-1) for 30 minutes at 4°C (dark), washed with 2mL PBS, pelleted, and resuspended in PBS for analysis. Samples were analyzed on the LSR Fortessa at the University of Michigan Flow Cytometry Core (details in Appendix D). FlowJo® software was used to quantify cell populations from human SVCs, which were gated according to Figure IV-2. As shown, after selecting for single cells, excluding debris, and selecting live cells, T cells ($CD45^{+}CD3^{+}$), macrophages ($CD45^{+}CD64^{+}CD206^{+}$), and dendritic cells (DC; $CD45^{-}CD64^{-}CD11c^{+}$) were gated off of $CD45^{+}$ total immune cells. Endothelial cells (EC; $CD45^{-}CD34^{+}CD31^{+}$) and preadipocytes ($CD45^{-}CD31^{-}CD29^{+}$) were selected from the $CD45^{-}$ non-hematopoeitic fraction. Given the variability in sample size obtained with the needle aspiration technique, all cell populations were normalized to the total number of live cells analyzed. The gating strategy is depicted in Figure IV-2.

Blood measurements. Plasma glucose (Thermo Scientific, Waltham, MA, USA), non-esterified fatty acid (Wako Chemicals USA, Richmond, VA, USA), triacylglyceride (Triacylglyceride reagent; Sigma Aldrich), and total- and high-density lipoprotein (HDL; Cholesterol E and HDL-Cholesterol E; Wako Chemicals USA) cholesterol concentrations were measured using commercially available colorimetric assay kits. Plasma insulin concentration was measured with a chemiluminescent immunoassay (Siemens IMMULITE 1000, Flanders NJ, USA). Matsuda insulin sensitivity index (ISI) was calculated as described by Matsuda & DeFronzo (13).

Statistics

Paired student's t-tests, were performed to assess differences between SED and EX. Two-way repeated measures ANOVAs (repeated for exercise and preadipocyte subtype) were used to assess differences in preadipocyte subpopulations, with Sidak's multiple comparison test used when required. Statistical significance was defined as $P<0.05$.

RESULTS

Baseline subject characteristics

Seven obese women and three obese men completed the study (Table IV-2). All subjects were regular exercisers (4 ± 1 sessions of moderate/vigorous exercise per week) in order to avoid the confounding influence of a novel exercise task on inflammation. Despite being regular exercisers, all subjects were classified having impaired glucose regulation/insulin resistance, based on their Matsuda ISI (14), which was measured after abstaining from exercise for three days (Table IV-2).

Exercise effects on fasting blood profile

Fasting plasma concentrations of non-esterified fatty acids, triglycerides, Total-, HDL-, and LDL cholesterol were not affected by the exercise session performed the previous day (SED vs. EX; Table IV-3). Similarly, fasting plasma glucose and insulin concentrations were nearly identical between EX and SED (Table IV-3). There was also no change in circulating cytokine concentrations of IL6 or TNFα (Figure IV-3).

Effects of exercise on stromal cell number

The exercise session (performed 12 hours before adipose tissue collection) did not affect the proportion of $CD45^{-}CD31^{+}CD34^{+}$ endothelial cells, total $CD45^{+}$ immune cells, or any of the other immune cell populations we measured (i.e. $CD45^{+}CD64^{-}CD11c^{+}$ dendritic cells, $CD45^{+}CD3^{+}$ T cells, and $CD45^{+}CD64^{+}CD206^{+}$ macrophages) (Figure IV-4). In contrast, exercise reduced the proportion of total preadipocytes in the SVC fraction (P = 0.04; Figure IV-5A).

We stratified preadipocytes into three subtypes according to CD34 and CD29 expression as previously outlined by Raajendiran et al. (5). In Figure IV-2D, we refer to these three populations as $CD34^{hi}$ ($CD29^{+}CD34^{hi}$), $CD34^{lo}$ ($CD29^{+}CD34^{lo}$), and $CD34^{-}$ ($CD29^{+}CD34^{-}$). These populations also express variable CD29 expression, with the $CD34^{-}$ population expressing the highest level of CD29 (Figure IV-2D). Interestingly, the reduction in the preadipocytes in the SVC appeared to be due to a reduction in the proportion of the $CD34^{hi}$ subtype (P=0.002), while $CD34^{-}$ and $CD34^{lo}$ preadipocytes were not different in SED vs. EX (Figure IV-4B). There was no effect of exercise on preadipocyte subtypes expressed as a proportion of total preadipocytes (P = 0.59). By t-test, there was a trend for $CD34^{hi}$ to decrease as a proportion of total preadipocytes (P = 0.08), and $CD34^{lo}$ preadipocytes increased (P = 0.04), while there was no change in $CD34^{-}$ preadipocytes relative to total SVC or preadipocytes.

Assessing the influence of blood contamination on stromal vascular cell quantification

It was important to establish the influence of blood contamination on our SVC quantification, because traces of blood are very common in the adipose tissue samples collected using the lipo-aspirate procedure. In Figure IV-6, panels A-F present whole blood stained with the same antibody panel as the adipose tissue SVC's. T cell (Figure IV-6B) and DC (Figure IV-6C) gating show considerable presence of blood cells, and therefore the quantification presented in Figure IV-4 should be considered to reflect adipose tissue T cell/DC numbers including local tissue blood cells. Despite this potential for blood contamination in the T cell and DC quantification, contamination was likely uniform in samples collected in the EX and SED visits, and therefore it likely doesn't affect the interpretation of our findings. There was no positive endothelial cell (Figure IV-6E) or preadipocyte (Figure IV-6F) staining on the whole blood control. Using an anti-CD206 antibody, we were able to identify adipose tissue-specific

macrophages. Figure IV-6H shows the CD206 FMO on SVC's confirming the presence of $CD206^{hi}$ and $CD206^{lo}$ macrophages. Figure IV-6C shows that there is a large population of blood cells that stain positive for CD64, a typical macrophage marker. Therefore, we relied on CD206 to exclude these potential contaminating blood cells (likely monocytes), because Figure IV-6D identifies the majority of these cells to be $CD206^{-}$. Figure IV-6H (CD206 FMO on SVCs) shows that the $CD206^{-}$ population of blood contamination was distinct from a population of $CD206^{lo}$ macrophages (which has been previously reported; (15)).

DISCUSSION

This is the first study to assess changes in stromal cell composition in human subcutaneous adipose tissue after an acute session of endurance-type exercise. A key finding of this study was that preadipocyte content in the SVC fraction of subcutaneous adipose tissue was reduced twelve hours after a session of exercise. Importantly, this reduction in preadipocyte content was driven by a reduction in $CD34^{hi}$ preadipocytes – a population of adipocyte precursor cells that has been linked to the formation of an adipocyte phenotype with elevated lipolytic rate (5). In contrast to these exercise induced changes in preadipocytes, there were no effects of acute exercise on total immune cell number, immune cell subtypes (macrophages, T cells, and dendritic cells), or endothelial cell number in subcutaneous adipose tissue. Therefore, these data suggest that a single session of exercise may provide a stimulus to remodel the preadipocyte pool within human subcutaneous adipose tissue, without altering immune cell or endothelial cell number 12h after exercise.

Preadipocytes are most often identified by the expression of CD34 (16), which is a transmembrane phosphoglycoprotein typically associated with hematopoietic stem/progenitor cells. However, CD34 expression is not exclusive to these cells and its function is not well-described beyond some role in cytoadhesion, proliferation, and differentiation (reviewed in (17)). Preadipocytes are now commonly described to express CD29, Sca-1, and CD24 (on Lin^{-} cells), with CD24 in particular linked to adipocyte commitment (18). The most reliable preadipcoyte cell surface markers remain unresolved, particularly in human adipose tissue, but CD34 (in combination with $CD45^{+}/CD31^{+}$ exclusion) is the primary marker used in most studies. Recently, Raajendiran et al. (5) isolated 3 distinct $CD45^{-}CD31^{-}CD29^{+}$ preadipocyte populations based on the abundance of CD34 ($CD34^{-}$, $CD34^{lo}$, $CD34^{hi}$), and reported these preadipocyte

subpopulations feature unique metabolic properties *ex vivo*. In particular, $CD34^{hi}$ preadipocytes differentiate into adipocytes with markedly elevated lipolytic rate, and high rates of lipolysis have been clearly linked with impaired insulin sensitivity (19,20). Along these lines, $CD34^{hi}$ preadipocytes are more prevalent in adipose SVCs from people with diabetes compared with non-diabetic controls (5). Our finding that exercise lowered the proportion of $CD34^{hi}$ cells in the SVC suggests that the proportion of preadipocyte subtypes in human subcutaneous adipose tissue is plastic, and exercise may lead to a shift towards a more favorable preadipocyte phenotype, primed to generate adipose tissue with a lower average lipolytic rate.

The session of exercise did not affect the relative abundance of $CD34^{-}$ cells, a subset of preadipocytes with high CD29 expression that that has been reported to generate beige-like adipocytes (5,21). It has been suggested that exercise may induce a beige-like phenotype in white adipose tissue via adrenergic signaling and myokine release from skeletal muscle (22). Our finding that exercise did not alter the abundance of $CD34^{-}$ ($CD29^{hi}$) preadipocytes could be interpreted to suggest that the exercise session did not remodel the preadipocyte pool towards beige-like precursors, which is consistent with several studies indicating that exercise training does not induce a beige-like phenotype within subcutaneous adipose tissue (23–25). Tsiloulas et al. (23) surmised that insufficient $CD29^{+}$ precursors could explain their observation that exercise training did not induce "beiging" within subcutaneous abdominal adipose tissue from obese subjects - although they did not assess $CD29^{+}$ progenitor content in their study. The identification of $CD34^{-}$ ($CD29^{hi}$) preadipocytes as about one third of total preadipocytes in our cohort of obese regular exercisers suggests that the presence of $CD29^{+}$ preadipocytes in human subcutaneous adipose tissue may not be a limiting factor for the beiging potential of exercise in healthy obese adults. However, longer-term exercise training studies would be required to ascertain whether regular exercise alters the $CD34^{-}CD29^{hi}$ preadipocyte pool thereby creating an environment with higher capacity for beiging.

Adipose tissue is a primary source of circulating inflammatory factors in obesity (26–28), but the effects of acute exercise on changes in adipose tissue immune cell composition have not been directly measured. Using transcriptomic analysis, Fabre et al. reported an increased expression of macrophage genes in human subcutaneous adipose tissue from previously untrained lean adults 4 h after a single session of exercise (29). In contrast, using immunofluorescence, MacPherson et al. (30) found reduced $F4/80^{+}CD11c^{+}$ cells (representing pro-inflammatory macrophages) in

inguinal white adipose tissue from HFD mice two hours after completing a two hour treadmill exercise session. Unfortunately, neither of these methodologies directly quantifies macrophage number from the adipose tissue, so the phenotype of adipose tissue macrophages cannot be determined from these studies. Our study is the first work to our knowledge to quantify adipose tissue macrophage content after acute exercise in subcutaneous adipose tissue from human subjects using flow cytometry. Contrary to our hypothesis, we found no change in macrophage number 12 hours after a session of exercise in this obese cohort. It is possible that an exercise-induced change in adipose tissue macrophage number is transient, and we may have missed this change in our samples collected 12 hours after exercise. It is also possible that acute exercise may not change macrophage number, but may modify the macrophage phenotype instead, consistent with the gene expression-level changes observed by Fabre et al. (29). In attempt to stratify macrophage subtypes, we used surface markers CD11c and CD206, but we were unable to achieve consistent separation of macrophage subtypes between cytometer runs. As well as being unable to quantify macrophage subtypes, we observed that most macrophages were $CD11c^{+}CD206^{+}$, which is in contrast with some previous studies assessing human subcutaneous adipose tissue macrophages (15); therefore, further clarification on the response of different macrophage subtypes to exercise needed.

To assess the ability of exercise to signal cellular remodeling of the broader adipose tissue immune environment, we also quantified dendritic cell and T cell content. While T cells (in particular TRegs and Th2 cells) are important for maintaining adipose tissue health in lean subjects, T cell accumulation in adipose tissue has been shown to precede macrophage infiltration; indicating that these cells are an important player in the early adipose tissue immune response. Furthermore, there is some data linking $CD11c^{-}$expressing adipose tissue DC's to immune cell recruitment, and specifically to T cell phenotype (Th17 vs. Th1 polarization; (31)). However, there are not much data assessing the contribution of DC's identified by markers truly distinguishing them from adipose tissue macrophages, as typical DC markers share overlap with macrophages and other cells (32). Using the general T cell marker CD3, and a specific DC marker $CD64^{-}CD11c^{+}$ (33), we found that total T cell and DC numbers did not change 12h after exercise. Similar to adipose tissue macrophages, this does not preclude the possibility that sampling 12 hours after the exercise session omits changes that may have occurred earlier (or later); or that exercise induces a phenotypic shift within these cell populations. Furthermore,

given the importance of these immune cell populations in the response to adipocyte hypertrophy, the effects of exercise on these cell populations may only be apparent during periods when adipose tissue is undergoing dynamic change (i.e., periods of weight gain or weight loss). For example, Kawanishi et al. (2010) reported that mice that exercised while actively gaining weight on a high fat diet (HFD) were largely protected from the large increase in inflammatory cytokines and markers of pro-inflammatory macrophage infiltration commonly found in adipose tissue from sedentary mice that gained the same amount of weight on the HFD.

Previous work from our lab and others (9,34) suggests that exercise may augment subcutaneous adipose tissue angiogenesis, a process that is required for effective adipose tissue remodeling. Because endothelial cells are central to the process of angiogenesis, we hypothesized that exercise would increase the abundance of these cells in adipose tissue. Contrary to this hypothesis, we did not detect a measurable increase in endothelial cell number in adipose tissue collected 12 hours after exercise. However, based on evidence that 12 weeks of exercise training increased adipose tissue capillarization (Walton, et al), along with cross-sectional findings from our lab reporting elevated expression of CD31 in regular exercisers compared with sedentary control subjects, we contend it may take longer to detect changes in endothelial cell number.

Among the limitations to this study are that we did not power the study to explore sex differences, and we were unable to assess depot differences. While differences in adipose tissue metabolism are known to exist between men and women, we anticipate that these sex related differences may be rather subtle compared with the robust effects of exercise on our measures. In addition, because we were interested here in studying exercise-mediated signals within *subcutaneous* adipose tissue after each exercise session in order to assess the potential for exercise to improve the capacity for lipid storage within this depot, our findings may not translated to responses in other adipose tissue depots (e.g. visceral or gluteofemoral adipose tissue). While we did not find a change in immune or endothelial cell content, it remains possible that these cell populations may change earlier after exercise than we measured, or that the exercise-induced signals related to inflammation and angiogenesis might be more potent in a less healthy population that the participants in our study. While our experiments do not identify a specific mechanism for the reduction in preadipocytes, the preferential reduction in $CD34^{hi}$ preadipocytes suggests future work should continue to explore these three preadipocyte subtypes

($CD34^{hi}$, $CD34^{lo}$, and $CD34^{-}$) to measure transcriptional/function changes related to differentiation or proliferation. This may be important in the quest to understand how exercise can regulate preadipocyte function as well as to identify pathways for the independent regulation of these progenitor subtypes.

The most novel finding from these experiments was the exercise-induced reduction in preadipocyte number, and this was achieved by a reduction in the abundance of $CD34^{hi}$ preadipocytes, which in turn differentiate into mature adipocytes with high lipolytic rates. Given that high adipose tissue lipolytic rate is linked to insulin resistance (19,35), this phenotype could lead to improved adipose tissue and whole body metabolism. Our finding that there was no change in immune cell, macrophage, T cell, or dendritic cell content in this cohort of obese, regular exercisers suggests that immune cell number is unchanged 12h after exercise in obese regular exercisers. Furthermore, the lack of change in endothelial cell number 12 h after the endurance-type exercise session likely indicates that adipose tissue angiogenesis takes several repeated exercise exposures to accrue. Overall, these data suggest the rapid effects of exercise on adipose tissue stromal cell number feature a remodeling of the preadipocyte pool that could lead to improved adipose tissue lipolytic rate, thereby improving tissue and systemic insulin sensitivity.

ACKNOWLEDGEMENTS

This project was supported by NIH R01#DK077966 and CIHR DFS #0077000623. I am thankful to Emily Krueger, Toree Baldwin, Michael Schleh, Lindsey Muir, Cara Porsche, Benjamin Ryan, Thomas Rode, Michelle Aube, Kanakadurga Singer, and Carey Lumeng for their intellectual and technical contributions to these experiments. This work was possible through use of the University of Michigan Flow Cytometry Core. Additional thanks to Suzette Howton for subject recruitment and coordination.

FIGURES

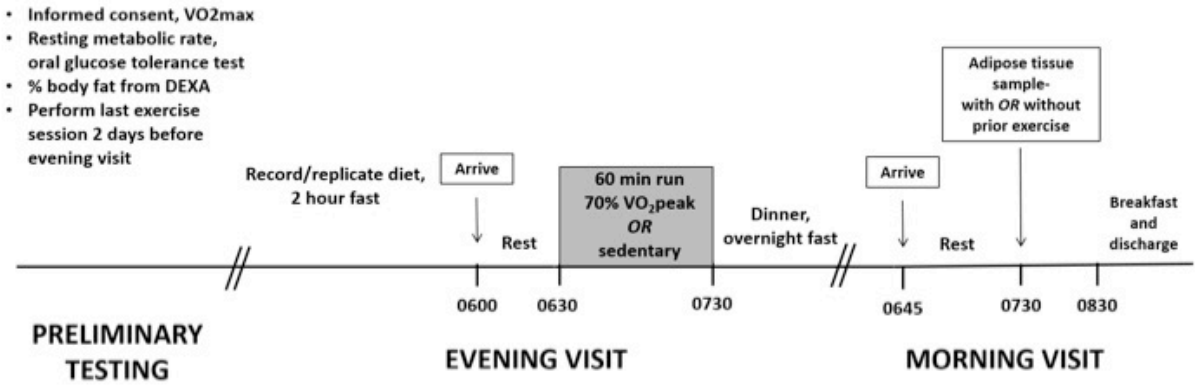

Figure IV-1 Experimental Design.

All participants completed an evening and morning visit for both exercise and sedentary control collections, in randomized order. DEXA: dual-energy X-ray absorptiometry.

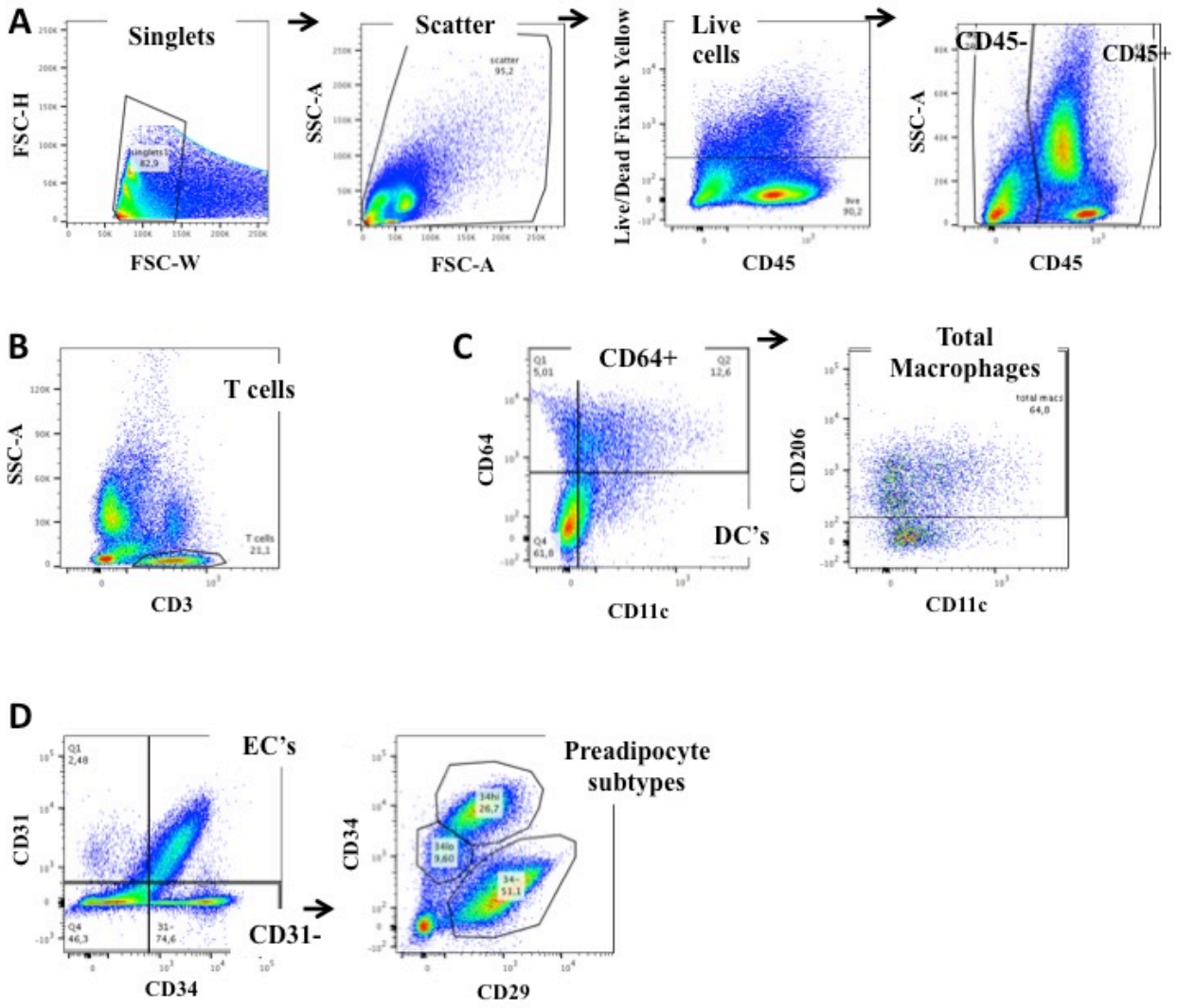

Figure IV-2 Representative flow cytometry gating scheme.

A) CD45+/- cell populations were gated off of single cells→scatter→live cell selection. *From CD45+ (immune cells)*: CD3+ T cell selection is shown (2B); as well as total macrophages, CD64+ with the addition of a subsequent CD206- exclusion (2C). *From CD45- (non-immune cells)*: EC's were selected as CD31+CD34+. Preadipocyte subtypes were gated off of the CD31- selection, based on CD34 and CD29 expression (2D). DC: dendritic cells; EC: endothelial cells.

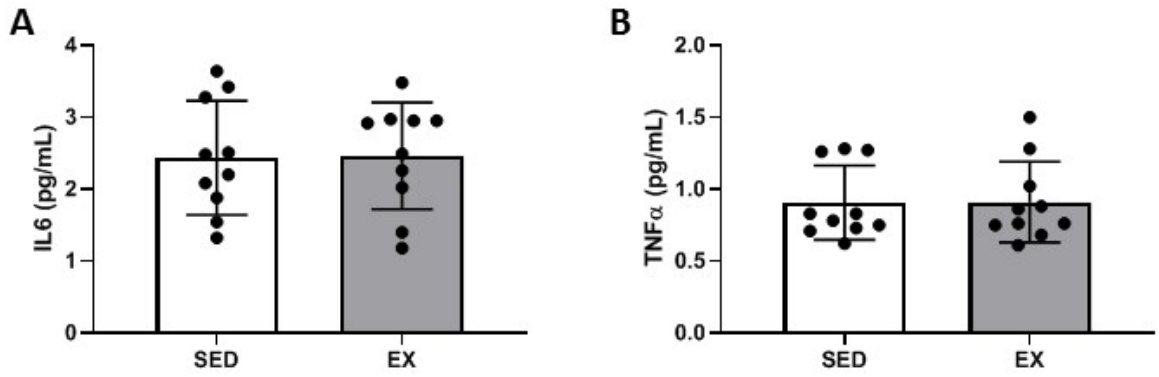

Figure IV-3 Plasma cytokine concentrations.

There was no change in circulating plasma cytokine concentrations of IL6 (P = 0.86; A) or TNFα (P = 0.91; B). N = 10. Data are Mean ± SD.

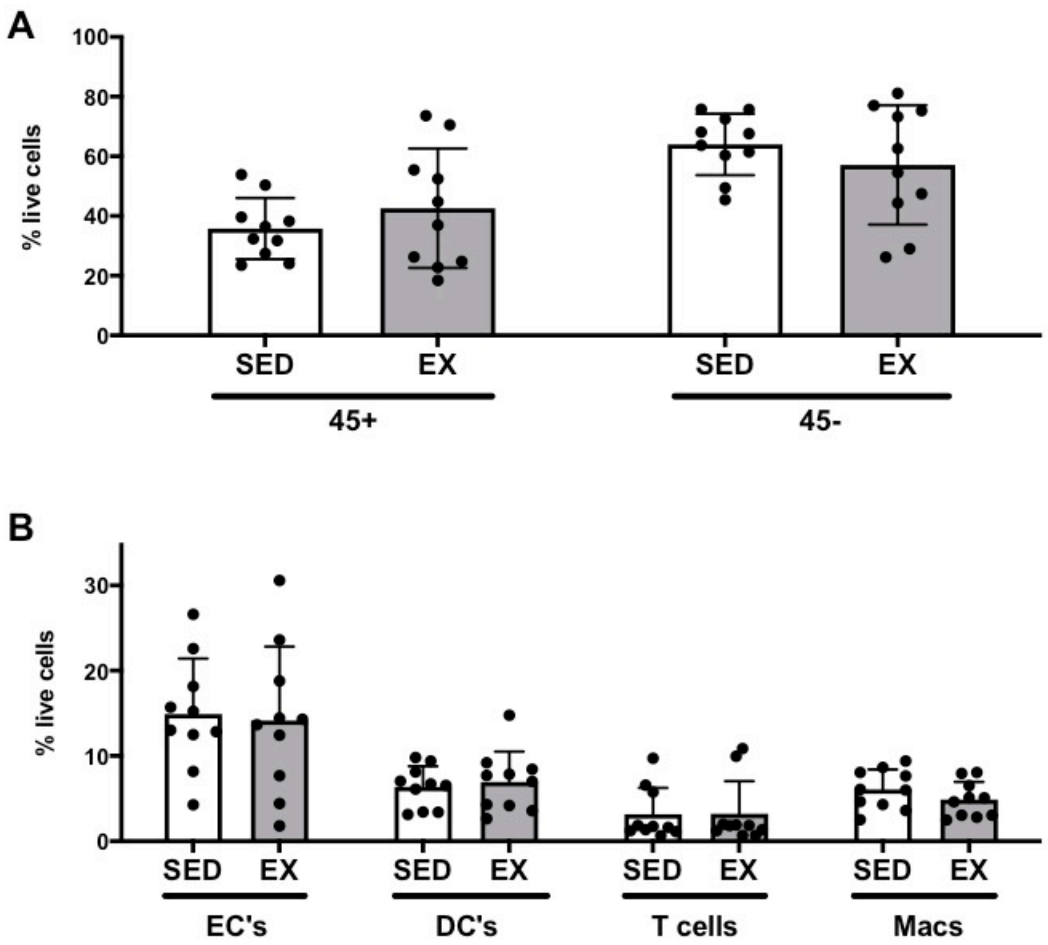

Figure IV-4 Stromal vascular cell content of adipose tissue samples following SED and EX visits.

(A) Immune cells as CD45+ and non-immune cells as CD45-; (B) Subsets selected from CD45+ or CD45- parent populations. SVC: stromal vascular cells; EC: endothelial cells; DC: dendritic cells; Macs: macrophages. All cell populations are represented as % SVC per that sample. N = 10. Data are Mean ± SD.

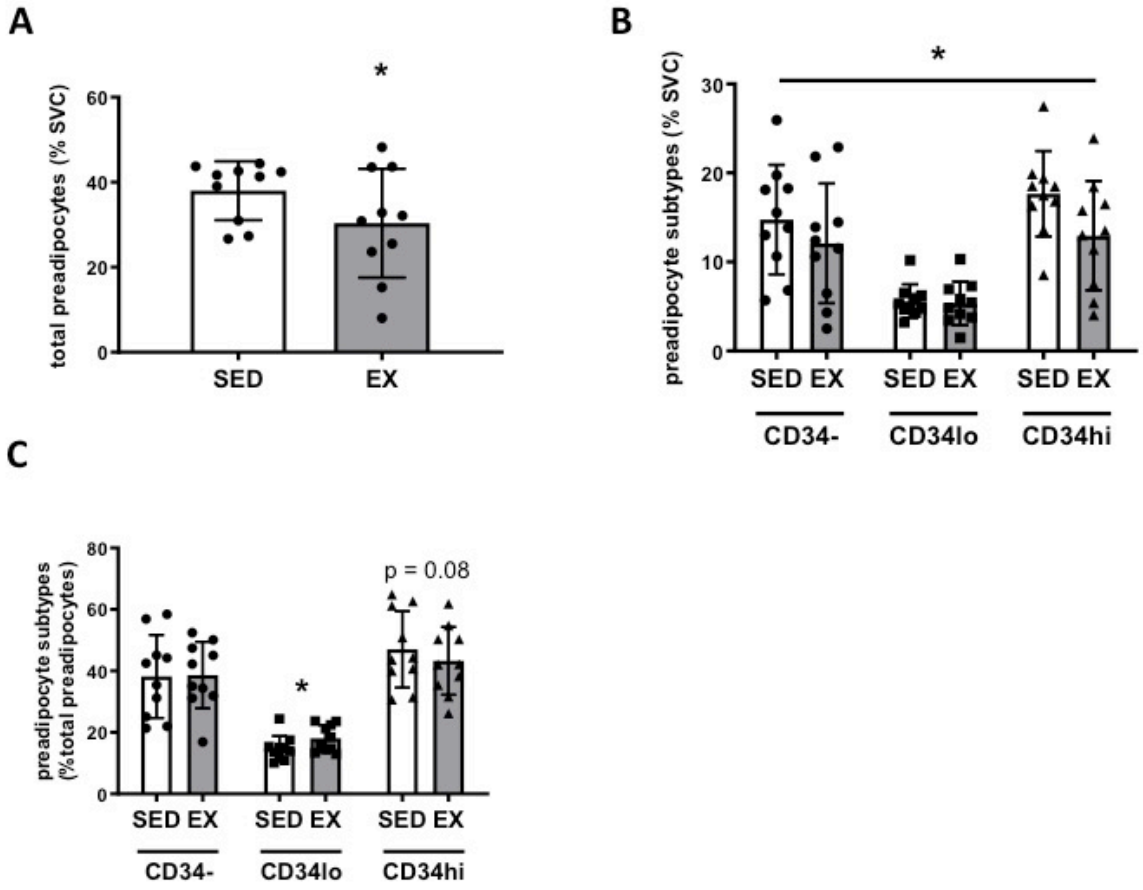

Figure IV-5 Preadipocyte phenotype.

SVC: stromal vascular cells. (A) Total preadipocytes in the stromalvascular fraction decreased in EX (P = 0.04). (B) CD34hi preadipocytes decreased as % SVC (P = 0.002; interaction between exercise and preadipocyte subtype P = 0.046). (C) Relative to total preadipocyte content: CD34hi preadipocytes trended to increase in EX (P = 0.08), CD34lo preadipocytes decreased (P = 0.04), and CD34- preadipocytes did not change (P = 0.86). N = 10. Data are Mean ± SD.

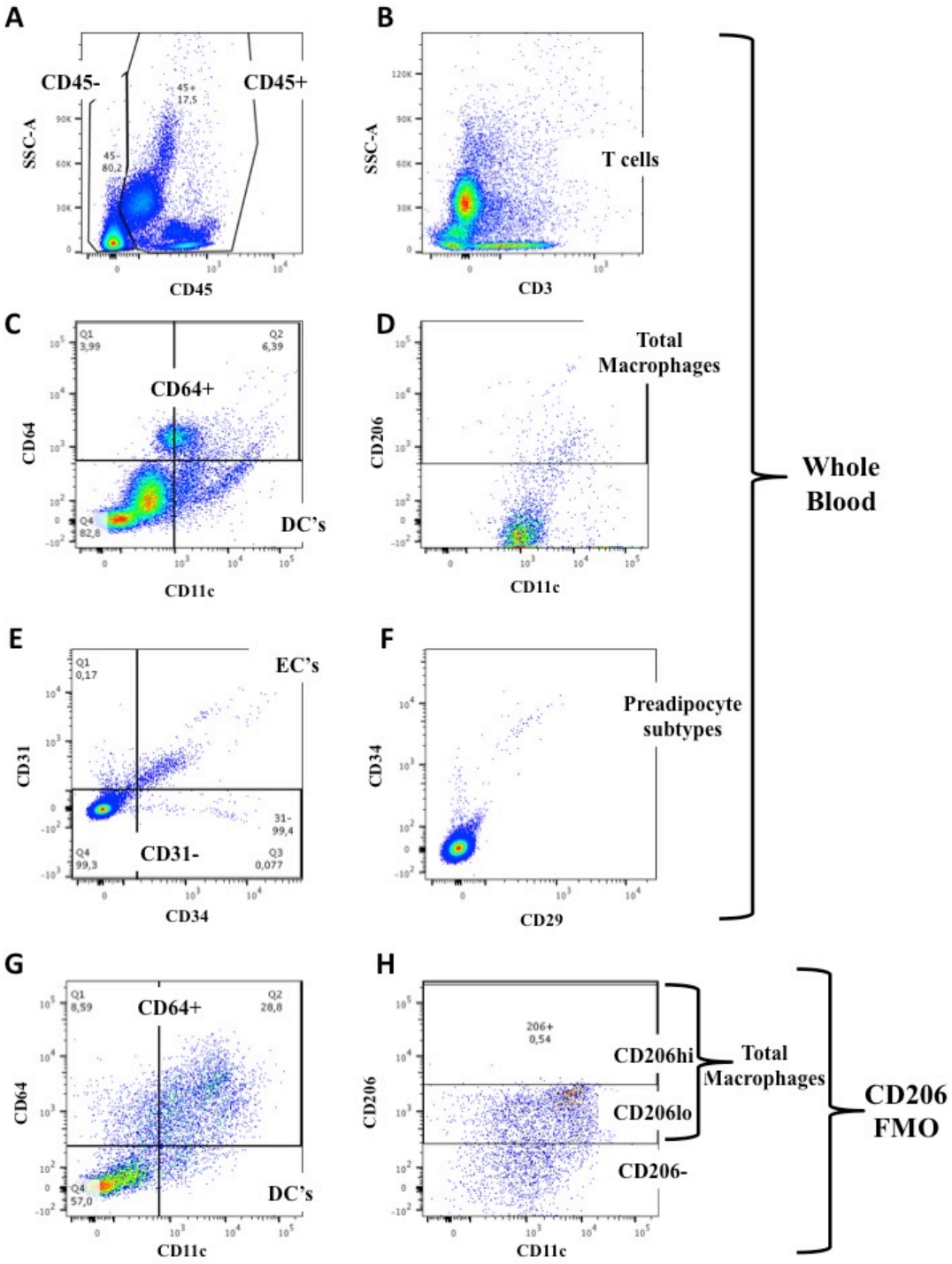

Figure IV-6 Assessment of the influence of blood contamination in SVC quantification.

(A-F) Whole blood control to assess the presence of blood cells within tissue SVC gating. (G-H) CD206-based selection of a total macrophage population clean from blood cells (blood sample with same gating in 6D). All plots were gated off of singlets, scatter, and live cell gating similar to Figure IV-2.

TABLES

Table IV-1 Flow cytometry antibodies

Marker	Color	Clone	Supplier
Live/Dead	Live/Dead Fix Yellow	N/A	Thermo Fisher Scientific L34967
CD45	e450	HI30	eBiosciences 48-0459-41
CD64	APC	10.1.1	BioLegend 305013
CD34	Percp-Cy5.5	581	BioLegend 353521
CD31	APC-Cy7	WM59	BioLegend 303119
CD11c	PE-Cy7	3.9	BioLegend 301608
CD29	PE	TS2/16	BioLegend 303004
CD3	FITC	OKT3	BioLegend 317305
CD206	BV650	19.2	BD Optibuild 740598
Trustain human FC block	-	-	Biolegend 422301

Table IV-2 Baseline characteristics

Age (years)	26 ± 5
Body mass (kg)	96 ± 11
BMI (kg/m^2)	33 ± 3
% Body Fat (DEXA)	41 ± 7
Fat mass (kg)	39 ± 7
Fat free mass (kg)	56 ± 7
VO_{2peak} (L/min)	3.0 ± 0.5
Matsuda ISI	4.1 ± 1.4

Baseline data collected during screening visits. n = 10. Data are Mean ± SD.

Table IV-3 Exercise effects on fasting blood profile

	SED	EX	P
NEFA (mg/dL)	344 ± 70	346 ± 71	0.97
Triglycerides (mg/dL)	82 ± 40	66 ± 25	0.30
Total Cholesterol (mg/dL)	145 ± 27	137 ± 29	0.10
HDL Cholesterol (mg/dL)	36 ± 13	34 ± 9	0.27
LDL Cholesterol (mg/dL)	109 ± 26	101 ± 24	0.21
Fasting glucose (mg/dL)	78 ± 10	79 ± 10	0.76
Fasting insulin (uIU/mL)	12 ± 5	11 ± 6	0.90

NEFA: non-esterified fatty acids; HDL: high density lipoprotein; LDL: low density lipoprotein. n = 10. Data are Mean ± SD.

Chapter V. Project 3
Effects of Habitual Exercise on Adipose Tissue Responses to Overeating

ABSTRACT

Overeating and the resultant weight gain have been linked to the ectopic lipid deposition and inflammation that underlie many obesity-related diseases. Effective storage of excess energy in subcutaneous adipose tissue during periods of overeating may help reduce weight-gain-related insulin resistance. Furthermore, exercise can alter the expression of genes involved in regulating adipose tissue storage capacity. The aim of this study was to assess changes in the expression of factors regulating adipose tissue storage capacity and inflammation in response to a brief exposure of overeating in non-obese adults who are either regular exercisers (EX) or non-exercisers (nonEX). Eleven EX and 11 nonEX who were well matched for BMI (22 ± 2 vs. 23 ± 3 kg/m^2) ate 30% above their estimated daily energy requirements for one week. Fasting blood and abdominal subcutaneous adipose tissue samples were collected before and after the overeating intervention. Both EX and nonEX gained ~1 kg ($P<0.01$), and Matsuda ISI was reduced ~15% in both groups ($P=0.04$), with no difference in the response to overeating between EX and nonEX. Similarly, gene expression of factors involved in lipid metabolism (HSL, ATGL, DGAT, PPARγ) and angiogenesis (HIF1α, KDR) were increased ($P<0.05$), with no differences observed between EX and nonEX. The modest overeating stimulus did not increase markers of inflammation in the systemic circulation (plasma C-reactive protein; $P = 0.30$) or adipose tissue (pERK/ERKtot $P = 0.33$; MCP-1 $P=0.85$). Overall our findings indicate that short exposure to a modest overeating stimulus can impair insulin sensitivity and upregulate genes involved in regulating adipose tissue storage capacity, with no major differences in responses between exercisers and non-exercisers in the early stages of weight gain.

INTRODUCTION

Obesity afflicts over one third of Americans, and is a leading cause of insulin resistance and the associated comorbidities (1,2). Obesity typically develops over months and years, as a result of episodic overeating (i.e., energy intake > energy expenditure), which requires adipose tissue to expand considerably in order to store the excess energy as triglycerides within the adipocytes. Unfortunately, with excessive weight gain, the capacity of adipose tissue to expand effectively/healthfully is often surpassed, which can lead to pathological features within the tissue, including hypoxia and fibrosis (3). Therefore, understanding the regulation of the processes involved in enhancing adipose tissue storage capacity during overeating is a crucial step for developing targeted therapies for adipose tissue (and systemic) insulin resistance. Exercise is known to rapidly improve systemic insulin resistance, but its effects on adipose tissue are not well explored. Understanding the effects of exercise on factors regulating adipose tissue storage capacity during episodes of overeating could reveal new mechanisms for improving metabolic health in obesity.

Healthy adipose tissue expansion requires several remodeling processes including adipogenesis (the formation of new adipocytes), angiogenesis (the formation of new blood vessels) and extracellular matrix (ECM) remodeling. Increased adipogenesis is thought to support healthier adipose tissue expansion by providing more small adipocytes for storing excess energy, which may attenuate the hypoxia that can result from extensive adipocyte hypertrophy (4). Similarly, it has been proposed that adipose tissue vascularity in obesity may be insufficient to provide oxygen to the hypertrophic adipocytes (5), and interventions designed to increase adipose tissue angiogenesis have been found to improve systemic glucose metabolism in mice (6–8). Furthermore, overexpression of HIF1α (the master regulator of hypoxic signaling) in mice triggers dramatic ECM fibrosis and inflammation (9). Chronic low-grade inflammation is a hallmark of obese adipose tissue, and can directly impair local and systemic insulin resistance by inhibiting insulin signal transduction. Immune cell expansion within adipose tissue can develop within days in mice on a high fat diet (10), though the onset of inflammation during weight gain in humans is not well established. Together, better understanding the regulation of key factors linked to enhancing adipose tissue storage capacity (e.g., angiogenesis, ECM remodeling, and

inflammation) in response to overeating, could identify mechanisms to improve healthy adipose tissue expansion and mitigate the negative consequences of weight gain and obesity.

Exercise can alter the expression of genes that have been shown to increase adipogenesis, angiogenesis, and ECM remodeling (11–14), suggesting that exercise may trigger events that could lead to enhanced storage capacity in adipose tissue. In fact, exercise training studies in mice have demonstrated animals that exercise while gaining weight on a high fat diet were protected from adipose tissue fibrosis and inflammation, compared with sedentary mice that gained the same amount of body fat on the same high fat diet (12,15). There is also evidence that exercise training can trigger adipose tissue angiogenesis in humans (16). Importantly, to test the effects of exercise on factors regulating adipose tissue storage capacity it is best to conduct longitudinal experiments while adipose tissue is stimulated to expand (i.e., during periods of sustained overeating). This project sought to determine the effects of exercise on factors related to adipose tissue storage capacity (e.g. angiogenesis, ECM remodeling, immune response) in response to one-week of overeating. Our hypothesis was that brief overeating would trigger factors regulating adipose tissue storage capacity, and that the response would be enhanced in regular exercisers.

METHODS

Subjects

We recruited two cohorts of health adults; one group of regular exercisers (EX; a least 4 days/wk of ≥30 min aerobic exercise of moderate-vigorous intensity for ≥6 months) and one group of non-exercisers (nonEX; no regularly planned exercise for at least 6 months). In total, 11 EX and 11 nonEX completed the study and the groups were well matched for body mass index (BMI; 20-30 m/kg^2). All subjects were non-smokers and weight-stable (±3 kg for at least 6 months). Exclusion criteria included blood pressure > 140/90 mmHg, history of cardiovascular or metabolic disease, or regular use of medications known to affect metabolism. The study protocol was approved by the University of Michigan Institutional Review Board.

Preliminary testing

Preliminary testing included measurement of weight, height, blood pressure, and peak oxygen consumption (VO_2peak) to assess aerobic capacity/fitness. VO_2peak was determined using a graded exercise test to exhaustion on either a stationary bike or treadmill, beginning with a 4-minute warm up, followed by an increasing workload every 1-2 minutes until volitional fatigue.

Experimental protocol

Experimental visit. Subjects completed two experimental visits; one immediately before (Pre) and another immediately after (Post) the one-week overeating intervention. The study design is depicted in Figure V-1. The evening before the experimental trial, EX completed an exercise session at 1630h (45 min at ~65% VO_2peak, monitored by heart rate). All subjects were provided with strict guidelines for dinner to ensure standard macronutrient composition (33% of daily energy expenditure; 55% carbohydrate, 30% fat, 15% protein). This meal was consumed by 2100h, after which subjects fasted until arriving for their experimental trial the next morning.

Subjects arrived to the laboratory at 0700h the next morning, at which time, body weight and resting blood pressure were collected, and an intravenous catheter was inserted for blood sampling. Then an abdominal subcutaneous adipose tissue sample was obtained by needle aspiration at 0800h (details of adipose tissue biopsy procedure are provided in Appendix A – and details of adipose tissue processing are provided below). Subjects then completed an oral glucose tolerance test (OGTT), with blood samples collected every 15 min for 2 hours after drinking a 75g dextrose drink (Azer Scientific). The Post overeating experimental trial was identical to the Pre trial.

Overeating intervention. For one week, subjects overate ~30% excess calories per day above their estimated daily energy expenditure based on fat free mass from underwater weighing: [{370 + (21.6 x fat free mass)} x 1.5] x 1.3 (17). To achieve this daily energy surplus, subjects consumed their normal diets to reach energy balance requirements, and supplemental calories were provided in the form of Boost Plus® (50% carbohydrate, 35% fat, and 15% protein) or other snacks with the same macronutrient composition if participants had dietary restrictions that precluded the use of Boost Plus®. Diet and exercise were monitored daily using MyFitnessPal and subjects also reported daily to a study team member: (1) consumption of their supplemental

calories; (2) detailed exercise information, and (3) body weight, taken at the same time each day. Importantly, EX were required to eat more than nonEX (i.e. to replace energy expended during exercise) in order for both groups to be in 30% caloric excess each day. On the final evening of the overeating intervention (the night before the "Post" trial), subjects consumed the same meal for dinner that they consumed the evening before the "Pre" trial.

Analytical procedures

Adipose tissue processing. Adipose tissue biopsies were immediately saline-rinsed, and divided for analysis. Approximately 300 mg was flash frozen for RNA and protein analysis. The remaining ~1-1.5 g was immediately digested in collagenase for separation of the SVCs and mature adipocytes; full protocol in Appendix E. Mature adipocytes were washed and allocated for *ex vivo* lipolysis (see below).

Lipolysis assay. An *ex vivo* lipolysis assay was performed on freshly extracted cells to assess basal and stimulated lipolytic rates of isolated mature adipocytes (200μL per well). Samples were incubated for two hours (rocking at 37 °C) in Krebs-Ringer Bicarbonate Buffer + 4% BSA, 5mM glucose, 200 nM adenosine, 20nM 2-phenylisopropyl adenosine, and 1U/mL adenosine deaminase in a sterile 96-well plate. Stimulated samples were also exposed to: $1x10^{-8}$ mM isoproterenol and $1x10^{-6}$ mM isoproterenol during this incubation. Immediately after the 2-hour incubation, the assay plate was placed on ice to arrest lipolysis, and media was collected to determine lipolytic rate as [glycerol] by colorimetric assay (Sigma Free Glycerol Reagent).

Adipose tissue mRNA expression. Gene expression was measured using qPCR (full protocol in Appendix F). Briefly, RNA was isolated by chloroform separation following homogenization in 1 mL RNA Stat-60 (Tel-Test Inc., Friendswood, TX). Reverse transcription was performed with 200 ng RNA input, using Life Technologies reverse transcriptase (4368813, Life Technologies, Grand Island, NY). Predesigned primer and probe sequences were purchased from IDT PrimeTime qPCR Assays and are listed in Table V-1. The qPCR data was normalized to expression of 2 housekeeping genes (peptidylprolyl isomerase A (PPIA) and beta-2-microglobulin (B2M)) using the -ΔCt method (18) and expressed as fold induction ($2^{-\Delta\Delta Ct}$) of mRNA expression compared with before overeating.

Western blotting. Western blotting was performed to assess protein content of a subset of genes whose expression was found to change using qPCR. Protein content was measured by loading 15-20 ug protein from subcutaneous adipose tissue homogenate (full details in Appendix G). All nitrocellulose membranes were stained with Memcode Reversible Protein Stain (ThermoScientific cat 24580) after transfer, and this total protein stain was quantified by AlphaView and used as a loading control in our quantification of protein abundance. Primary antibodies were purchased from Cell Signaling and incubated overnight. As noted above, protein content (AU) was normalized to total protein content from that subject's lane (Memcode) to correct for variability in loading, as well as an internal standard (pooled adipose tissue homogenate) that was loaded into each gel to correct for differences in running and transferring when multiple membranes were combined.

Plasma/serum concentration measurements. Blood samples were centrifuged at 2000rpm at 4^{o}C for 15 minutes and stored at -80 °C until analysis; serum samples were left to clot at room temperature for 30 min before centrifugation. Plasma glucose (Thermo Scientific, Waltham, MA, USA), fatty acid (Wako Chemicals USA, Richmond, VA, USA), triacylglyceride (Triacylglyceride reagent; Sigma Aldrich), and total- and high-density lipoprotein (HDL; Cholesterol E and HDL-Cholesterol E;Wako Chemicals USA) concentrations were measured using commercially available colorimetric assay kits. Serum insulin concentration was measured with a chemiluminescent immunoassay (Siemens IMMULITE 1000, Flanders NJ, USA). Plasma C-reactive protein was measured by a high-sensitivity ELISA (Calbiotech, CR120C). A panel of circulating inflammatory markers (IFN-γ, IL-10, IL-13, IL1Rα, IL-1α, IL-1β, IL-6, IL-8, MCP-1, TNFα, IL-4, VEGF) was measured by multiplex (Luminex L200, Luminex, Austin, TX, USA) using a kit purchased from Millipore (#HCVD3-67CK, Milliplex MAP Kit, Millipore, Billerica, MA, USA).

Calculations

Glucose and insulin concentrations during the OGTT were used to calculate insulin sensitivity using the Matsuda Insulin Sensitivity Index (ISI) (19).

Statistical analysis

A student's t-test was used to determine baseline differences between EX and nonEX. A 2-way mixed model ANOVA (overeating x exercise) was used to assess the response to overeating within, and between the groups. A P-value of < 0.05 was considered statistically significant.

RESULTS

Baseline subject characteristics

As designed, EX and nonEX were well matched for age, body weight, and BMI (Table V-2). Also, as anticipated, VO_2peak was nearly 25% greater in EX vs. nonEX ($p = 0.03$; Table V-2), reflecting the expected enhanced aerobic capacity/fitness in EX. Baseline insulin sensitivity (as assessed by the Matsuda ISI) was greater in EX vs. nonEX ($p = 0.01$; Table V-2), and there was a trend for fasting plasma triglyceride concentrations to be higher in nonEX vs. EX ($p = 0.06$; Table V-2) but all other baseline blood lipid measures were similar between groups (Table V-2).

Whole-body metabolic responses to overeating

After our one-week overeating intervention, body weight increased by ~1 kg in both EX (75.1 ± 10 to 75.9 ± 11 kg) and nonEX (75.0 ± 16 to 75.9 ± 16 kg) (both $p < 0.01$). Importantly, weight gain was identical between groups ($p = 0.99$). Matsuda ISI was reduced by ~10% after overeating ($p = 0.04$), and this impairment in insulin sensitivity was similar between groups (Figure V-2). The one-week overeating intervention did not significantly alter any of the measured blood lipid markers or C-reactive protein in either group (Table V-3).

Adipose tissue responses to overeating

Adipocyte size, lipolysis, and inflammation. The very modest (~1 kg) weight gain from the one-week overeating intervention did not translate to a measurable increase in average adipocyte area in either EX (4268 ± 1252 to 4346 ± 1178 μm^2) or nonEX (5078 ± 1251 to 5284 ± 1873 μm^2). Overeating also did not alter basal or stimulated *ex vivo* lipolytic rate in isolated adipocytes in either group (Figure V-3), suggesting our overeating intervention did not impact the primary function of adipocytes. The one-week overeating intervention did not appear to affect a measure of tissue inflammatory status, ERK phosphorylation (Figure V-4). Unfortunately, 9 of the 10 cytokines measured by Luminex (see METHODS) were not detectable in the healthy subjects

enrolled in this study. MCP-1 was the only measureable cytokine, and it was not affected by overeating in either group ($P \geq 0.85$; data not shown).

Factors regulating adipose tissue metabolism and remodeling. In agreement with our *ex vivo* adipocyte lipolytic measurements, overeating did not alter the protein abundance or phosphorylation state of factors regulating lipolysis or esterification (Figure V-4). There was a significant main effect for the abundance of HSL and ATGL between EX and nonEX ($P < 0.05$; Figure V-4), but again this did not translate to differences in lipolysis (Figure V-3).

In contrast to protein abundance measures, the mRNA expression of several key factors regulating lipolysis and lipid storage (Figure V-5A) as well as angiogenesis (Figure V-5B) were upregulated after overeating. This suggests that the overeating stimulus triggered signals to augment these processes, but the stimulus may not have been robust enough (or long-lasting enough) to translate to a measurable increase at the protein level. Unlike the increased gene expression of lipid metabolism and angiogenic factors, mRNA expression of some of the important factors involved in ECM remodeling did not change (Figure V-5C). Contrary to our hypothesis, we also did not observe any measurable differences in gene expression in response to overeating between EX and nonEX.

DISCUSSION

Major findings from our study indicate that even a modest overeating stimulus can impair insulin sensitivity after one week in healthy adults, and regular exercise did not protect against this rapid maladaptive response to overeating. In contrast to the decline in insulin sensitivity, overeating did not significantly affect blood lipid profile, adipocyte lipolysis, or markers of inflammation in adipose tissue or plasma. Interestingly, overeating did increase gene expression for factors regulating lipid metabolism and angiogenesis in adipose tissue, but this did not evoke changes in the abundance of their respective proteins. Therefore, while systemic insulin sensitivity may decline rapidly after even mild overeating, it may take a more robust overeating stimulus (duration of overeating and/or magnitude of weight gain) for other clinical and subclinical measures to respond.

Overeating can rapidly impact key markers of metabolic health (20–23). Our finding that insulin sensitivity was impaired after just one week of overeating aligns with previous work demonstrating a relatively rapid decline in insulin sensitivity with overeating (20,24–27). The mechanism(s) underlying the rapid reduction in insulin sensitivity with overeating are not clear, but may be due to several factors, including: oxidative stress (24), ectopic lipid deposition (liver, visceral adipose tissue; (28)), and tissue and/or systemic inflammation (10). It has been suggested that regular exercise may help protect against the insulin resistance that often accompanies overeating (25,27). For example, Walhin et al. (25) reported that in subjects required to overeat 50% more than their calculated energy needs for 1 week, glucose tolerance was impaired in those who reduced their daily physical activity to low levels (<4000 steps/day), but not in subjects who remained physically active. In contrast, here we found insulin sensitivity declined similarly in regular exercisers and non-exercisers. This discrepancy may be due in part to the relatively modest overeating stimulus employed in our study (30%) compared with previous studies (≥50%). Perhaps even more notable, in previous studies (25,27), subjects who exercised while overeating gained a bit less weight or body fat during the intervention than those who remained sedentary, and this difference in body weight/fat gain could have a profound impact on their metabolic outcomes. In our study, exercisers and non-exercisers were tightly matched for weight gain during our intervention, suggesting that when controlling for weight gain, exercise may not provide additional protection against systemic insulin resistance in response to brief exposure to overeating. Furthermore, the "inactive" groups in previous studies (25,27) were required to markedly reduce their habitual physical activity behaviour *in addition to* overeating, and this simultaneous change confounds the interpretation of their findings - whereas here we assessed the effects of maintained habitual physical activity status in our subject.

During periods of overeating and weight gain, the vast majority of the excess energy is stored in adipocytes in the adipose tissue. Correspondingly, weight gain can increase the abundance of factors regulating lipolysis and lipid storage in the expanding subcutaneous adipose tissue (29). For example, overfeeding studies have reported changes in proteins involved in regulating adipose tissue esterification (DGAT2) and lipolysis (pHSL, PLIN, ATGL) after 8 weeks of weight gain in mice and humans (30,31). Our observation that the gene expression of many of these same factors were increased after only one week of overeating suggests that the signaling events triggering these adaptive responses in adipose tissue occur rather quickly in response to an

energy surplus. We surmise that the lack of change in the abundance of corresponding proteins may have been largely due to the short exposure of a relatively modest overeating stimulus in our study, although other factors, such as the effects of overeating on adipose tissue endoplasmic reticulum (ER) stress (32) may contribute as well. The ER is the primary site of protein synthesis, so ER stress, and a resultant disruption in ER function may attenuate protein translation.

Adipose tissue expansion during periods of weight gain requires not only adipocyte hypertrophy, but also accommodation by the surrounding anatomical environment. For example, if expanding adipocytes do not experience a compensatory increase in angiogenesis/vascularity, insufficient capillarization may contribute to tissue hypoxia/inflammation, as well as tissue and systemic insulin resistance (33,34). Although angiogenic capacity has been reported to increase in response to overeating and weight gain (35), adipocyte capillary density is still often found to be compromised in obesity (6,7). Our findings expand on these data by demonstrating that even a very modest overeating stimulus in human subjects can trigger a pro-angiogenic response, as evidenced by our observed increase in the expression of several pro-angiogenic genes. Interestingly, this included HIF1a gene expression, which could suggest increased hypoxic signaling; but unfortunately we did not have sufficient tissue to establish HIF1a localization (HIF1a nuclear content would be a better index of HIF1a activation). It appears that the pro-angiogenic signalling we observed did not translate to a measurable increase in adipose vascularity, as noted by the lack of change the gene expression of *CD31* or protein abundance of VEGFα (both markers of an adaptive response in angiogenesis).

Contrary to our hypothesis, exercise did not further augment this angiogenic response to overeating. This is in apparent contrast with recent findings from our lab that adipose tissue VEGFA mRNA expression increased in the hour(s) after exercise (11,36), which we interpreted to suggest that angiogenic signaling is upregulated in the few hours after each session of exercise. This discrepancy could be a factor of the timing of the measurements (12h after exercise in the present study vs. 1-3 hours after exercise in previous work). Alternatively, it is possible that the pro-angiogenic effects of overeating we observed in both EX and nonEX may have overwhelmed the more subtle effects of exercise in our study.

Although obesity-related insulin resistance is often linked with increased systemic and/or adipose tissue inflammatory response (37–42), we found no increase in tissue or systemic

inflammation in response to overeating. This aligns with some human studies dissociating impaired insulin sensitivity from changes in circulating pro-inflammatory cytokines and adipose tissue macrophages in the early stages of weight gain (24,43). Development of insulin resistance with an accompanying pro-inflammatory response likely requires more robust alterations in adipose tissue morphology than our 1 week overeating intervention would provide (reviewed in (44)). For example, Muir et al. (10) reported that in overfed mice, peak CD11c+ adipose tissue macrophage infiltration was observed when adipocytes hypertrophied to their peak size. Therefore, while increased circulating inflammatory factors and an increase in adipose tissue inflammatory pathway activation may indeed contribute to impaired insulin action in obesity, they may not be required for the onset of insulin resistance during the early stages of weight gain. This is consistent with other work in mice suggesting that early diet-induced insulin resistance is linked to lipid overload and lipid toxicity in skeletal muscle and liver, rather than inflammation (45). Notably, cytokine concentrations are often well below the clinical range in healthy adults (46), and even overeating for one week did not bring many of these adipose tissue cytokines into the measurable range in our healthy subjects (Luminex, data not shown).

Although our findings indicate regular exercise did not protect against insulin resistance or alter the changes in adipose tissue we found in response with this brief exposure to overeating, it is still quite possible that exercise might modify the adaptive responses to longer-term overeating and weight gain. Along these lines, an overwhelming amount of epidemiological evidence demonstrates improved markers of metabolic health outcomes and fewer incidences of metabolic disease in those who live physically active lives vs. sedentary adults (47,48). Several factors may underlie the long-term health benefits of exercise, including improved weight maintenance with exercise (49), but much of the health benefits of a physically active lifestyle remain even when controlling for body weight/body fat. Because most people experience at least some weight gain throughout adulthood (50), it is possible that at least a portion of the long-term metabolic health benefits of regular exercise may be due to exercise-mediated modifications in adipose tissue structure and metabolic function as people experience episodes of weight gain throughout their lifetime.

Conducting controlled overeating experiments in human subjects presents considerable challenges, and several limitations exist. This experiment was conducted in free-living conditions, and although subjects' diets were tightly monitored, we were not able to directly

control dietary adherence. All subjects gained weight after the one-week intervention supporting the prospect that they were indeed overeating, and importantly, weight gain was tightly matched between EX and nonEX. In addition, our study was designed to test the effects of overeating in healthy adults to assess consequences of early stages of weight gain, but it is possible that the response to a similar overeating challenge in obese adults may be different from what we observed here. Also, we only collected samples from abdominal subcutaneous adipose tissue in our study, due to its major role in fatty acid delivery to the systemic circulation (51), but it is important to consider that adipose depot differences likely exist in the response to overeating. In particular, visceral adipose tissue typically develops more inflammation than subcutaneous adipose tissue, and so the responses to overeating might be different in visceral fat. Furthermore, there are differences in the adipose tissue immune response to overeating between males and females (52). While we anticipate that these sex-based differences in the response to overeating may be rather subtle, it is important to acknowledge that the study was not powered to assess sex differences in this response. Finally, all samples were collected in the overnight fasted state, so the responses presented here do not reflect the overeating effects in postprandial conditions.

In summary, our main findings indicate that a brief and modest overeating intervention triggered an increase in the expression of genes involved in lipid metabolism and angiogenesis in abdominal subcutaneous adipose tissue. These early adaptive responses to overeating and weight gain could lead to long-term alterations in adipose tissue lipid storage capacity. Future work aimed at understanding the regulation of angiogenesis, adipogenesis, and ECM remodeling in response to more extensive weight gain will be very impactful. This study also provided a free-living, practical model to suggest that brief overeating (inducing just ~1 kg weight gain) significantly impaired insulin sensitivity in healthy adults, without affecting *ex-vivo* lipolytic rate, or markers of adipose tissue and systemic inflammation. This suggests that the early induction of insulin resistance with weight gain is likely independent of adipose tissue or systemic inflammation, and (consistent with previous work) could result from ectopic lipid deposition. Importantly, we found no difference in the response to overeating in regular exercisers vs. non-exercisers, suggesting exercise may not protect against the negative consequences of the *initial* exposure to overeating.

ACKNOWLEDGEMENTS

This project was supported by NIH R01#DK077966 and CIHR DFS #0077000623. I am thankful to Emily Krueger, Jenna Gillen, Natalie Taylor, Darby Middlebrook, Toree Baldwin, Konstantinos Karabetsos, and Michael Schleh for their intellectual and technical contributions to these experiments. Additional thanks to Suzette Howton and Haojia Jing for participant recruitment and dietary control, and to Benjamin Ryan, and Thomas Rode, and Benjamin Reinheimer for assistance.

FIGURES

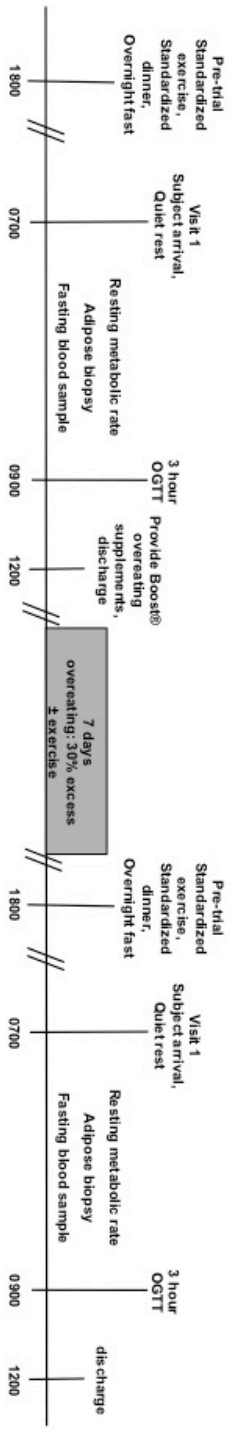

Figure V-1 Overeating study design.

The day before the study visits, subjects consumed identical diets, with the addition of supplemental kcal during the intervention. Visit 1 was identical to Visit 2, as subjects reported to the lab following an overnight fast for collection of adipose tissue and blood samples. Overeating was performed in free-living conditions and monitored daily. OGTT: oral glucose tolerance test.

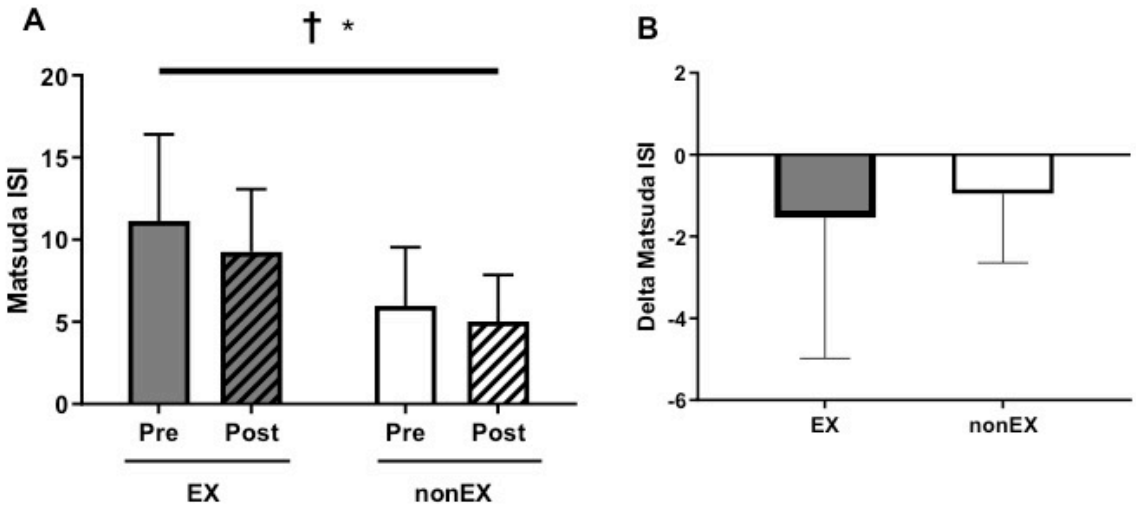

Figure V-2 Insulin sensitivity response to overeating.

ISI: insulin sensitivity index *P<0.05 for effect of exercise. †P<0.05 for effect of overeating. N = 9-11 per group. Data are Mean ± SD.

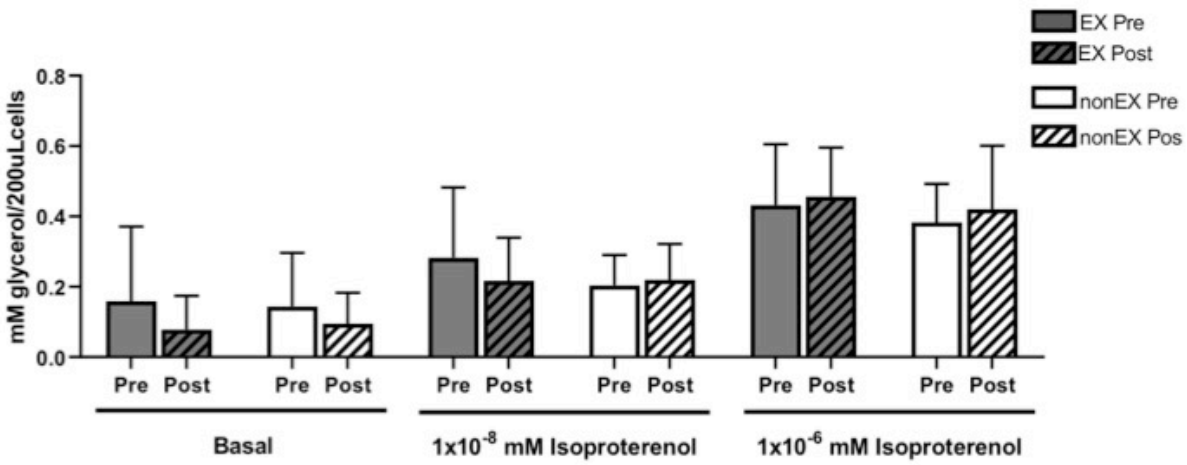

Figure V-3 Ex Vivo Adipocyte Lipolysis.

Basal lipolysis (no isoproterenol), low-dose isoproterenol-stimuled lipolysis, and high-dose isoproterenol-stimulated lipolysis as mM glycerol in media from 200uL fresh mature adipocytes following a 2-hour incubation. N = 8-11.

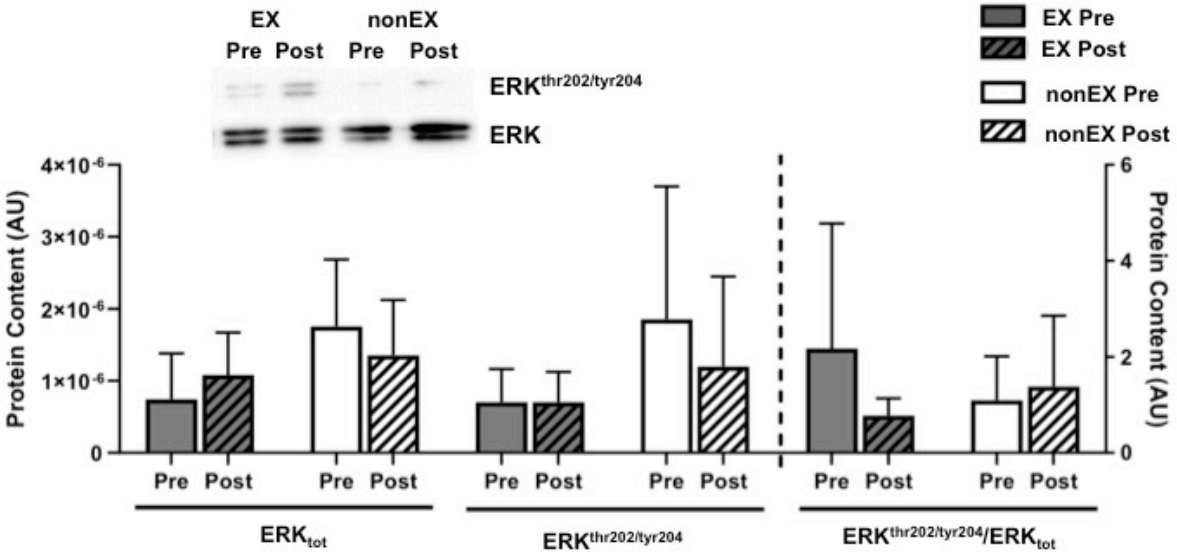

Figure V-4 Adipose Tissue ERK Protein.

Representative images and quantified protein content for ERK_{tot}, pERK, and $pERK/ERK_{tot}$ as a marker of ERK activity. N = 5-9. Data are Mean ± SD.

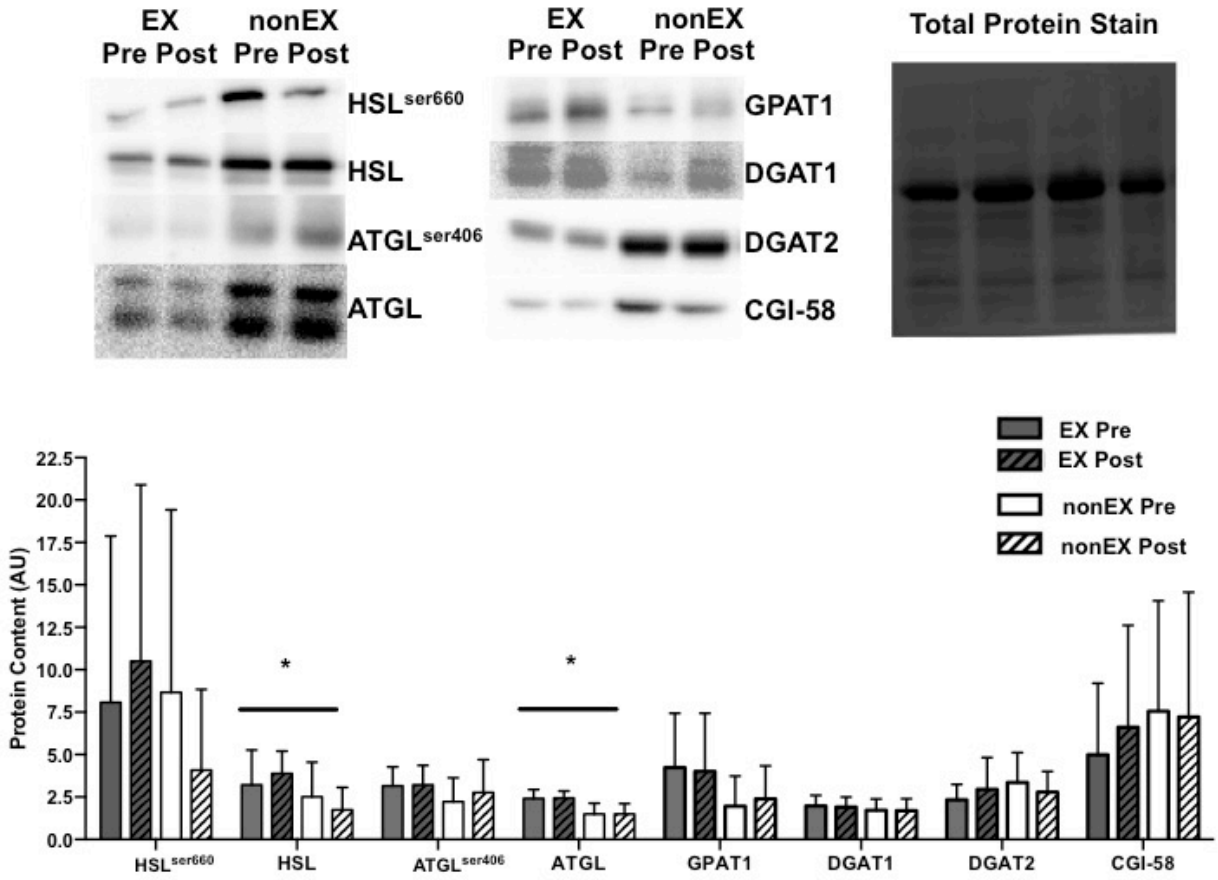

Figure V-5 Adipose Tissue Lipolysis/Esterification Proteins.

No change in the content of eight proteins involved in lipolysis or esterification in response to overeating. Inset: representative images for all proteins measured, with representative Memcode total protein image at right. *P<0.05 for effect of exercise. N = 8-10. Data are Mean ± SD.

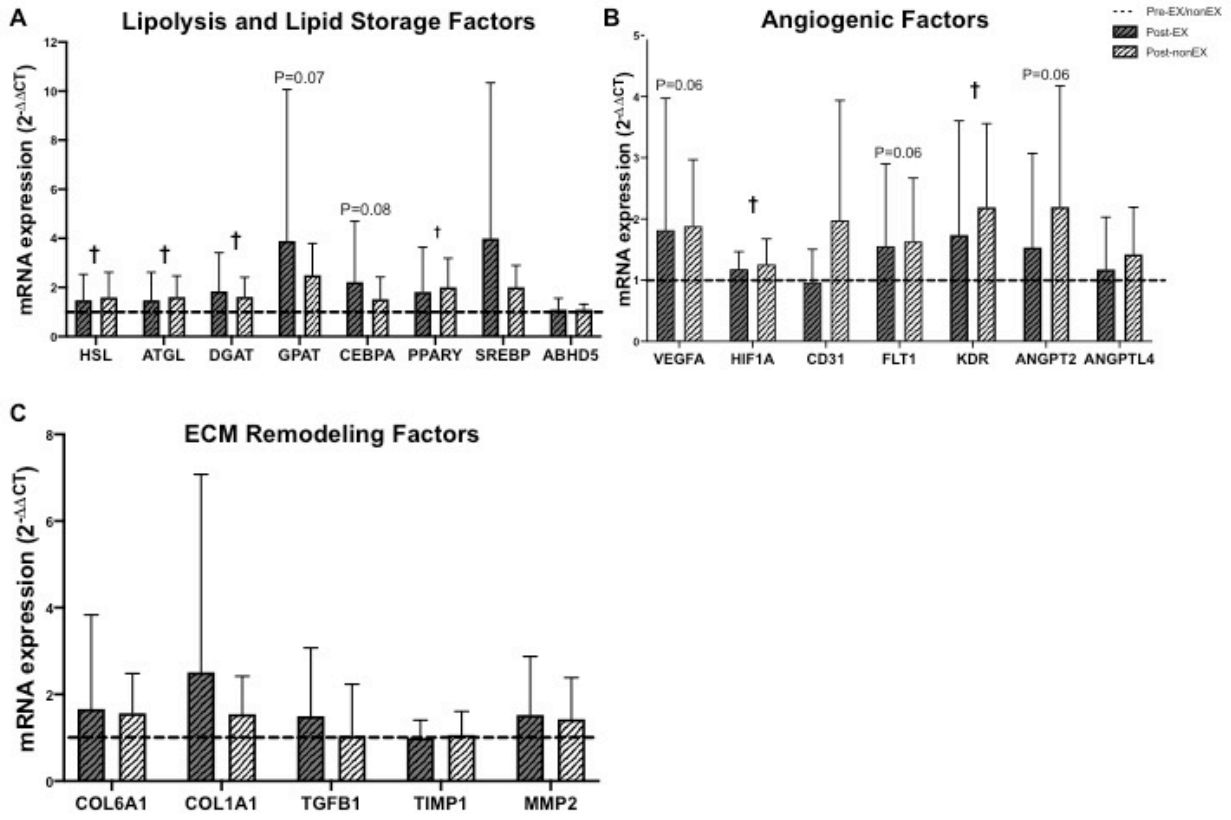

Figure V-6 Gene expression.

mRNA was upregulated in response to overeating in a panel of genes involved in lipolysis and lipid storage (A) and angiogenesis (B), but there was no change in the expression of genes involved in extracellular matrix remodeling (C). †P<0.05 for effect of overeating. N = 8-10. Data are Mean ± SD.

TABLES

Table V-1 qPCR targets in the subcutaneous adipose tissue

Gene symbol	Protein encoded
HSL	hormone-sensitive lipase (HSL)
ATGL	adipose triglyceride lipase (ATGL)
DGAT1	diacylglyceride acyltransferase 1 (DGAT1)
GPAT1	glycerol-3-phosphate Acyltransferase-1 (GPAT1)
CEBPA	CCAAT enhancer binding protein alpha (CEBPα)
PPARG	proliferator-activated receptor gamma (PPARγ)
SREBP1C	sterol regulatory element-binding protein 1 (SREBP1c)
ABHD5	1-acylglycerol-3-phosphate O-acyltransferase (ABHD5)
VEGFA	vascular endothelial growth factor (VEGF)
HIF1A	hypoxia inducible factor 1 alpha (HIF1α)
CD31	cluster of differentiation 31 (CD31)
FLT1	vascular endothelial growth factor receptor 1 (VEGFR1)
KDR	vascular endothelial growth factor receptor 2 (VEGFR2)
ANGPT2	angiopoietin-2 (ANGPT2)
ANGPTL4	angiopoietin-like 4 (ANGPTL4)
COL6A1	collagen alpha-1 (VI) chain (COL6A1)
COL1A1	collagen alpha-1 (I) chain (COL1A1)
TGFB1	transforming growth factor beta 1 (TGF-β1)
TIMP1	tissue inhibitor of matrix metalloproteinases 1 (TIMP1)
MMP2	matrix metallopeptidase 2 (MMP2)

Table V-2 Baseline characteristics of subjects

	EX	NONEX	P
Age (years)	22 ± 2	23 ± 3	0.70
Body mass (kg)	75.1 ± 9.9	75.0 ± 15.6	0.99
BMI (kg/m^2)	24.6 ± 2.9	24.6 ± 2.3	0.99
VO_{2peak} (ml/kg FFM/min)	3.2 ± 0.7	2.6 ± 0.6*	0.03
Matsuda ISI	11.1 ± 5.3	6.0 ± 3.6*	0.02
Triglycerides (mg/dL)	54 ± 22	80 ± 35	0.06
Total Cholesterol (mg/dL)	138 ± 24	131 ± 31	0.59
HDL Cholesterol (mg/dL)	46 ± 12	38 ± 10	0.13
LDL Cholesterol (mg/dL)	92 ± 25	93 ± 28	0.94

BMI: body mass index, ISI: insulin sensitivity index, HDL: high density lipoprotein, LDL: low density lipoprotein.
* $P<0.05$ compared with EX. n = 9-11 per group. Data are Mean ± SD.

Table V-3 Metabolic responses to overeating

	EX		NONEX				
	Pre	**Post**	**Pre**	**Post**	**ME: Exercise**	**ME: Overeating**	**Interaction**
Triglycerides (mg/dL)	54 ± 22	61 ± 40	80 ± 35	75 ± 32	0.12	0.87	0.39
Total Cholesterol (mg/dL)	138 ± 24	129 ± 18	131 ± 31	139 ± 34	0.89	0.99	0.08
HDL Cholesterol (mg/dL)	46 ± 12	48 ± 10	38 ± 10	41 ± 9	0.07	0.22	0.93
LDL Cholesterol (mg/dL)	92 ± 25	81 ± 14	93 ± 28	98 ± 36	0.41	0.58	0.11
Fasting NEFA (uM)	395 ± 191	270 ± 133	336 ± 205	337 ± 210	0.96	0.10	0.09
CRP (mg/L)	1.7 ± 1.3	1.8 ± 1.6	1.6 ± 1.3	2.0 ± 1.4	0.94	0.30	0.58

BMI: body mass index, ISI: insulin sensitivity index, HDL: high density lipoprotein, LDL: low density lipoprotein, NEFA: non-esterified fatty acids, CRP: high-sensity C-reactive protein. n = 9-11 per group. Data are Mean ± SD.

Chapter VI. Overall Discussion

Together, the projects of my dissertation shed light on some pathways through which exercise modifies adipose tissue in ways that could impact metabolic health. In this chapter, I will summarize the key findings from all of my dissertation projects and provide an integrated interpretation of the results. Then, I will outline some ensuing questions that could help move these findings towards understanding the signals that regulate adipose tissue and systemic inflammation and insulin resistance in humans.

SUMMARY OF KEY FINDINGS

Project 1: *The effects of a single session of moderate-intensity and high-intensity exercise on factors regulating adipose tissue structure and metabolic function*

In Project 1, I used RNA-sequencing and qPCR analyses to explore changes in the subcutaneous adipose tissue transcriptome in obese adults after an exercise session of either high intensity interval training (HIIT) or moderate intensity continuous training (MICT). Subcutaneous abdominal adipose tissue samples were collected before exercise and one hour after exercise.

Key Findings:

- HIIT and MICT resulted in similar upregulation of gene sets related to the inflammatory response (IL6-JAK-STAT3 Signaling, Allograft Rejection, TNFA Signaling via NFKB, and Inflammatory Response)
- Gene sets involved in Oxidative Phosphorylation, Peroxisome, and Adipogenesis were downregulated one hour after exercise
- The expression of several genes involved in adipose tissue remodeling (VEGFA, IL6, ANGPTL4, TIMP1) were increased after exercise
- The rapid gene set response to a single exercise session appears to be largely independent of exercise intensity

Overall, this project identified the coordinated upregulation of inflammatory genes to be the major adipose tissue signaling response one hour after a single session of HIIT or MICT.

Project 2: *The effects of acute moderate-intensity exercise on adipose tissue cellular composition and function in lean and obese humans*

Project 2 used flow cytometry to assess changes in the cellular composition of the adipose tissue stromal vascular fraction from obese adults collected 12 h after exercise (60 min at 80 ± 3% HR_{peak}; EX) compared with a within-subject sedentary control (SED).

Key Findings:

- Exercise decreased both total preadipocyte number, and CD34hi preadipocytes, without a corresponding change in CD34- and CD34lo preadipocytes
- There were no changes in adipose tissue EC's, total (CD45+) immune cells, DC's, T cells, or adipose tissue macrophages in SED vs. EX

The decrease in CD34hi preadipocytes after exercise suggests a shift towards a preadipocyte phenotype that may confer a healthier whole adipose tissue metabolic profile (i.e. lower lipolytic rate).

Project 3: *The effects of habitual exercise on adipose tissue responses to overeating*

In Project 3, habitual exercisers (≥30 min planned exercise, ≥5 days/week) and non-exercisers (no planned weekly exercise) consumed ~30% more calories than that required for weight maintenance. They gained ~1kg (matched between exercisers and non-exercisers) over one week, while maintaining regular exercise or inactivity. Subcutaneous abdominal adipose tissue biopsies were collected before and after overeating to assess *ex vivo* lipolytic rate (isolated adipocytes), gene expression, and protein content of factors related to adipose tissue remodeling. Peripheral insulin sensitivity was calculated by Matsuda insulin sensitivity index (ISI) from a 3 h oral glucose tolerance test before and after overeating.

Key Findings:

- One week of modest overeating impaired ISI in healthy adults by 10%
- Regular exercise did not protect against this rapid maladaptive response to overeating
- Overeating did not alter blood lipid profile, adipocyte lipolysis, or tissue/systemic inflammation

- Overeating increased gene expression of factors regulating lipid metabolism and angiogenesis (HSL, ATGL, DGAT, PPARγ, HIF1A, KDR) in adipose tissue, without changing the corresponding proteins

Together, the brief overeating exposure (1 week) resulted in a similar reduction in insulin sensitivity and tissue gene expression changes in exercisers and non-exercisers, without impacting other tissue and circulating markers of metabolic health/inflammation.

INTEGRATED INTERPRETATION OF RESULTS

Rapid adipose tissue inflammatory response to exercise

A key novel finding from my dissertation was the upregulation of inflammatory signaling genes one hour after exercise in adipose tissue from obese adults (Project 1). However, our observation in Project 2 that adipose tissue total immune cell number, macrophage, T cell, and dendritic cell content did not change 12 hours after exercise in adipose tissue samples from a similar cohort of obese, regular exercisers suggests this transcriptional response may not increase immune cell number within the adipose tissue, at least in this timeframe. It is well-documented that blood leukocyte number increases during exercise, biased towards cytotoxic/effector and mature/differentiated cells; cells with tissue migration phenotypes; and cells with a higher adenoreceptor/glucocorticoid receptor expression (reviewed in Simpson et al. (149)). After exercise, lymphocyte number decreases (lymphocytopenia), and there is an increase in neutrophil number relative to pre-exercise baseline, which has been suggested to reflect leukocyte egress to tissues like the spleen, lungs, and gut (151). However, despite accelerating interest/appreciation in adipose tissue's role as an immunological tissue, there is essentially no work examining the effects of exercise on changes in adipose tissue immune cells in human subjects. My dissertation projects were designed in part to expand our understanding in this regard. Characterizing the adipose tissue immune response to exercise could provide a novel understanding of the signals regulating adipose tissue inflammation, and inform therapeutic strategies to attenuate the chronic low-grade inflammation characteristic of obesity.

My observation from Project 2 indicating that immune cell number was stable 12 h after exercise suggests the leukocytes mobilized by exercise may not be migrating to adipose tissue in

the several hours after exercise. Therefore, it is more likely that exercise may trigger a change in macrophage or other immune cell *phenotype* (i.e. transcriptional profile of a given cell population), independently of cell number. For example, MacPherson et al. (19) reported a reduction in pro-inflammatory (F4/80+CD11c+) macrophages, but no change in total (F4/80+) macrophage content 2h post-exercise in mouse inguinal adipose tissue – suggesting exercise might regulate macrophage phenotype independent of total number. Given the time course of monocyte differentiation within tissue (i.e. days), an acute exercise-induced change in macrophage phenotype would likely occur via transcriptional changes within resident adipose tissue macrophages (rather than influx and differentiation of circulating monocytes). However, monocytes and neutrophils could be rapidly recruited to adipose tissue in response to exercise, but I was unable to quantify these cells in this dissertation due to tissue limitations. Therefore, future projects could expand on this work by measuring these other immune cell populations, as well as immune cell subtypes (e.g. CD11c+/- macrophages) to more completely define the adipose tissue response to exercise.

Effects of exercise on adipose tissue angiogenesis and vascularization

Our findings that VEGFA gene expression increased (trend $P = 0.07$) one hour after exercise (Project 1), with no change in endothelial cell content 12 hours after exercise (Project 2) suggest that even though each exercise session may upregulate pro-angiogenic genes, this does not trigger endothelial cell migration by 12 hours after exercise. Understanding if and how exercise induces angiogenesis could have important therapeutic implications because angiogenesis is essential for tissue oxygenation, paracrine function, and fatty acid transport – all of which typically become pathologic in the context of adipose tissue expansion. Angiogenesis is necessary for adipogenesis (77), implicating this process as central in adipose tissue expansion. It has also been suggested that insufficient angiogenesis to accommodate adipocyte hypertrophy can drive adipose tissue inflammation and fibrosis through the resulting hypoxic signaling (161). Min et al. (193) recently reported that exercise protected against the reduction in adipose tissue capillary density normally observed with weight gain in mice on a high fat diet. This suggests that exercise may help maintain vascularity in obese adipose tissue, but this will need to be explored with a model of overeating long enough to achieve functional changes in human adipose tissue vasculature. While we did not collect samples for histology in Project 3, there was

no change in adipose tissue CD31 mRNA expression, which provided a crude indication that the angiogenic signaling from this modest one-week overeating stimulus did not increase adipose tissue vascularity.

Effects of exercise on adipose tissue extracellular matrix (ECM) remodeling

ECM remodeling is regulated in part by the cumulative balance of matrix metalloproteinases (MMPs) and tissue inhibitors of MMPs (TIMPs) in the local adipose tissue environment. Although we did not perform an exhaustive assessment of ECM remodeling factors, we found an increase in TIMP1 one hour after HIIT/MICT (Project 1), but no difference in COL1 or COL6 gene expression between non-obese exercisers and non-exercisers (Project 3). Future work would merit from more functional measures of adipose tissue ECM remodeling factors in response to acute and chronic exercise, such as zymography and histological analyses. Furthermore, Marcelin et al. (204) recently showed that PDGFRα signaling regulates the proportion of $CD9^{hi}$ progenitors that are linked to a pro-fibrotic phenotype in mice and humans, suggesting regulation of the progenitor pool could alter adipose tissue fibrosis. Although we did not comprehensively assess the impact of exercise on progenitors within adipose tissue, Project 2 did identify a change in preadipocyte phenotype and number within adipose tissue 12 hours after exercise, suggesting exercise-related signals can influence at least a subset of the progenitor populations in human subcutaneous adipose tissue.

When we addressed the effects of regular exercise on the angiogenic and ECM remodeling signaling responses to overeating in adipose tissue, there was no difference in the response between exercisers and non-exercisers (Project 3). However, our finding that angiogenic factors increase within one week of overeating while ECM remodeling factors do not, suggests that angiogenesis may be triggered more rapidly than ECM remodeling; at least in response to overeating. Overall, overeating/weight gain and the result increased stimulus for triglyceride storage is likely a much more robust signal for these remodeling processes in adipose tissue compared with exercise alone, given that these processes are typically triggered to support adipocyte hypertrophy/hyperplasia. Therefore, assessing the effects of exercise in the context of more robust adipose tissue expansion and energy surplus may shed light on its ability to regulate angiogenesis and ECM remodeling.

Effects of exercise on adipose tissue metabolism

One of the most compelling findings from my dissertation was a decrease in total preadipocyte content 12 hours after a single exercise session (Project 2). This was observed along with a rapid downregulation of the hallmark adipogenic gene set one hour after exercise (Project 1). We speculate here that the rapid downregulation of adipogenic genes in response to exercise is likely distinct from longer-term adaptations that might feature enhanced adipogenesis, given preliminary findings from our lab suggesting that incubating preadipocytes in exercise serum increases the rate of adipogenesis (154). It is unclear from the reduction in preadipocytes in Project 2 whether this decrease results from increased adipogenesis, reduced proliferation, or increased apoptosis. However, given the time course of *in vivo* preadipocyte differentiation (~8% per year (79)), it is likely one of the latter. Overall, the broad takeaway from the observed decrease in preadipocyte content (driven by CD34hi preadipocytes) is that the preadipocyte phenotype can be modified rapidly. Therefore, better understanding the mechanisms regulating the exercise-induced decrease in preadipocytes (e.g. regulation of proliferation and apoptosis) could elucidate the potential for therapeutic regulation of these cells by exercise or pharmacological means. Importantly, Raajendiran et al. (166) demonstrated that distinct preadipocyte subtypes secrete different proteins and differentiate into adipocytes with different lipolytic rates. Therefore, exploring the relationship between preadipocyte phenotype and *in vivo* adipose tissue function (e.g. lipolytic rate or secretome) would inform whether manipulating this cell population could alter whole adipose tissue metabolic function.

Assessing the adipose tissue structural response to overeating requires robust energy surplus

A key working hypothesis at the outset of this dissertation was that regular exercise protects against the negative consequences of weight gain within adipose tissue. While Projects 1 and 2 identified some immune and progenitor cell responses to acute exercise in obese regular exercisers, Project 3 found no difference in the adipose tissue responses (gene expression, protein content, *ex vivo* lipolytic rate) to short-term overeating between regular exercisers and non-exercisers. These data suggest that in non-obese adults, exercise may not impact the adipose tissue response to brief and modest overeating. However, the 1 kg weight gain induced by overeating did not correspond to an increase in adipocyte size, which is the key demand for structural remodeling within adipose tissue. Therefore, although genes involved in adipose tissue

metabolism and angiogenesis were upregulated by overeating in Project 3, it was not surprising that there were no changes in gene expression of extracellular matrix remodeling factors, or protein content of the key fat storage and angiogenic proteins we measured – and in fact this informs a model wherein some minimum adipocyte hypertrophy is required to trigger measureable structural changes within adipose tissue. That threshold may be dependent on baseline adipocyte size or adipose tissue composition, and so working with an obese population may also be important to capture the remodeling response that is relevant to pathological adipose tissue.

DIRECTIONS FOR FUTURE RESEARCH

Time course of the adipose tissue immune response to exercise

Findings from Project 1 suggests immune signaling is rapidly upregulated following each session of exercise, but in Project 2 I found no change in immune cell number (total, macrophages, T cells, and dendritic cells) 12 hours after exercise. To my knowledge, no work to date has measured the changes in immune cell abundance between 0-12 hours after exercise, when changes in circulating immune cell numbers are known to be dynamic (149). Therefore, obtaining a time course of immune cell changes in adipose tissue (e.g. 1, 4, 8, and 12 hours after exercise) would help elucidate the short-term dynamics of immune cells in adipose tissue. Importantly, the inflammatory signaling response to exercise could result from a phenotypic change in immune cells, rather than a change in cell number. Collecting sorted cells and/or imaging tissue samples could be a key step to assess phenotypic shifts in immune cell populations in response to exercise. Further exploring these changes will be important to identify the exercise related signals that may influence adipose tissue health during weight gain and obesity.

Effects of exercise on adipose tissue structural remodeling during weight gain

My dissertation projects have helped to expand our understanding about the effects of exercise on signaling and cell population profile in adipose tissue – as well as attempts to examine the effects of exercise on adipose tissue during a brief exposure to overeating and weight gain. However, to assess whether these effects of exercise may truly modify adipose

tissue in ways to protect against the negative health consequences of weight gain, we must employ a longer, more robust overeating/weight intervention. In rodents, longer-term high fat diet interventions do indeed demonstrate protective effects of exercise on adipose tissue fibrosis (44), macrophage infiltration (43) and angiogenesis (193); but there have been no well-controlled long-term overeating interventions in humans to establish whether exercise could be an effective tool to mitigate adipose tissue dysfunction. Importantly, in order to assess the *direct effects* of exercise on adipose tissue in response to weight gain, it is imperative to match weight gain (more importantly match the gain in body fat mass) between exercisers and non-exercisers. In these types of overeating experiments, exercisers must eat more than non-exercisers in order to compensate for the energy expended during exercise. If not, the exercisers will gain less weight and it will be impossible to discern the direct effects of exercise on changes in adipose tissue structure, inflammation, function, etc, from the indirect effects of just gaining less body fat. The inclusion of more functional measurements into these experiments would also better characterize the effects of exercise on the structural response to overeating. For example, conducting *ex vivo* measurements of angiogenic capacity (205) in addition to histological assessments of adipose tissue capillarization and protein and mRNA measures of factors regulating angiogenesis; would provide a more comprehensive evaluation of the effects of exercise on angiogenesis. Similarly, the addition of adipose tissue histology paired with more functional assays such as co-culture of decellularized adipose tissue with other cells (e.g. preadipocytes) would provide more comprehensive assessment of influence of exercise while overeating on ECM function and composition. For example, co-culture of preadipocytes and decellularized adipose tissue from exercisers and non-exercisers who undergo weight gain could reveal whether the ECM from exercisers might promote adipogenesis better than non-exercisers following a period of tissue expansion. Together, these experiments would help to (1) more thoroughly characterize the changes during the early response to overeating in human adipose tissue, and (2) identify regulators (through exercise or other means) that could improve the ability of adipose tissue to expand.

OVERALL CONCLUSIONS

Adipose tissue dysfunction is central to the development of obesity-related metabolic dysfunction. Hallmarks of adipose tissue dysfunction include hypertrophic adipocytes, accompanied by adipose tissue hypoxia, fibrosis, and chronic low-grade inflammation, which are all associated with tissue and systemic insulin resistance. Overall, Projects 1 and 2 of this dissertation provided some of the first evidence that acute exercise can signal changes in inflammatory gene expression and stromal vascular fraction composition within subcutaneous adipose tissue from obese humans. In particular, the remodeling of the adipocyte progenitor pool after acute aerobic exercise provides novel evidence that exercise can rapidly impact adipose tissue composition. Collectively, Projects 1 and 2 contribute to our working knowledge of the rapid post-exercise (1h and 12h) adipose tissue responses to exercise (conceptual model in Figure VI-1). Project 3 demonstrated that brief, modest overeating resulted in increased angiogenic and lipid metabolism gene expression in adipose tissue from non-obese people, with no accompanying structural changes during the brief overeating exposure. Furthermore, there was no difference in the signaling response between regular exercisers and non-exercisers in response to this mild and brief overeating stimulus. These data suggest that perhaps some minimum adipocyte hypertrophy may be required to trigger structural adaptations in the adipose tissue stroma. Therefore, future work measuring the impact of long-term weight gain or weight loss resulting in appreciable changes in cell size could shed light on the potential for the signals associated with regular exercise to influence adipose tissue remodeling (angiogenesis, ECM remodeling, and inflammation). This has important implications for effectively using exercise as a therapeutic intervention, and more globally for understanding the coordinated signals regulating adipose tissue remodeling during the episodes of weight gain that most people in developed countries experience throughout adulthood.

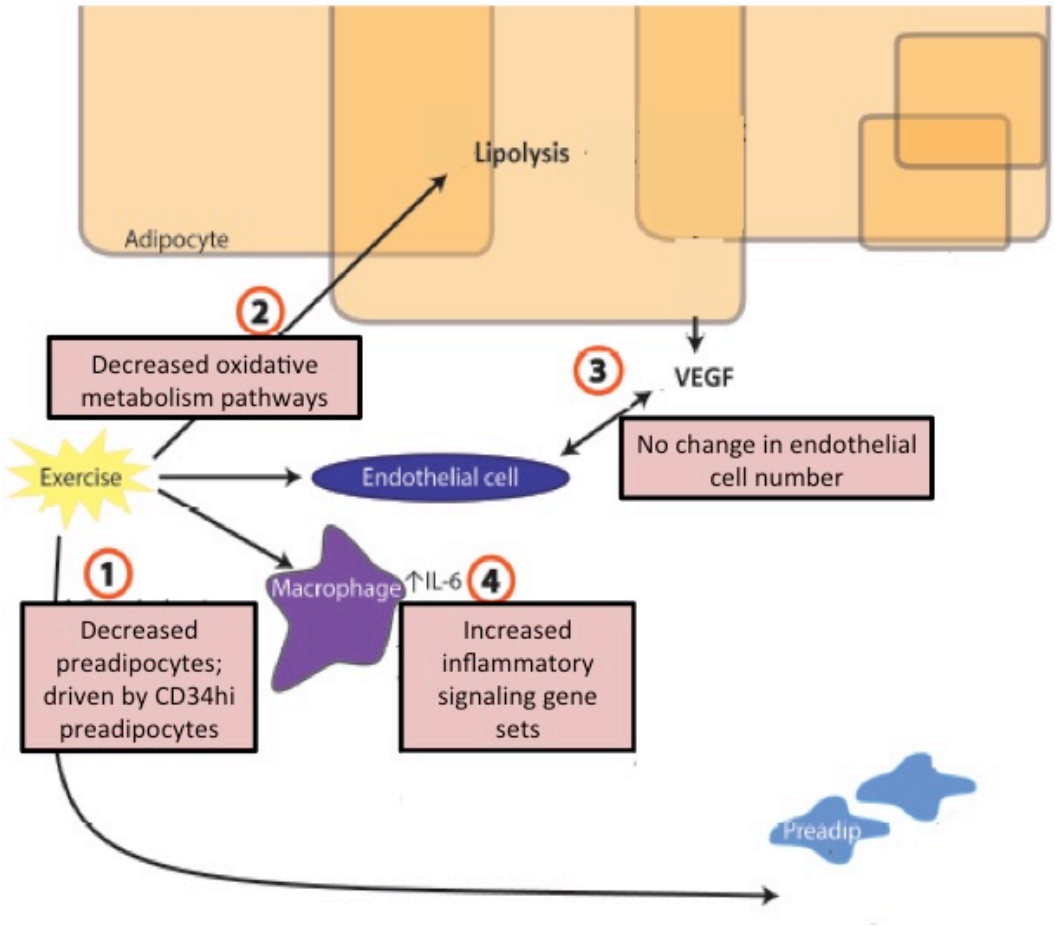

Figure VI-1 Conceptual Model.

Novel acute exercise-induced signals in adipose tissue include (1) decreased total and CD34^{hi} preadipocytes; (2) decreased oxidative metabolism pathways; (3) no change in endothelial cell content; and (4) increased inflammatory signaling pathways.

REFERENCES

1. Ogden CL, Carroll MD, Fryar CD, Flegal KM. Prevalence of Obesity Among Adults and Youth: United States, 2011-2014. NCHS Data Brief. 2015;(219):1–8.
2. Flegal KM, Graubard BI, Williamson DF, Gail MH. Underweight , Overweight , and Obesity. JAMA. 2017;293(15):1861–7.
3. Nguyen NT, Nguyen X-MT, Lane J, Wang P. Relationship Between Obesity and Diabetes in a US Adult Population: Findings from the National Health and Nutrition Examination Survey, 1999–2006. Obes Surg. 2011;21(3):351–5.
4. Hubert H, Feinleib M, McNamara P, Castelli W. Obesity as an Independent Risk Factor for Cardiovascular Disease: A 26-year Follow-up of Participants in the Framingham Heart Study. Circulation. 1983;67(5):968–77.
5. Tremmel M, Gerdtham U-G, Nilsson P, Saha S. Economic Burden of Obesity: A Systematic Literature Review. Int J Environ Res Public Health. 2017;14(4):435.
6. Van Pelt DW, Guth LM, Wang AY, Horowitz JF. Factors regulating subcutaneous adipose tissue storage, fibrosis, and inflammation may underlie low fatty acid mobilization in insulin sensitive obese adults. Am J Physiol - Endocrinol Metab. 2017;313(4):429–39.
7. Pasarica M, Rood J, Ravussin E, Schwarz JM, Smith SR, Redman LM. Reduced oxygenation in human obese adipose tissue is associated with impaired insulin suppression of lipolysis. J Clin Endocrinol Metab. 2010;95(8):4052–5.
8. Lumeng CN, Saltiel AR. Inflammatory links between obesity and metabolic disease. Life Sci. 2011;121(6):2111–7.
9. O'Connell J, Lynch L, Cawood TJ, Kwasnik A, Nolan N, Geoghegan J, et al. The Relationship of Omental and Subcutaneous Adipocyte Size to Metabolic Disease in Severe Obesity. PLoS One. 2010;5(4):e9997.
10. Cotillard A, Poitou C, Torcivia A, Bouillot J, Dietrich A, Klöting N, et al. Adipocyte Size Threshold Matters : Link with Risk of Type 2 Diabetes and Improved Insulin Resistance After Gastric Bypass. J Clin Endocrinol Metab. 2016;99(8):1466–70.
11. Virtue S, Vidal-Puig A. Adipose tissue expandability, lipotoxicity and the Metabolic Syndrome - An allostatic perspective. Biochim Biophys Acta - Mol Cell Biol Lipids. Elsevier B.V.; 2010;1801(3):338–49.
12. Gray SL, Vidal-Puig AJ. Adipose Tissue Expandability in the Maintenance of Metabolic

Homeostasis. Nutr Rev. 2007;65(SUPPL.1):7–12.

13. Kohlgruber A, Lynch L. Adipose Tissue Inflammation in the Pathogenesis of Type 2 Diabetes. Curr Diab Rep. 2015;15(11):1–11.

14. Thompson D, Karpe F, Lafontan M, Frayn K. Physical Activity and Exercise in the Regulation of Human Adipose Tissue Physiology. Physiol Rev. 2012;92:157–91.

15. Townsend LK, Knuth CM, Wright DC. Cycling our way to fit fat. Physiol Rep. 2017;5(7):1–9.

16. Gauthier M-S, Miyoshi H, Souza SC, Cacicedo JM, Saha AK, Greenberg AS, et al. AMP-activated protein kinase is activated as a consequence of lipolysis in the adipocyte. J Biol Chem. 2008;283(24):16514–24.

17. Hoier B, Hellsten Y. Exercise-induced capillary growth in human skeletal muscle and the dynamics of VEGF. Microcirculation. 2014;21(4):301–14.

18. Dudley GA, Tullson PC, Terjung RL. Influence of mitochondrial content on the sensitivity of respiratory control. J Biol Chem. 1987 Jul 5;262(19):9109–14.

19. Macpherson REK, Huber JS, Frendo-Cumbo S, Simpson JA, Wright DC. Adipose Tissue Insulin Action and IL-6 Signaling after Exercise in Obese Mice. Med Sci Sports Exerc. 2015;47(10):2034–42.

20. Oliveira AG, Araujo TG, Carvalho BM, Guadagnini D, Rocha GZ, Bagarolli RA, et al. Acute exercise induces a phenotypic switch in adipose tissue macrophage polarization in diet-induced obese rats. Obesity. 2013;21(12):2545–56.

21. Guh DP, Zhang W, Bansback N, Amarsi Z, Birmingham CL, Anis AH. The incidence of co-morbidities related to obesity and overweight: A systematic review and meta-analysis. BMC Public Health. 2009;9(1):88.

22. Benjamin RM. The Surgeon General's vision for a healthy and fit nation. US Dep Heal Hum Serv. 2010;125:514–5.

23. U.S. Department of Health and Human Services. Fact sheets from the Surgeon General's Call to Action to Prevent and Decrease Overweight and Obesity. W V Med J. 2002;98(6):234–43.

24. Frühbeck G. Overview of Adipose Tissue and Its Role in Obesity and Metabolic Disorders. In: Yang K, editor. Adipose Tissue Protocols. Totowa, NJ: Humana Press; 2008. p. 1–22.

25. Sun K, Tordjman J, Clement K, Scherer PE. Fibrosis and Adipose Tissue Dysfunction. Cell Metab. 2014;18(4):470–7.

26. Shulman GI. Ectopic Fat in Insulin Resistance, Dyslipidemia, and Cardiometabolic Disease. N Engl J Med. 2014;371(12):1131–41.

27. Wildman RP, Muntner P, Reynolds K, Mcginn AP. The Obese Without Cardiometabolic Risk Factor Clustering and the Normal Weight With Cardiometabolic Risk Factor Clustering. Arch Intern Med. 2008;168(15):1617–24.

28. Pasarica M, Sereda OR, Redman LM, Albarado DC, Hymel DT, Roan LE, et al. Reduced adipose tissue oxygenation in human obesity. Diabetes. 2009;58(3):718–25.

29. Divoux A, Tordjman J, Lacasa D, Veyrie N, Hugol D, Aissat A, et al. Fibrosis in Human Adipose Tissue : Composition , Distribution , and Link With Lipid Metabolism and Fat. Diabetes. 2010;59(November):2817–25.

30. Hotamisligil GS., Shargill NS., Spiegelman BM. Adipose Expression of Tumor Necrosis Factor-α : Direct Role in Obesity-Linked Insulin Resistance. Science (80-). 1993;259(5091):87–91.

31. Kern PA, Ranganathan S, Li C, Wood L, Ranganathan G. Adipose tissue tumor necrosis factor and interleukin-6 expression in human obesity and insulin resistance. Am J Physiol Endocrinol Metab. 2001;72205(208):745–51.

32. Martinez-Santibañez G, Nien-Kai Lumeng C. Macrophages and the Regulation of Adipose Tissue Remodeling. Annu Rev Nutr. 2014;34(1):57–76.

33. Van Pelt DW, Newsom SA, Schenk S, Horowitz JF. Relatively low endogenous fatty acid mobilization and uptake helps preserve insulin sensitivity in obese women. Int J Obes. Nature Publishing Group; 2014;39(1):149–55.

34. Magkos F, Fabbrini E, Conte C, Patterson BW, Klein S. Relationship between Adipose Tissue Lipolytic Activity and Skeletal Muscle Insulin Resistance in Nondiabetic Women. J Clin Endocrinol Metab. 2012;97(7):E1219–23.

35. Heath GW, Gavin 3rd JR, Hinderliter JM, Hagberg JM, Bloomfield SA, Holloszy JO. Effects of exercise and lack of exercise on glucose tolerance and insulin sensitivity. J Appl Physiol Respir Environ Exerc Physiol. 1983;55(2):512–7.

36. Newsom SA, Everett AC, Hinko A, Horowitz JF. A single session of low-intensity exercise is sufficient to enhance insulin sensitivity into the next day in obese adults. Diabetes Care. 2013;36(9):2516–22.

37. Boström P, Wu J, Jedrychowski MP, Korde A, Ye L, Lo JC, et al. A PGC1-α-dependent myokine that drives brown-fat-like development of white fat and thermogenesis. Nature. 2012;481(7382):463–8.

38. Stanford KI, Middelbeek RJW, Townsend KL, Lee MY, Takahashi H, So K, et al. A novel role for subcutaneous adipose tissue in exercise-induced improvements in glucose homeostasis. Diabetes. 2015;64(6):2002–14.

39. Huh JY, Panagiotou G, Mougios V, Brinkoetter M, Vamvini MT, Schneider BE, et al. FNDC5 and irisin in humans: I. Predictors of circulating concentrations in serum and plasma and II. mRNA expression and circulating concentrations in response to weight loss and exercise. Metabolism. Elsevier B.V.; 2012;61(12):1725–38.

40. Kurdiova T, Balaz M, Vician M, Maderova D, Vlcek M, Valkovic L, et al. Effects of obesity, diabetes and exercise on *Fndc5* gene expression and irisin release in human skeletal muscle and adipose tissue: *in vivo* and *in vitro* studies. J Physiol. 2014;592(5):1091–107.

41. Norheim F, Langleite TM, Hjorth M, Holen T, Kielland A, Stadheim HK, et al. The effects of acute and chronic exercise on PGC-1a, irisin and browning of subcutaneous adipose tissue in humans. FEBS J. 2014;281(3):739–49.

42. Walton RG, Finlin BS, Mula J, Long DE, Zhu B, Fry CS, et al. Insulin-resistant subjects have normal angiogenic response to aerobic exercise training in skeletal muscle, but not in adipose tissue. Physiol Rep. 2015;3(6):1–15.

43. Kawanishi N, Yano H, Yokogawa Y, Suzuki K. Exercise training inhibits inflammation in adipose tissue via both suppression of macrophage infiltration and acceleration of phenotypic switching from M1 to M2 macrophages in high-fat-diet- induced obese mice. Exerc Immunol Rev. 2010;16:105–18.

44. Kawanishi N, Niihara H, Mizokami T, Yano H, Suzuki K. Exercise training attenuates adipose tissue fibrosis in diet-induced obese mice. Biochem Biophys Res Commun. Elsevier Inc.; 2013;440(4):774–9.

45. Oral EA. Lipoatrophic diabetes and other related syndromes. Rev Endocr Metab Disord. 2003;4(1):61–77.

46. Gavrilova O, Marcus-Samuels B, Graham D, Kim JK, Shulman GI, Castle AL, et al. Surgical implantation of adipose tissue reverses diabetes in lipoatrophic mice. J Clin Invest. 2000;105(3):271–8.

47. Santomauro A, Boden G, Silva M, Rocha D, Santos R, Ursich M, et al. Overnight lowering of free fatty acids with Acipimox improves insulin resistance and glucose tolerance in obese diabetic and nondiabetic subjects. Diabetes. 1999;48(9):1836–41.

48. Nguyen T, Mijares A, Johnson M, Jensen M. Postprandial in nonobese leg and splanchnic men and women fatty acid metabolism. Am J Physiol. 1996;271(34):E965-72.

49. Ramakrishnan VM, Boyd NL. The Adipose Stromal Vascular Fraction as a Complex Cellular Source for Tissue Engineering Applications. Tissue Eng Part B Rev. 2017;00(00):ten.teb.2017.0061.

50. Rosen ED, Spiegelman BM. Adipocytes as regulators of energy balance and glucose homeostasis. Nature. 2006;444(7121):847–53.

51. Frayn, K; Arner, P; Yki-Jarvinen H. Fatty acid metabolism in adipose tissue, muscle, and liver in health and disease. Essays Biochem. 2006;42:89–103.

52. Wang H, Eckel RH. Lipoprotein lipase: from gene to obesity. AmJPhysiol EndocrinolMetab. 2009;297(1522–1555 (Electronic)):E271–88.

53. Kazantzis M, Stahl A. Fatty acid transport proteins, implications in physiology and disease. Biochim Biophys Acta - Mol Cell Biol Lipids. Elsevier B.V.; 2012;1821(5):852–7.

54. Cadoudal, T; Distel, E; Durant, S; Fouque, F; Blouin, J; Collinet, M; Bortoli, S; Forest, C; Benelli C. Regulation by thiazolidinediones and implication in glyceroneogenesis in adipose tissue. Diabetes. 2008;57(September):2272–9.

55. Coleman RA, Lee DP. Enzymes of triacylglycerol synthesis and their regulation. Prog Lipid Res. 2004;43(2):134–76.

56. Frühbeck G, Méndez-Giménez L, Fernández-Formoso J-A, Fernández S, Rodríguez A. Regulation of adipocyte lipolysis. Nutr Res Rev. 2014;27(01):63–93.

57. Brasaemle DL, Subramanian V, Garcia A, Marcinkiewicz A, Rothenberg A. Perilipin A and the control of triacylglycerol metabolism. Mol Cell Biochem. 2009;326(1–2):15–21.

58. Sztalryd C, Xu G, Dorward H, Tansey JT, Contreras JA, Kimmel AR, et al. Perilipin A is essential for the translocation of hormone-sensitive lipase during lipolytic activation. J Cell Biol. 2003;161(6):1093–103.

59. Haemmerle G, Lass A, Zimmermann R, Gorkiewicz G, Meyer C, Rozman J, et al. Defective Lipolysis and Altered Energy Metabolism in Mice Lacking Adipose Triglyceride Lipase. Science (80-). 2006;211(May):734–7.

60. Sahu-Osen A, Montero-Moran G, Schittmayer M, Fritz K, Dinh A, Chang Y-F, et al. CGI-58/ABHD5 is phosphorylated on Ser239 by protein kinase A: control of subcellular localization. J Lipid Res. 2015;56(1):109–21.

61. Tsiloulis T, Watt MJ. Exercise and the Regulation of Adipose Tissue Metabolism. 1st ed. Vol. 135, Progress in Molecular Biology and Translational Science. Elsevier Inc.; 2015. 175-201 p.

62. Egan JJ, Greenberg AS, Chang MK, Wek SA, Moos MC, Londos C. Mechanism of hormone-stimulated lipolysis in adipocytes: translocation of hormone-sensitive lipase to the lipid storage droplet. Proc Natl Acad Sci U S A. 1992;89(18):8537–41.

63. Arner P, Kriegholm E, Engfeldt P, Bolinder J. Adrenergic Regulation of Lipolysis Insitu At Rest and During Exercise. J Clin Invest. 1990;85(3):893–8.

64. Arner P. Human fat cell lipolysis: Biochemistry, regulation and clinical role. Best Pract Res Clin Endocrinol Metab. 2005;19(4):471–82.

65. Roepstorff C, Vistisen B, Donsmark M, Nielsen JN, Galbo H, Green KA, et al. Regulation of hormone-sensitive lipase activity and Ser563 and Ser565 phosphorylation in human skeletal muscle during exercise. J Physiol. 2004;560:551–62.

66. Lafontan M, Langin D. Lipolysis and lipid mobilization in human adipose tissue. Prog Lipid Res. Elsevier Ltd; 2009 Sep [cited 2014 Jul 13];48(5):275–97.

67. Jaworski K, Sarkadi-Nagy E, Duncan RE, Ahmadian M, Sul HS. Regulation of triglyceride metabolism. IV. Hormonal regulation of lipolysis in adipose tissue. Am J Physiol Gastrointest Liver Physiol. 2007;293(1):G1–4.

68. Mulla N a, Simonsen L, Bülow J. Post-exercise adipose tissue and skeletal muscle lipid metabolism in humans: the effects of exercise intensity. J Physiol. 2000;524 Pt 3:919–28.

69. Obesity E, Distribution BF, Diet E, Kanaley JA, Cryer PE, Jensen MD. Fatty Acid Kinetic Responses to Exercise. J Clin Invest. 1993;92:255–61.

70. Horowitz JF, Coppack SW, Paramore D, Cryer PE, Zhao G, Klein S, et al. Effect of short-

term fasting on lipid kinetics in lean and obese women. Am J Physiol. 1999;276(2 Pt 1):E278-84.

71. Yen C-LE, Farese R V. Fat breakdown: A function for CGI-58 (ABHD5) provides a new piece of the puzzle. Cell Metab. 2006;3(5):305–7.

72. Kim J, Wall E Van De, Laplante M, Azzara A, Trujillo ME, Hofmann SM, et al. Obesity-associated improvements in metabolic profile through expansion of adipose tissue. J Clin Invest. 2007;117(9):2621–37.

73. Choe SS, Huh JY, Hwang IJ, Kim JI, Kim JB. Adipose tissue remodeling: Its role in energy metabolism and metabolic disorders. Front Endocrinol (Lausanne). 2016;7(APR):1–16.

74. Gealekman O, Guseva N, Hartigan C, Apotheker S, Gorgoglione M, Gurav K, et al. Depot-Specific Differences and Insufficient Subcutaneous Adipose Tissue Angiogenesis in Human Obesity. Circulation. 2011;123(2):186–94.

75. Muir LA, Neeley CK, Meyer KA, Baker NA, Brosius AM, Washabaugh AR, et al. Adipose tissue fibrosis, hypertrophy, and hyperplasia: Correlations with diabetes in human obesity. Obesity. 2016;24(3):597–605.

76. Khan T, Muise ES, Iyengar P, Wang Z V, Chandalia M, Abate N, et al. Metabolic dysregulation and adipose tissue fibrosis: role of collagen VI. Mol Cell Biol. 2009;29(6):1575–91.

77. Cao Y. Angiogenesis modulates adipogenesis and obesity. J Clin Invest. 2007;117(9):2362–8.

78. Christiaens V, Lijnen HR. Role of the fibrinolytic and matrix metalloproteinase systems in development of adipose tissue. Arch Physiol Biochem. 2006;112(4–5):254–9.

79. Strawford A, Christiansen M, Helerstein MK. Adipose tissue triglyceride turnover, de novo lipogenesis, and cell proliferation in humans measured with 2H2O. Am J Physiol Endocrinol Metab. 2004;286:E577–88.

80. Allister CA, Liu L, Lamendola CA, Craig CM, Cushman SW, Hellerstein MK, et al. In vivo 2H2O administration reveals impaired triglyceride storage in adipose tissue of insulin-resistant humans. J Lipid Res. 2015;56(2):435–9.

81. Acosta JR, Douagi I, Andersson DP, Bäckdahl J, Rydén M, Arner P, et al. Increased fat cell size: a major phenotype of subcutaneous white adipose tissue in non-obese individuals with type 2 diabetes. Diabetologia. 2016 Mar 25;59(3):560–70.

82. McLaughlin T, Sherman A, Tsao P, Gonzalez O, Yee G, Lamendola C, et al. Enhanced proportion of small adipose cells in insulin-resistant vs insulin-sensitive obese individuals implicates impaired adipogenesis. Diabetologia. 2007;50(8):1707–15.

83. Jeffery E, Wing A, Holtrup B, Sebo Z, Kaplan JL, Saavedra-Peña R, et al. The Adipose Tissue Microenvironment Regulates Depot-Specific Adipogenesis in Obesity. Cell Metab. 2016;24(1):142–50.

84. Lacasa D, Taleb S, Keophiphath M, Miranville A, Clement K. Macrophage-secreted factors impair human adipogenesis: Involvement of proinflammatory state in preadipocytes. Endocrinology. 2007;148(2):868–77.

85. Xie L, Ortega MT, Mora S, Chapes SK. Interactive changes between macrophages and adipocytes. Clin Vaccine Immunol. 2010;17(4):651–9.

86. Liu LF, Craig CM, Tolentino LL, Choi O, Morton J, Rivas H, et al. Adipose tissue macrophages impair preadipocyte differentiation in humans. PLoS One. 2017;12(2):e0170728.

87. Rosen ED, MacDougald O a. Adipocyte differentiation from the inside out. Nat Rev Mol Cell Biol. 2006;7(12):885–96.

88. Cristancho AG, Lazar MA. Forming functional fat: a growing understanding of adipocyte differentiation. Nat Rev Mol Cell Biol. Nature Publishing Group; 2011;12(11):722–34.

89. Chawla a, Lazar M a. Peroxisome proliferator and retinoid signaling pathways co-regulate preadipocyte phenotype and survival. Proc Natl Acad Sci U S A. 1994;91(5):1786–90.

90. Tontonoz P, Hu E, Spiegelman BM. Stimulation of adipogenesis in fibroblasts by PPARγ2, a lipid-activated transcription factor. Cell. 1994;79(7):1147–56.

91. Macdougald O a, Lane MD. Transcriptional Regulation of Gene Expression During Adipocyte Differentiation. Annu Rev Biochem. 1995;64:345–73.

92. Hausman GJ, Richardson RL. Adipose Tissue Angiogenesis. J Anim Sci. 2004;82:925–34.

93. Scherer PE. Adipose tissue: From lipid storage compartment to endocrine organ. Diabetes. 2006;55(6):1537–45.

94. Frayn KN, Karpe F. Regulation of human subcutaneous adipose tissue blood flow. Int J Obes (Lond). Nature Publishing Group; 2013;38(October):1–29.

95. Coppack SW, Evans RD, Fisher RM, Frayn KN, Gibbons GF, Humphreys SM, et al. Adipose tissue metabolism in obesity: Lipase action in vivo before and after a mixed meal. Metabolism. 1992;41(3):264–72.

96. Bülow J. Human adipose tissue blood flow during prolonged exercise, III. Effect of beta-adrenergic blockade, nicotinic acid and glucose infusion. Scand J Clin Lab Invest. 1981;41(4):415–24.

97. Crandall DL, Hausman GJ, Kral JG. A Review of the Microcirculation of Adipose Tissue : Anatomic, Metabolic, and Angiogenic Perspectives. Microcirculation. 1997;4(2):211–32.

98. Silha J V, Krsek M, Sucharda P, Murphy LJ. Angiogenic factors are elevated in overweight and obese individuals. Int J Obes. 2005;29(11):1308–14.

99. Sun K, Wernstedt Asterholm I, Kusminski CM, Bueno AC, Wang Z V, Pollard JW, et al. Dichotomous effects of VEGF-A on adipose tissue dysfunction. Proc Natl Acad Sci U S

A. 2012;109(15):5874–9.

100. Sung HK, Doh KO, Son JE, Park JG, Bae Y, Choi S, et al. Adipose vascular endothelial growth factor regulates metabolic homeostasis through angiogenesis. Cell Metab. Elsevier; 2013;17(1):61–72.

101. Bråkenhielm E, Veitonmäki N, Cao R, Kihara S, Matsuzawa Y, Zhivotovsky B, et al. Adiponectin-induced antiangiogenesis and antitumor activity involve caspase-mediated endothelial cell apoptosis. Proc Natl Acad Sci U S A. 2004;101(8):2476–81.

102. Haas TL, Nwadozi E. Regulation of skeletal muscle capillary growth in exercise and disease. Appl Physiol Nutr Metab. 2015;40(12):1221–32.

103. Eilken HM, Adams RH. Dynamics of endothelial cell behavior in sprouting angiogenesis. Curr Opin Cell Biol. Elsevier Ltd; 2010;22(5):617–25.

104. Corvera S, Gealekman O. Adipose tissue angiogenesis: Impact on obesity and type-2 diabetes. Biochim Biophys Acta - Mol Basis Dis. Elsevier B.V.; 2014;1842(3):463–72.

105. Nakayama K, Frew IJ, Hagensen M, Skals M, Habelhah H, Bhoumik A, et al. Siah2 regulates stability of prolyl-hydroxylases, controls HIF1a abundance, and modulates physiological responses to hypoxia. Cell. 2004;117(7):941–52.

106. Halberg N, Khan T, Trujillo ME, Wernstedt-Asterholm I, Attie AD, Sherwani S, et al. Hypoxia-Inducible Factor 1α Induces Fibrosis and Insulin Resistance in White Adipose Tissue. Mol Cell Biol. 2009;29(16):4467–83.

107. Hong KH, Ryu J, Han KH. Monocyte chemoattractant protein-1 – induced angiogenesis is mediated by vascular endothelial growth factor-A. Blood. 2015;105(4):1405–8.

108. Tabruyn SP, Griffioen AW. NF-κB: A new player in angiostatic therapy. Angiogenesis. 2008;11(1):101–6.

109. Olsson A-K, Dimberg A, Kreuger J, Claesson-Welsh L. VEGF receptor signalling — in control of vascular function. Nat Rev Mol Cell Biol. 2006;7(5):359–71.

110. Suganami T, Ogawa Y. Adipose tissue macrophages: their role in adipose tissue remodeling. J Leukoc Biol. 2010;88(1):33–9.

111. Townsend LK, Knuth CM, Wright DC. Cycling our way to fit fat. Physiol Rep. 2017;5(7):1–9.

112. Van Pelt DW, Guth LM, Horowitz JF. Aerobic exercise elevates markers of angiogenesis and macrophage IL6 gene expression in the subcutaneous adipose tissue of overweight-to-obese adults. J Appl Physiol. 2017;jap.00614.2017.

113. Ludzki AC, Pataky MW, Cartee GD, Horowitz JF. Acute endurance exercise increases *Vegfa* mRNA expression in adipose tissue of rats during the early stages of weight gain. Appl Physiol Nutr Metab. 2018;43(7):751–4.

114. Spencer M, Unal R, Zhu B, Rasouli N, McGehee RE, Peterson C a, et al. Adipose tissue extracellular matrix and vascular abnormalities in obesity and insulin resistance. J Clin Endocrinol Metab. 2011;96(12):E1990-8.

115. Lin D, Chun TH, Kang L. Adipose extracellular matrix remodelling in obesity and insulin resistance. Biochem Pharmacol. Elsevier Inc.; 2016;119:8–16.

116. Kos K, Wong S, Tan B, Gummesson A, Jernas M, Franck N, et al. Regulation of the Fibrosis and Angiogenesis Promoter SPARC / Osteonectin in Human Adipose Tissue by Weight. Diabetes. 2009;58(August):1780–8.

117. Yurchenco PD. Basement membranes: Cell scaffoldings and signaling platforms. Cold Spring Harb Perspect Biol. 2011;3(2):1–27.

118. Zhou J, Ding M, Zhao Z, Reeders ST. Complete primary structure of the sixth chain of human basement membrane collagen, α6(IV). Isolation of the cDNAs for α6(IV) and comparison with five other type IV collagen chains. J Biol Chem. 1994;269(18):13193–9.

119. Ryan MC, Christiano AM. The functions of laminins: Lessons from in vivo studies. Matrix Biol. 1996;15(6):369–81.

120. Pasarica M, Gowronska-Kozak B, Burk D, Remedios I, Hymel D, Gimble J, et al. Adipose tissue collagen VI in obesity. J Clin Endocrinol Metab. 2009;94(12):5155–62.

121. Divoux A, Clément K. Architecture and the extracellular matrix: The still unappreciated components of the adipose tissue. Obes Rev. 2011;12(501):494–503.

122. Williams AS, Kang L, Wasserman DH. The extracellular matrix and insulin resistance. Trends Endocrinol Metab. Elsevier Ltd; 2015;26(7):357–66.

123. Guglielmi V, Cardellini M, Cinti F, Corgosinho F, Cardolini I, D'Adamo M, et al. Omental adipose tissue fibrosis and insulin resistance in severe obesity. Nutr Diabetes. 2015;5(February).

124. Martinez-santiba G, Lumeng CN. Macrophages and the Regulation of Adipose Tissue Remodeling. Annu Rev Nutr. 2014;34:57–76.

125. Nagase H, Woessner J. Matrix metalloproteinases. J Biol Chem. 1999;(37):1–4.

126. Hopps E, Lo Presti R, Montana M, Noto D, Averna MR, Caimi G. Gelatinases and their tissue inhibitors in a group of subjects with metabolic syndrome. J Investig Med. 2013;61(6):978–83.

127. Jiang H, Zhu H, Chen X, Peng Y, Wang J, Liu F, et al. TIMP-1 transgenic mice recover from diabetes induced by multiple low-dose streptozotocin. Diabetes. 2007;56(1):49–56.

128. Jaworski DM, Sideleva O, Stradecki HM, Langlois GD, Habibovic A, Satish B, et al. Sexually dimorphic diet-induced insulin resistance in obese tissue inhibitor of metalloproteinase-2 (TIMP-2)-deficient mice. Endocrinology. 2011;152(4):1300–13.

129. Pincu Y, Huntsman HD, Zou K, De Lisio M, Mahmassani ZS, Munroe MR, et al. Diet-induced obesity regulates adipose-resident stromal cell quantity and extracellular matrix gene expression. Stem Cell Res. The Authors; 2016;17(1):181–90.

130. Reilly SM, Saltiel AR. Adapting to obesity with adipose tissue inflammation. Nat Rev Endocrinol. Nature Publishing Group; 2017;13(11):633–43.

131. Mathis D. Immunological goings-on in visceral adipose tissue. Cell Metab. Elsevier Inc.; 2013;17(6):851–9.

132. Lumeng CN, Bodzin JL, Saltiel AR. Obesity induces a phenotypic switch in adipose tissue macrophage polarization. J Clin Invest. 2007;117(1):175–84.

133. Yudkin JS, Stehouwer CDA, Emeis JJ, Coppack SW. C-Reactive Protein in Healthy Subjects: Associations with Obesity , Insulin Resistance , and Endothelial Dysfunction. Arter Thromb Vasc Biol. 1999;19:972–9.

134. Weisberg SP, McCann D, Desai M, Rosenbaum M, Leibel RL, Ferrante AW. Obesity is associated with macrophage accumulation in adipose tissue. J Clin Invest. 2003;112(12):1796–808.

135. Lumeng CN, DeYoung SM, Saltiel AR. Macrophages block insulin action in adipocytes by altering expression of signaling and glucose transport proteins. Am J Physiol Endocrinol Metab. 2007;292(1):E166–74.

136. de Luca C, Olefsky JM. Inflammation and insulin resistance. FEBS Lett. 2008;582(1):97–105.

137. Kern PA, Saghizadeh M, Ong JM, Bosch RJ, Deem R, Simsolo RB. The expression of tumor necrosis factor in human adipose tissue. Regulation by obesity, weight loss, and relationship to lipoprotein lipase. J Clin Invest. 1995;95(5):2111–9.

138. Hotamisligil GS, Peraldi P, Budavari A, Ellis R, Morris F, Hotamisligil GS, et al. IRS-1-Mediated Inhibition of Insulin Receptor Tyrosine Kinase Activity in TNF-α-and Obesity-Induced Insulin Resistance. Science (80-). 1996;271(5249):665–8.

139. Orr JS, Puglisi MJ, Ellacott KLJ, Lumeng CN, Wasserman DH, Hasty AH. Toll-like receptor 4 deficiency promotes the alternative activation of adipose tissue macrophages. Diabetes. 2012;61(11):2718–27.

140. Saltiel AR, Olefsky J. Inflammatory mechanisms linking obesity an metabolic disease. J Clin Invest. 2017;127(1):1–4.

141. Drenth JP, Van Uum SH, Van Deuren M, Pesman GJ, Van der Ven-Jongekrijg J, Van der Meer JW. Endurance run increases circulating IL-6 and IL-1ra but downregulates ex vivo TNF-alpha and IL-1 beta production. J Appl Physiol. 1995;79(5):1497–503.

142. Petersen AMW, Pedersen BK. The anti-inflammatory effect of exercise. J Appl Physiol. 2005;98(4):1154–62.

143. Schmittgen TD, Livak KJ. Analyzing real-time PCR data by the comparative CT method. Nat Protoc. 2008;3(6):1101–8.

144. Mootha VK, Daly MJ, Patterson N, Mesirov JP, Golub TR, Tamayo P, et al. PGC-1α-responsive genes involved in oxidative phosphorylation are coordinately downregulated in human diabetes. Nat Genet. 2003;34(3):267–73.

145. Romijn J a, Coyle EF, Sidossis LS, Zhang XJ, Wolfe RR. Relationship between fatty acid delivery and fatty acid oxidation during strenuous exercise. J Appl Physiol. 1995

Dec;79(6):1939–45.

146. van Loon LJ, Greenhaff PL, Constantin-Teodosiu D, Saris WH, Wagenmakers AJ. The effects of increasing exercise intensity on muscle fuel utilisation in humans. J Physiol. 2001 Oct 1;536(Pt 1):295–304.

147. Fabre O, Ingerslev LR, Garde C, Donkin I, Simar D, Barrès R. Exercise training alters the genomic response to acute exercise in human adipose tissue. Epigenomics. 2018;10(8):1033–50.

148. Shinkai S, Shore S, Shek PN, Shephard RJ. Acute Exercise and Immune Function. Int J Sport Med. 1992;13(06):452–61.

149. Peake JM, Neubauer O, Walsh NP, Simpson RJ. Recovery of the immune system after exercise. J Appl Physiol. 2017;122(5):1077–87.

150. Simpson RJ, Bigley AB, Agha N, Hanley PJ, Bollard CM. Mobilizing Immune Cells with Exercise for Cancer Immunotherapy. Exercise and Sport Sciences Reviews. 2017. 1 p.

151. Krüger K, Lechtermann A, Fobker M, Völker K, Mooren FC. Exercise-induced redistribution of T lymphocytes is regulated by adrenergic mechanisms. Brain Behav Immun. 2008;22(3):324–38.

152. Shen Y, Zhou H, Jin W, Lee HJ. Acute exercise regulates adipogenic gene expression in white adipose tissue. Biol Sport. 2016;33(4):381–91.

153. Zeve D, Millay DP, Seo J, Graff JM. Exercise-Induced Skeletal Muscle Adaptations Alter the Activity of Adipose Progenitor Cells. PLoS One. 2016;11(3):e0152129.

154. Varshney P, GUTH LM, ANDERSON CM, RAAJENDIRAN A, WATT MJ, HOROWITZ JF. 287-OR: Acute Exercise Enhances the Differentiation Rate of Human Adipocyte Precursor Cells. Diabetes. 2019 Jun 1;68(Supplement 1):287–OR. Available from: http://diabetes.diabetesjournals.org/content/68/Supplement_1/287-OR.abstract

155. Stinkens R, Brouwers B, Jocken JW, Blaak EE, Teunissen-Beekman KF, Hesselink MK, et al. Exercise training-induced effects on the abdominal subcutaneous adipose tissue phenotype in humans with obesity. J Appl Physiol. 2018;125(5):1585–93.

156. Camera DM, Anderson MJ, Hawley JA, Carey AL. Short-term endurance training does not alter the oxidative capacity of human subcutaneous adipose tissue. Eur J Appl Physiol. 2010;109(2):307–16.

157. Larsen S, Danielsen JH, Søndergård SD, Søgaard D, Vigelsoe A, Dybboe R, et al. The effect of high-intensity training on mitochondrial fat oxidation in skeletal muscle and subcutaneous adipose tissue. Scand J Med Sci Sport. 2015;25(1):e59–69.

158. U.S. Department of Health and Human Services. Physical Activity Guidelines for Americans. 2018. 1-117 p.

159. Ghaben AL, Scherer PE. Adipogenesis and metabolic health. Nat Rev Mol Cell Biol. Springer US; 2019.

160. White U, Ravussin E. Dynamics of adipose tissue turnover in human metabolic health and

disease. Diabetologia. Diabetologia; 2019;62(1):17–23.

161. Sun K, Tordjman J, Clément K, Scherer PE. Fibrosis and adipose tissue dysfunction. Cell Metab. 2013;18(4):470–7.

162. Mifflin MD, St Jeor ST, Hill L a, Scott BJ, Daugherty S a, Koh YO. A new predictive equation in healthy individuals for resting energy. Am J Clin Nutr. 1990;51:241–7.

163. Muir LA, Geletka L, Kiridena S, Griffin C, Delproposto JB, Lucas H, et al. Rapid adipose tissue expansion triggers unique proliferation and lipid accumulation profiles in adipose tissue macrophages. J Leukoc Biol. 2018;(October 2017):1–14.

164. Matsuda M, DeFronzo R. Insulin Sensitivity Indices Obtained From Comparison with the Euglycemic Insulin Clamp. Diabetes Care. 1999;22(9):1462–70.

165. Radikova Z, Koska J, Huckova M, Ksinantova L, Imrich R, Vigas M, et al. Insulin sensitivity indices: A proposal of cut-off points for simple identification of insulin-resistant subjects. Exp Clin Endocrinol Diabetes. 2006;114(5):249–56.

166. Raajendiran A, Ooi G, Bayliss J, O'Brien PE, Schittenhelm RB, Clark AK, et al. Identification of Metabolically Distinct Adipocyte Progenitor Cells in Human Adipose Tissues. Cell Rep. Elsevier; 2019;27(5):1528–1540.e7.

167. Wentworth JM, Naselli G, Brown WA, Doyle L. Pro-inflammatory CD11c+ CD206+ adipose tissue macrophages are associated with insulin resistance in human obesity. Diabetes. 2010;59(July):1648–56.

168. Cawthorn WP, Scheller EL, MacDougald OA. Adipose tissue stem cells meet preadipocyte commitment: Going back to the future. J Lipid Res. 2012;53(2):227–46.

169. Sidney L, Branch M, Dunphy S, Dua H, Hopkinson A. Concise Review: Evidence for CD34 as a Common Marker for Diverse Progenitors. Stem Cells. 2014;32:1380–9.

170. Fairbridge NA, Southall TM, Ayre DC, Komatsu Y, Raquet PI, Brown RJ, et al. Loss of CD24 in mice leads to metabolic dysfunctions and a reduction in white adipocyte tissue. PLoS One. 2015;10(11):1–19.

171. Stanford KI, Goodyear LJ. Muscle-adipose tissue cross talk. Cold Spring Harb Perspect Med. 2018;8(8).

172. Tsiloulis T, Carey AL, Bayliss J, Canny B, Meex RCR, Watt MJ. No evidence of white adipocyte browning after endurance exercise training in obese men. Int J Obes. Nature Publishing Group; 2018;42(4):721–7.

173. Bulló M, García-Lorda P, Peinado-Onsurbe J, Hernández M, Argilés JM, Salas-Salvadó J. TNFα expression of subcutaneous adipose tissue in obese and morbid obese females: Relationship to adipocyte LPL activity and leptin synthesis. Int J Obes. 2002;26(5):652–8.

174. Bertola A, Ciucci T, Rousseau D, Bourlier V, Duffaut C, Bonnafous S, et al. Identification of adipose tissue dendritic cells correlated with obesity-associated insulin-resistance and inducing Th17 responses in mice and patients. Diabetes. 2012;61(9):2238–47.

175. Sundara Rajan S, Longhi MP. Dendritic cells and adipose tissue. Immunology.

2016;149(4):353–61.

176. Cho KW, Zamarron BF, Muir LA, Singer K, Porsche CE, Delproposto JB, et al. Adipose Tissue Dendritic Cells are Independent Contributors to Obesity-Induced Inflammation and Insulin Resistance. J Immunol. 2016;197(9):3650–61.

177. Flegal KM, Kruszon-Moran D, Carroll MD, Fryar CD, Ogden CL. Trends in obesity among adults in the United States, 2005 to 2014. JAMA - J Am Med Assoc. 2016;315(21):2284–91.

178. Hales CM, Carroll MD, Fryar CD, Ogden CL. Prevalence of Obesity Among Adults and Youth: United States, 2015–2016. NCHS data brief, no 288. Hyattsville, MD: National Center for Health Statistics. NCHS data brief, no 288 Hyattsville, MD Natl Cent Heal Stat. 2017;(288):2015–6.

179. Rudnicki M, Abdifarkosh G, Nwadozi E, Ramos S V., Makki A, Sepa-Kishi DM, et al. Endothelial-specific FoxO1 depletion prevents obesity-related disorders by increasing vascular metabolism and growth. Elife. 2018;7:1–25.

180. Cunningham J. Original Body composition a synthetic review general prediction of energy expenditure : as a determinant and a proposed. Am J Clin Nutr. 1991;54(6):963–9.

181. Cornford AS, Hinko A, Nelson RK, Barkan AL, Horowitz JF. Rapid development of systemic insulin resistance with overeating is not accompanied by robust changes in skeletal muscle glucose and. Appl Physiol Nutr Metab. 2013;38(5):512–9.

182. Tam CS, Chaudhuri R, Hutchison AT, Samocha-Bonet D, Heilbronn LK. Skeletal muscle extracellular matrix remodeling after short-term overfeeding in healthy humans. Metabolism. Elsevier Inc.; 2017;67:26–30.

183. McLaughlin T, Craig C, Liu LF, Perelman D, Allister C, Spielman D, et al. Adipose cell size and regional fat deposition as predictors of metabolic response to overfeeding in insulin-resistant and insulin-sensitive humans. Diabetes. 2016;65(5):1245–54.

184. Brøns C, Jensen CB, Storgaard H, Hiscock NJ, White A, Appel JS, et al. Impact of short-term high-fat feeding on glucose and insulin metabolism in young healthy men. J Physiol. 2009;587(10):2387–97.

185. Boden G, Homko C, Barrero CA, Stein TP, Chen X, Cheung P, et al. Excessive caloric intake acutely causes oxidative stress, GLUT4 carbonylation, and insulin resistance in healthy men. Sci Transl Med. 2015;7(304):1–10.

186. Walhin J, Richardson JD, Betts JA, Thompson D. Exercise counteracts the effects of short-term overfeeding and reduced physical activity independent of energy imbalance in healthy young men. J Physiol. 2013;591(24):6231–43.

187. Knudsen SH, Hansen LS, Pedersen M, Dejgaard T, Hansen J, Van Hall G, et al. Changes in insulin sensitivity precede changes in body composition during 14 days of step reduction combined with overfeeding in healthy young men. J Appl Physiol. 2012;113(1):7–15.

188. Krogh-madsen R, Pedersen M, Solomon TPJ, Knudsen SH, Hansen LS, Karstoft K, et al.

Normal physical activity obliterates the deleterious effects of a high-caloric intake. J Appl Physiol. 2014;116(3):231–9.

189. Johannsen DL, Tchoukalova Y, Tam CS, Covington JD. Effect of 8 Weeks of Overfeeding on Ectopic Fat Deposition and Insulin Sensitivity : Testing the " Adipose Tissue Expandability " Hypothesis. Diabetes Care. 2014;37(10):2789–97.

190. Virtue S, Vidal-Puig A. Adipose tissue expandability, lipotoxicity, and the Metabolic Syndrome - An allostatic perspective. Biochim Biophys Acta. 2010;(1801):338–49.

191. Alligier M, Meugnier E, Debard C, Lambert-Porcheron S, Chanseaume E, Sothier M, et al. Subcutaneous adipose tissue remodeling during the initial phase of weight gain induced by overfeeding in humans. J Clin Endocrinol Metab. 2012;97(2):183–92.

192. Gaidhu MP, Anthony NM, Patel P, Hawke TJ, Ceddia RB. Dysregulation of lipolysis and lipid metabolism in visceral and subcutaneous adipocytes by high-fat diet: Role of ATGL, HSL, and AMPK. Am J Physiol - Cell Physiol. 2010;298(4):961–71.

193. Min SY, Learnard H, Kant S, Gealikman O, Rojas-Rodriguez R, Desouza T, et al. Exercise rescues gene pathways involved in vascular expansion and promotes functional angiogenesis in subcutaneous white adipose tissue. Int J Mol Sci. 2019;20(8).

194. Nishimura S, Manabe I, Nagasaki M, Eto K, Yamashita H, Ohsugi M, et al. CD8+ effector T cells contribute to macrophage recruitment and adipose tissue inflammation in obesity. Nat Med. Nature Publishing Group; 2009;15(8):914–20.

195. Sun S, Ji Y, Kersten S, Qi L. Mechanisms of Inflammatory Responses in Obese Adipose Tissue. Annu Rev Nutr [Internet]. 2012;32(1):261–86.

196. Tam CS, Viardot A, Clément K, Tordjman J, Tonks K, Greenfield JR, et al. Short-term overfeeding may induce peripheral insulin resistance without altering subcutaneous adipose tissue macrophages in humans. Diabetes. 2010;59(9):2164–70.

197. Lee BC, Lee J. Cellular and molecular players in adipose tissue inflammation in the development of obesity-induced insulin resistance. Biochim Biophys Acta - Mol Basis Dis. Elsevier B.V.; 2014;1842(3):446–62.

198. Lee YS, Li P, Huh JY, Hwang IJ, Lu M, Kim JI, et al. Inflammation is necessary for long-term but not short-term high-fat diet-induced insulin resistance. Diabetes. 2011;60(10):2474–83.

199. Christiansen T, Bruun JM, Paulsen SK, Ølholm J, Overgaard K, Pedersen SB, et al. Acute exercise increases circulating inflammatory markers in overweight and obese compared with lean subjects. Eur J Appl Physiol. 2013;113(6):1635–42.

200. Lavie CJ, Arena R, Swift DL, Johannsen NM, Sui X, Lee DC, et al. Exercise and the cardiovascular system: Clinical science and cardiovascular outcomes. Circ Res. 2015;117(2):207–19.

201. Lee IM, Shiroma EJ, Lobelo F, Puska P, Blair SN, Katzmarzyk PT, et al. Effect of physical inactivity on major non-communicable diseases worldwide: An analysis of burden of disease and life expectancy. Lancet. Elsevier Ltd; 2012;380(9838):219–29.

202. Swift DL, McGee JE, Earnest CP, Carlisle E, Nygard M, Johannsen NM. The Effects of Exercise and Physical Activity on Weight Loss and Maintenance. Prog Cardiovasc Dis. Elsevier Inc.; 2018;61(2):206–13.

203. Jarrett B, Bloch GJ, Bennett D, Bleazard B, Hedges D. The influence of body mass index, age and gender on current illness: A cross-sectional study. Int J Obes. Nature Publishing Group; 2010;34(3):429–36.

204. Marcelin G, Ferreira A, Liu Y, Atlan M, Aron-Wisnewsky J, Pelloux V, et al. A PDGFRα-Mediated Switch toward CD9high Adipocyte Progenitors Controls Obesity-Induced Adipose Tissue Fibrosis. Cell Metab. 2017;25(3):673–85.

205. Raziel Rojas-Rodriguez, Olga Gealekman, Maxwell E. Kruse, Brittany Rosenthal, Kishore Rao, SoYun Min, Karl D. Bellve, Lawrence M. Lifshitz and SC. Adipose Tissue Angiogenesis Assay. Ethn Dis. 2010;20(1 Supplement):1–26.

APPENDICES

Appendix A – Subcutaneous Adipose Tissue Aspiration Biopsy

- The anterior abdominal wall in the periumbilical area will be cleaned with betadine
- All the following procedures performed using aseptic technique
- Create sterile field around biopsy site and inject 10cc of 1% lidocaine (no epinephrine) with 25g needle, to infiltrate biopsy site (at least 5cm lateral to the umbilicus)
- Inject up to 10cc of 0.5% lidocaine to supplement anesthesia, and to add more saline volume to the biopsy area (**Lidocaine administration should not exceed 4.5mg/kg body weight*)
- Make small incision (2-3mm) in anesthetized biopsy site with tip of #11 scalpel blade
- Insert Coleman aspiration needle into incision site (~3-5cm), blunt needle "cheater" is inserted into syringe to hold vacuum in syringe (blocking the plunger from retracting) during the aspiration process
- With needle inserted, one hand lightly pinches the surface of the biopsy site, while the other hand gentle maneuvers the biopsy needle under the skin for ~60 seconds to extract tissue.
- Remove aspiration needle from incision site and eject tissue onto abdominal pad for cleaning with saline
- Aspiration procedure is then repeated in the same incision, but the needle will be directed to a slightly different "track" within the anesthetized area in order to avoid tissue collection within exactly the same area.
- Aspiration procedure is repeated ~10 times.
- After completion of all tissue extraction, biopsy site will be cleaned with alcohol, steri-strip placed to close the small incision, and tegaderm bandage placed over the steri-strips
- Ice will be applied to biopsy site (as desired) for 10-20 min
- Participant is instructed to keep the bandages on for 5 days.

As an alternative approach, a 1.5in x 16g needle may be used for tissue aspiration instead of the Spirotri cannula, under the same conditions as described above.

Appendix B – RNA Sequencing Sample Preparation and Interpretation Tools

Prep/optimization

- Meet with RNA sequencing/bioinformatics core to create a project plan
- Run some test samples through RNA QC to determine if isolation with the kit of choice provided sufficient yield/quality of RNA – in our case, the Qiagen RNeasy Plus Universal Mini Kit + Turbo DNAse treatment had good quality and purity based on RIN, 260/230, and DNA Qubit – note quality scores are generally lower for fatty tissues
- Then did the same with our real samples before forwarding to sequencing core – i.e. created original submission with final samples as QC only; with a note that the samples would be forwarded for sequencing only after QC was discussed with the core.
    - Note: communication between parties was challenging here! Phone is best but not always available.

RNA Isolation

- Prep: cool tissue lyser blocks and centrifuge, acquire dry ice for chipping/homogenizing, reconstitute kit reagents for RNeasy kit, clean all supplies, gloves, and bench top with RNAse-away (repeat as needed throughout procedure→essential for RNA purity and yield), label tubes:
    - 1 set round bottom 2mL homogenization tubes
    - 1 set 0.6mL or smaller for Turbo purification
    - 3x1.5mL microcentrifuge tubes - label the final set with genomics core ID's (need to create online submission before isolation) if applicable
- Chip 40-60mg adipose tissue using clean scalpel in mortar with liquid nitrogen (blood contamination becomes a problem with larger pieces)
- Store samples in eppendorf tubes on dry ice until immediately before lysing in Cartee lab tissue lyser
- Prep 2mL heavy-duty round-bottom eppendorf tubes with 2 steel ball bearings (RNAse-cleaned) and 1mL RNA-Stat 60 on RNAse-cleaned ice bucket
- Add samples to RNA-Stat 60 quickly and lyse 60 seconds (max speed) on Cartee lab tissue lyser→check for homogenous slurry→repeat for 30-60 seconds as needed until sample is homogenous
- Spin samples at 12 000G, 10 min, 4C to separate fat to top
- Carefully waste top fat layer if too thick to access infranatant without contamination
- Transfer infranatant (avoiding pelleted waste) into new 1.5mL eppendorf, entering through middle of sample to avoid lipid contamination
- Proceed to step 5 of RNeasy Plus Universal Mini Kit Protocol (Qiagen Cat 73404) - adjustments are noted here, but see kit protocol for full details:

- Add 100uL gDNA eliminator solution (proportional to starting volume - in this case ~900uL starting volume), securely cap the tube containing the homogenate, and shake it vigorously for 15s (vortex). Addition of gDNA eliminator solution will effectively reduce genomic DNA contamination fo the aqueous phase; but contrary to the kit protocol, **an additional DNAse treatment has been found to be necessary in our hands**
- Add 180uL chloroform. Securely cap the tube containing the homogenate, and shake it vigorously for 15 s (vortex). Thorough mixing is important for subsequent phase separation.
- Place the tube containing the homogenate on the benchtop at room temperature for a full 3 min - we have occasionally observed insufficient separation following the spin; if this happens, mix samples and re-spin.
- Centrifuge at 12000G for 15 min at 4C. After centrifugation, heat the centrifuge to room temperature for subsequent steps.
- Transfer the upper aqueous phase (~500uL) to a new microcentrifuge tube
- Add one volume (e.g. 500uL) of 70% ethanol, mix thoroughly by pipetting, do not centrigure; proceed to next step immediately
- Transfer up to 700uL of the sample to an RNeasy mini spin column placed in a 2mL collection tube (supplied) by ejecting straight into the tube (no need to have the tip right on the membrane). Close the lid gently and centrifuge for 15s at ≥8000G at room temp. Discard the flow through (DO NOT BLEACH WASTE)
- Repeat with the remainder of the sample (can use suction to discard flow through for efficiency in large batch processing)
- Add 700uL buffer RWT to the RNeasy spin column: angle the tip and inject into the column inner rim; should be able to see the solutions swirl down and into the column using this technique; do not need to touch the tip to the rim in order to expedite by enabling the same tip throughout. Close lid gently and centrifuge for 15 s at ≥8000G to wash the membrane. Discard flow through.
- Add 500uL buffer RPE, cap, spin at same settings, discard flow through
- Add 500uL buffer RPE, cap, spin for 2 min, discard flow through
- Place the spin column in a new 2mL collection tube and discard the old tube with the flow through. Close the lid gently, centrifuge at full speed (kept at 8000G here) for 1 min to avoid flow through/RPE carryover.
- Place the RNeasy spin column in a new 1.5mL collection tube and add 30uL RNAse free water directly to the spin column membrane (pipet with tip close to membrane - can touch membrane if needed, but if not can use same tip throughout). Ensure accurate pipet especially for this step! Cap and elute RNA by spinning for 1 min at ≥8000G - stop at this step due to typically low yields.

- Proceed to Turbo DNAse treatment. Could add an on-column DNAse treatment to the steps above, but we had to clean already isolated RNA and therefore used the Turbo DNA-free kit for post-isolation DNA cleanup: Invitrogen cat AM1907. See kit protocol for cleanup, adjusted protocol outlined here:
  - Warm incubator to 37C
  - Transfer RNA to 0.6mL tubes or smaller for sufficient supernatant recvoery
  - Add 0.1x final volume 10X Turbo DNAse buffer and 1uL of Turbo DNase enzyme to the RNA and mix gently; final volume can be 10-100uL; typically:

        - 30uL RNA (based on availability from isolation procedure)
        - 1uL DNase (constant)
        - 3.4uL buffer (10% of final volume)
        - 34.4uL total
    - Incubate at 37C for 30 min
    - Resuspend the DNAse inactivation reagent by flicking or vortexing
    - Add resuspended DNase inactivation reagent (2uL or 0.1 volume - whichever is greater - 3.4uL in this case) and mix well
    - Incubate for 5 min at room temperature and flick 2-3 times during the incubation period to redisperse the DNase inactivation reagent
    - Centrifuge samples (10000G, 1.5 min, room temp) and carefully transfer the supernatant containing the RNA to a fresh tube (labeled for genomics core if needed); do not disturb the pellet of DNase inactivation reagent - this is the final purified RNA specimen
- Send 5uL to core for QC – or for proper sequencing samples, send the full 30uL to the core for QC and this means the tubes will have to have submission ID's on them and the tubes will get freeze-thawed one additional time following the QC discussion – this is not a big problem in the big picture – RNA quality has been stable for a couple freeze-thaws in our hands.

Library Prep

- QuantSeq library prep (by Lexogen) was run by Melissa Coon (uniqname ricotta)
- QC (by bioanalyzer) was emailed to us as a PDF (on SML drive)
- qPCR was performed to confirm these results (all by sequencing core). Melissa confirmed that QC looked good after library prep.

Analysis

- Data was then organized and processed and run through the pipeline by Grace Kenney (grkenney) - see report from core on the drive
- QC for alignment to the reference genome was performed by FastQC - see multiQC report on the drive - most important outcome is overall alignment (overall ~80%)
- LogCPM values were filtered for variance stabilization and removal of low/unexpressed genes
- edgeR normalization was performed using trimmed mean of M values technique prior to fitting the data
- Dispersion plot confirms that variation is not tightly linked to expression as a final check before fitting the data
- The linear model is described here, with the addition of paired variables used for each individual; the limma package of Bioconductor was used for fitting the model differential expression was assessed with sample-level quality weights used: https://www.bioconductor.org/packages/release/bioc/vignettes/limma/inst/doc/usersguide.pdf
- FDR p-value was used

- GSEA analysis was performed (BROAD institute) - steps outlined here:

GSEA analysis performed following user guide from the GSEA website:
http://software.broadinstitute.org/gsea/doc/GSEAUserGuideFrame.html

1. Download GSEA to run online via JAVA (there are various slightly different versions, I use the easiest one to launch, which runs online)
2. Prepare 2 key files:
    a. Expression dataset – I created in excel (for ease of sorting groups) and saved as a tab-delimited .txt - can follow existing template
    b. Phenotype labels – I created in excel and saved as .cls – see previous examples or user guide for formatting guidelines - first # = #samples, second # = #distinct groups, third # always 1. To save as .cls file:
        i. Save as tab-delimited text file
        ii. On a Mac: in the finder window, right click -> select "Get Info"
        iii. Name + extension
        iv. Uncheck hide extension
        v. Manually change .txt to .cls
3. Gene sets – can choose from the MSigDb – I used:
        i. GO - biological processes
        ii. Hallmark
        iii. Curated KEGG
        iv. Curated Reactome
        v. GO molecular function
        vi. GO cellular component

        Note: I had challenges running e.g. "GO - all" because I think it was too many gene sets combined for the processing of the computer (error message = JAVA heap space)
4. Run GSEA:
    a. Only need to use one expression data set as it works with both phenotype labels
    b. Gene sets database - toggle between the list above (or other options)
    c. Number of permutations - start with 10 to test the input; then run with 1000 as default
    d. Toggle between both phenotype labels: pre/post and hiit/mict (any of the hiit/mict comparisons can be made with that phenotype label sheet) depending on the comparison being run
    e. Note that *the same "feature" i.e. gene or probe identifiers need to be used across all these files;* I used the default from the data from the core, which didn't work with **"collapse data to symbols" set at True - I had to change it to false**
    f. Permutation type did not work with Phenotype; I had to change it to gene_set
    g. Chip annotations – I used NCBI by default

I ran comparisons: HIIT Pre vs. HIIT Post, MICT Pre vs. MICT Post

Interpretation: http://www.gsea-msigdb.org/gsea/doc/GSEAUserGuideFrame.html?_Interpreting_GSEA_Results

- GSEA goal = determine whether members of a gene set are randomly distributed throughout a list (which ranks genes by DE, with no minimum threshold) or whether they tend to occur toward the top or bottom; indicating if a gene set is related to the phenotype (e.g. pre vs. post exercise)
- Key outcome = Enrichment Score (ES) - reflects this degree to which a gene set is overrepresented at the extremes (top/bottom) of an entire ranked gene list - calculated by walking down the full list of genes and counting a running sum statistic upon encountering a gene from the gene set - or decreasing it when encountering a gene not in this gene set - so ES is the max deviation from 0 and corresponds to a weighted Kolmogorov-Smirnov-like statistic
    - Positive score = gene set enrichment at the top of the ranked list; increased by the intervention/disease phenotype
    - Negative score = enrichment at the bottom; decreased by the intervention/disease phenotype
- Significance level of ES is based on comparing to ES's of a ton of permutations of either phenotype labels or random gene sets - considered in the nominal p value - limited value because not corrected for multiple comparisons
- FDR is also calculated as the estimated probability that a given normalized ES (normalized for the size of the gene set) represents a false positive - computed by comparing the tails of the observed and null distributions for NES - so this is what we want to go by because it accounts for multiple comparisons

Appendix C – Leading Edge Genes from GSEA

IL6 JAK STAT3				
PROBE	RANK IN GENE LIST	RANK METRIC SCORE	RUNNING ES	CORE ENRICHMENT
PIM1	39	0.35023	0.042094	Yes
MAP3K8	258	0.246771	0.056007	Yes
IRF1	263	0.246124	0.087523	Yes
TNFRSF1B	268	0.244102	0.118777	Yes
A2M	282	0.238903	0.148615	Yes
PF4	283	0.238839	0.179519	Yes
ACVR1B	316	0.233403	0.207074	Yes
TNFRSF1A	356	0.227495	0.233287	Yes
STAT3	412	0.219341	0.257123	Yes
TYK2	422	0.217919	0.284576	Yes
IL17RA	483	0.210238	0.30682	Yes
IL1R2	563	0.201182	0.326322	Yes
LTB	673	0.191081	0.342038	Yes
CSF2RB	716	0.188037	0.362898	Yes
CSF3R	790	0.181934	0.380406	Yes
ITGB3	830	0.178058	0.400222	Yes
PTPN1	907	0.172388	0.416246	Yes
IL18R1	989	0.166961	0.431155	Yes
IL4R	1109	0.158119	0.44178	Yes
TLR2	1419	0.136729	0.433934	Yes
IL10RB	1492	0.132801	0.445167	Yes
PIK3R5	1536	0.129842	0.458414	Yes
BAK1	1614	0.1248	0.468198	Yes
IL2RG	1626	0.124225	0.483363	Yes
IL2RA	1682	0.121277	0.49451	Yes
CCR1	2025	0.103775	0.479673	Yes
CD14	2084	0.101401	0.488	Yes
TGFB1	2102	0.100768	0.499633	Yes
ITGA4	2252	0.093426	0.499408	Yes
PTPN2	2268	0.092617	0.510152	Yes
CNTFR	2345	0.089186	0.515411	Yes
SOCS3	2779	0.070914	0.488801	No
CD44	2824	0.068896	0.49408	No

IL13RA1	3244	0.052716	0.466273	No
CXCL9	3284	0.051116	0.469663	No
CXCL10	3290	0.050857	0.475831	No
PLA2G2A	3479	0.044581	0.466062	No
GRB2	3504	0.043988	0.46977	No
HMOX1	4354	0.015867	0.401658	No
ACVRL1	4782	0.002849	0.366737	No
STAT1	5339	-0.01321	0.322496	No
JUN	5523	-0.01781	0.309676	No
FAS	5978	-0.03021	0.276064	No
TNFRSF21	6129	-0.03416	0.268087	No
PTPN11	6240	-0.03696	0.263779	No
STAT2	6430	-0.04194	0.253586	No
IRF9	6500	-0.04371	0.253539	No
IFNGR2	6743	-0.05066	0.240094	No
IFNAR1	6795	-0.05196	0.242602	No
PDGFC	7191	-0.06215	0.217998	No
CBL	8258	-0.09011	0.141559	No
IL15RA	8270	-0.0906	0.152373	No
CD9	8282	-0.09092	0.163227	No
HAX1	8360	-0.0934	0.168949	No
MYD88	8475	-0.09729	0.172115	No
CD36	8583	-0.10021	0.176239	No
CSF1	8596	-0.10059	0.188262	No
OSMR	8710	-0.10427	0.192416	No
IL1R1	8925	-0.1109	0.18908	No
IL6ST	9526	-0.13086	0.156425	No
LEPR	9633	-0.13514	0.16515	No
IFNGR1	10342	-0.16569	0.128077	No
STAM2	10486	-0.17199	0.138512	No

ALLOGRAFT REJECTION				
PROBE	RANK IN GENE LIST	RANK METRIC SCORE	RUNNING ES	CORE ENRICHMENT
CCR2	161	0.273351	0.003238	Yes
CCND3	204	0.262347	0.015705	Yes
CCL5	265	0.245956	0.025677	Yes
PF4	283	0.238839	0.038793	Yes
HLA-E	294	0.237077	0.052384	Yes
ELF4	307	0.234343	0.065642	Yes
EGFR	378	0.224706	0.07349	Yes
IFNAR2	408	0.219636	0.08444	Yes

SPI1	411	0.219397	0.097621	Yes
BCL3	418	0.218644	0.110423	Yes
LY75	546	0.202693	0.112191	Yes
TLR1	581	0.199413	0.121494	Yes
LTB	673	0.191081	0.12555	Yes
CFP	674	0.191069	0.137174	Yes
LYN	677	0.190784	0.148614	Yes
HCLS1	707	0.188488	0.157668	Yes
PTPRC	713	0.188202	0.168702	Yes
APBB1	720	0.187452	0.179606	Yes
CD1D	740	0.185949	0.189338	Yes
SRGN	791	0.181817	0.196241	Yes
GBP2	794	0.181486	0.207115	Yes
PRKCB	913	0.172171	0.207774	Yes
MAP4K1	971	0.168024	0.213255	Yes
IL16	976	0.167751	0.223128	Yes
LCP2	1000	0.165986	0.231313	Yes
NCF4	1054	0.162273	0.236776	Yes
TAP1	1100	0.158569	0.24268	Yes
IL4R	1109	0.158119	0.251634	Yes
TLR6	1203	0.151238	0.253099	Yes
TAPBP	1239	0.14855	0.259225	Yes
ITGAL	1247	0.148209	0.26766	Yes
PTPN6	1252	0.147826	0.27632	Yes
TRAF2	1253	0.147807	0.285312	Yes
CD3G	1401	0.137756	0.281466	Yes
TLR2	1419	0.136729	0.28837	Yes
CSK	1521	0.131294	0.287956	Yes
JAK2	1525	0.130903	0.29567	Yes
CD2	1551	0.128763	0.301424	Yes
ICOSLG	1567	0.127834	0.307954	Yes
HIF1A	1584	0.126683	0.31433	Yes
IL2RG	1626	0.124225	0.318477	Yes
IL2RA	1682	0.121277	0.32128	Yes
CCL19	1691	0.120851	0.327967	Yes
WAS	1720	0.119089	0.332883	Yes
CD247	1745	0.117995	0.338065	Yes
B2M	1766	0.117205	0.343531	Yes
RPL39	1780	0.116504	0.349538	Yes
CD96	1830	0.113469	0.352365	Yes
CCR1	2025	0.103775	0.342542	Yes
CTSS	2045	0.102894	0.347222	Yes
GLMN	2064	0.102235	0.351944	Yes

TGFB1	2102	0.100768	0.354997	Yes
HLA-A	2157	0.098282	0.356485	Yes
IRF7	2180	0.096929	0.360551	Yes
PRF1	2189	0.096619	0.365764	Yes
HLA-DOA	2343	0.089241	0.358467	Yes
CD74	2346	0.089176	0.363726	Yes
GZMB	2370	0.08827	0.367183	Yes
NPM1	2476	0.083262	0.363515	No
FGR	2563	0.07965	0.361208	No
CD86	2656	0.075952	0.358176	No
ACVR2A	2836	0.068484	0.347454	No
F2R	2974	0.063265	0.339908	No
GPR65	3059	0.059966	0.33657	No
EIF3A	3102	0.058042	0.336607	No
GZMA	3206	0.054607	0.331362	No
CXCL9	3284	0.051116	0.328068	No
HLA-DRA	3289	0.050917	0.330832	No
HLA-DMB	3323	0.050056	0.331133	No
FCGR2B	3854	0.031497	0.288967	No
RPS9	4142	0.02246	0.266462	No
TIMP1	4254	0.019041	0.258388	No
BCL10	4294	0.017611	0.256216	No
ICAM1	4401	0.014576	0.248286	No
ST8SIA4	4488	0.011639	0.241841	No
IL27RA	4491	0.011527	0.242376	No
HLA-DQA1	4590	0.008873	0.234765	No
PSMB10	4882	-5.08E-04	0.210592	No
IGSF6	4934	-0.0021	0.206478	No
TAP2	5008	-0.00432	0.200669	No
GCNT1	5203	-0.00928	0.185098	No
STAT1	5339	-0.01321	0.174673	No
RPS19	5507	-0.01733	0.161837	No
FLNA	5539	-0.01822	0.160368	No
ABI1	5643	-0.02139	0.153102	No
STAB1	5805	-0.02536	0.141254	No
CD47	5870	-0.02705	0.137576	No
FAS	5978	-0.03021	0.130514	No
IKBKB	6050	-0.03186	0.126547	No
EIF3D	6210	-0.03632	0.115532	No

RPL9	6252	-0.03733	0.114393	No
CD4	6267	-0.03784	0.11553	No
KLRD1	6325	-0.03917	0.113172	No
CCL13	6328	-0.03922	0.115392	No
WARS	6355	-0.03993	0.115658	No
UBE2D1	6406	-0.0414	0.114018	No
IFNGR2	6743	-0.05066	0.089154	No
ITGB2	6778	-0.05156	0.089463	No
LY86	6921	-0.05482	0.080987	No
MMP9	7044	-0.05808	0.074374	No
MAP3K7	7336	-0.06586	0.054176	No
EIF4G3	7345	-0.06603	0.057528	No
TPD52	7573	-0.07123	0.042981	No
HLA-DMA	7973	-0.08193	0.014779	No
IL15	7993	-0.08239	0.018211	No
C2	8177	-0.08745	0.00831	No
RIPK2	8192	-0.08773	0.012483	No
RPS3A	8224	-0.08877	0.015305	No
DEGS1	8533	-0.09873	-0.00431	No
CSF1	8596	-0.10059	-0.00334	No
RARS	8659	-0.10257	-0.00226	No
INHBB	8690	-0.10373	0.001554	No
CCL4	8744	-0.10548	0.003563	No
TGFB2	8807	-0.1076	0.004951	No
EIF3J	8863	-0.10896	0.007005	No
DARS	8866	-0.10903	0.013472	No
CCL2	8870	-0.10908	0.019858	No
AARS	8898	-0.11005	0.024307	No
THY1	8997	-0.11332	0.02305	No
TLR3	9009	-0.11386	0.029062	No
CD28	9031	-0.11445	0.034278	No
CAPG	9056	-0.11524	0.039292	No
MTIF2	9112	-0.11698	0.041834	No
CCND2	9543	-0.13165	0.014078	No
BCAT1	9703	-0.13808	0.009254	No
CD40	9710	-0.13828	0.017167	No
NME1	9906	-0.1465	0.00986	No
GALNT1	10206	-0.15896	-0.00534	No
IFNGR1	10342	-0.16569	-0.00649	No
NCK1	10415	-0.16876	-0.00221	No
IRF8	10480	-0.17181	0.002921	No
ETS1	10688	-0.18286	-0.00317	No

EIF5A	10897	-0.19538	-0.00859	No
ABCE1	11423	-0.23605	-0.03789	No
BRCA1	11443	-0.23774	-0.02501	No
MRPL3	11560	-0.25048	-0.01942	No
AKT1	11588	-0.25375	-0.00623	No
UBE2N	11782	-0.28175	-0.00514	No
SOCS5	11856	-0.29412	0.00668	No
HDAC9	11916	-0.30719	0.020461	No

TNFA SIGNALING VIA NFKB

PROBE	RANK IN GENE LIST	RANK METRIC SCORE	RUNNING ES	CORE ENRICHMENT
IER3	14	0.402595	0.018994	Yes
ZC3H12A	16	0.395612	0.038722	Yes
RNF19B	21	0.383896	0.057613	Yes
NFIL3	30	0.364614	0.075205	Yes
EHD1	74	0.317851	0.08754	Yes
SERPINB8	86	0.308278	0.102061	Yes
REL	88	0.305275	0.117265	Yes
KLF10	120	0.289926	0.129201	Yes
NINJ1	184	0.266677	0.137307	Yes
KDM6B	248	0.248453	0.144501	Yes
MAP3K8	258	0.246771	0.156109	Yes
IRF1	263	0.246124	0.1681	Yes
CCL5	265	0.245956	0.180334	Yes
IER2	302	0.234982	0.189102	Yes
NR4A2	363	0.225825	0.195412	Yes
MXD1	383	0.224009	0.205047	Yes
BCL3	418	0.218644	0.213164	Yes
SLC2A3	439	0.215758	0.222302	Yes
PTPRE	440	0.215469	0.233092	Yes
IL7R	471	0.211884	0.241204	Yes
YRDC	551	0.202178	0.244747	Yes
NAMPT	554	0.202081	0.2547	Yes
CEBPB	668	0.191321	0.254868	Yes
BTG2	682	0.190508	0.263325	Yes
DUSP4	694	0.18975	0.271911	Yes
DDX58	701	0.18888	0.28087	Yes
RELA	843	0.177197	0.277998	Yes
BHLHE40	899	0.172826	0.282071	Yes
SNN	930	0.171236	0.288147	Yes
CCNL1	948	0.169946	0.295241	Yes

CFLAR	1065	0.161145	0.293648	Yes
TANK	1066	0.161049	0.301713	Yes
TAP1	1100	0.158569	0.306904	Yes
RELB	1124	0.157228	0.312862	Yes
LITAF	1147	0.155674	0.318825	Yes
MAP2K3	1151	0.155437	0.326359	Yes
IFIT2	1245	0.148274	0.326037	No
TLR2	1419	0.136729	0.318473	No
ICOSLG	1567	0.127834	0.31263	No
HES1	1569	0.127701	0.318941	No
BIRC3	1759	0.117654	0.309089	No
ATP2B1	1782	0.116478	0.31309	No
DUSP5	1861	0.11116	0.312159	No
TGIF1	1910	0.109159	0.313627	No
PPP1R15A	1928	0.108454	0.317642	No
FOSL2	2137	0.099309	0.305289	No
ZBTB10	2160	0.098208	0.308374	No
MCL1	2227	0.094797	0.307623	No
JUNB	2235	0.09419	0.311757	No
ABCA1	2341	0.089301	0.307482	No
F3	2355	0.08877	0.310845	No
PFKFB3	2501	0.082248	0.302885	No
SDC4	2534	0.080734	0.304262	No
EFNA1	2630	0.076859	0.300198	No
SOCS3	2779	0.070914	0.291421	No
PDE4B	2808	0.069623	0.292575	No
CD44	2824	0.068896	0.294775	No
DENND5A	2891	0.066235	0.292595	No
TNFAIP6	2956	0.064195	0.290478	No
TNC	2966	0.063684	0.292917	No
SLC2A6	2987	0.062886	0.294401	No
PLEK	2996	0.06261	0.296869	No
SMAD3	3255	0.052328	0.277999	No
CXCL10	3290	0.050857	0.277713	No
GADD45A	3309	0.0504	0.278738	No
PDLIM5	3352	0.049091	0.277698	No
KLF9	3367	0.048396	0.278955	No
B4GALT1	3423	0.046745	0.276714	No
SAT1	3442	0.046065	0.277522	No
SOD2	3488	0.044359	0.275995	No
ZFP36	3540	0.042564	0.273878	No
PLK2	3645	0.03837	0.267136	No
TRIP10	3957	0.02803	0.242634	No

GPR183	3986	0.026971	0.241652	No
SPSB1	4119	0.02299	0.231808	No
TSC22D1	4145	0.022317	0.230843	No
GFPT2	4161	0.021907	0.230691	No
TNFAIP8	4305	0.017105	0.219635	No
TNIP1	4318	0.01671	0.219473	No
VEGFA	4380	0.015145	0.21515	No
B4GALT5	4395	0.01477	0.214723	No
ICAM1	4401	0.014576	0.215037	No
TRAF1	4517	0.010914	0.206004	No
PMEPA1	4533	0.010568	0.205284	No
FOS	4598	0.008663	0.200386	No
KYNU	4756	0.003582	0.187488	No
PLAUR	5005	-0.00427	0.167044	No
MAFF	5040	-0.00508	0.164466	No
DRAM1	5190	-0.00889	0.152499	No
BTG3	5205	-0.00932	0.1518	No
ID2	5261	-0.01087	0.147763	No
BIRC2	5278	-0.01148	0.147005	No
JUN	5523	-0.01781	0.127572	No
BCL2A1	5541	-0.01825	0.12707	No
BMP2	5576	-0.01927	0.125203	No
NFE2L2	5652	-0.02152	0.120033	No
IRS2	5918	-0.02866	0.099394	No
TRIB1	5937	-0.02915	0.099354	No
ACKR3	5938	-0.02915	0.100814	No
RCAN1	5979	-0.03021	0.098995	No
IFNGR2	6743	-0.05066	0.037975	No
PHLDA1	7077	-0.05893	0.013187	No
TNFAIP2	7157	-0.06116	0.009669	No
CDKN1A	7289	-0.06459	0.001992	No
ETS2	7440	-0.06851	-0.00707	No
STAT5A	7525	-0.0702	-0.01055	No
PLAU	7599	-0.07198	-0.01303	No
MYC	7606	-0.07212	-0.00992	No
CEBPD	7622	-0.07244	-0.00754	No
DNAJB4	7722	-0.07504	-0.01203	No
TIPARP	7732	-0.0753	-0.00901	No
RHOB	7788	-0.07677	-0.00975	No
IFIH1	8001	-0.08262	-0.02327	No
RIPK2	8192	-0.08773	-0.0347	No
LAMB3	8243	-0.08958	-0.03438	No
IL15RA	8270	-0.0906	-0.03201	No

EGR3	8428	-0.09555	-0.0403	No
MSC	8497	-0.0978	-0.04107	No
KLF4	8499	-0.09781	-0.03625	No
CSF1	8596	-0.10059	-0.03921	No
PTGER4	8655	-0.10248	-0.03891	No
TNIP2	8656	-0.10248	-0.03378	No
CCND1	8668	-0.10305	-0.02954	No
SQSTM1	8709	-0.10426	-0.02765	No
PNRC1	8729	-0.10494	-0.02398	No
CCL4	8744	-0.10548	-0.01986	No
CCL2	8870	-0.10908	-0.02481	No
EIF1	8965	-0.11224	-0.02702	No
TUBB2A	9167	-0.11857	-0.03783	No
NFAT5	9190	-0.11934	-0.03368	No
CD83	9348	-0.12488	-0.04051	No
KLF2	9525	-0.13084	-0.04862	No
IL6ST	9526	-0.13086	-0.04206	No
PANX1	9581	-0.13319	-0.03989	No
DUSP1	9745	-0.13983	-0.04647	No
KLF6	9917	-0.14697	-0.05335	No
SERPINE1	10028	-0.15133	-0.05494	No
GADD45B	10211	-0.15906	-0.06213	No
MARCKS	10219	-0.1595	-0.05473	No
SGK1	10244	-0.16047	-0.04869	No
EDN1	10297	-0.16336	-0.04484	No
PHLDA2	10346	-0.16579	-0.04054	No
ATF3	10507	-0.17301	-0.0452	No
HBEGF	10658	-0.18115	-0.04862	No
G0S2	10669	-0.18164	-0.04036	No
NFKB2	10783	-0.18742	-0.04039	No
EGR1	10921	-0.19696	-0.04194	No
SPHK1	11094	-0.20906	-0.0458	No
BTG1	11135	-0.21265	-0.03848	No
IER5	11179	-0.21556	-0.03127	No
NFKB1	11234	-0.21946	-0.02478	No
JAG1	11275	-0.22356	-0.01691	No
TNFAIP3	11314	-0.22708	-0.00871	No
LDLR	11658	-0.26305	-0.02411	No
BCL6	11689	-0.26717	-0.01323	No
CCRL2	11793	-0.28362	-0.0076	No
NFKBIA	12095	-0.38042	-0.01363	No
FUT4	12098	-0.3819	0.005331	No

INFLAMMATORY RESPONSE				
PROBE	RANK IN GENE LIST	RANK METRIC SCORE	RUNNING ES	CORE ENRICHMENT
RAF1	116	0.29082	0.007594	Yes
ADM	211	0.259639	0.015169	Yes
IRF1	263	0.246124	0.025518	Yes
CCL5	265	0.245956	0.040013	Yes
TNFRSF1B	268	0.244102	0.054315	Yes
ACVR1B	316	0.233403	0.064242	Yes
CD55	317	0.233291	0.07807	Yes
FFAR2	375	0.224862	0.08666	Yes
MXD1	383	0.224009	0.099355	Yes
RASGRP1	419	0.218449	0.109393	Yes
PROK2	433	0.216515	0.121146	Yes
PTPRE	440	0.215469	0.133419	Yes
IL10RA	461	0.213037	0.144383	Yes
IL7R	471	0.211884	0.156194	Yes
KCNA3	487	0.209764	0.16738	Yes
CCR7	553	0.202094	0.173955	Yes
NAMPT	554	0.202081	0.185933	Yes
TLR1	581	0.199413	0.195591	Yes
IFITM1	587	0.198972	0.206969	Yes
FPR1	597	0.197512	0.217928	Yes
TNFSF10	663	0.191865	0.223896	Yes
LYN	677	0.190784	0.234124	Yes
BTG2	682	0.190508	0.245083	Yes
SELL	724	0.187377	0.252781	Yes
CSF3R	790	0.181934	0.258161	Yes
ITGB3	830	0.178058	0.265473	Yes
PTAFR	832	0.177936	0.275936	Yes
RELA	843	0.177197	0.285608	Yes
IL18R1	989	0.166961	0.28345	Yes
LCP2	1000	0.165986	0.292457	Yes
SEMA4D	1103	0.158442	0.293369	Yes
CD82	1105	0.158325	0.30267	Yes
IL4R	1109	0.158119	0.311792	Yes
TAPBP	1239	0.14855	0.309873	Yes
AQP9	1285	0.145308	0.314745	Yes
TLR2	1419	0.136729	0.311793	Yes
PIK3R5	1536	0.129842	0.309845	Yes
ICOSLG	1567	0.127834	0.314928	Yes
HIF1A	1584	0.126683	0.321107	Yes
ATP2B1	1782	0.116478	0.311634	No

CD14	2084	0.101401	0.292621	No
C5AR1	2092	0.101165	0.298036	No
IRF7	2180	0.096929	0.296548	No
SLC7A2	2196	0.096397	0.301015	No
ABCA1	2341	0.089301	0.294337	No
RHOG	2348	0.08903	0.299115	No
F3	2355	0.08877	0.303878	No
RNF144B	2398	0.08714	0.305552	No
CD48	2523	0.08109	0.30005	No
NMI	2589	0.078581	0.299304	No
EIF2AK2	2742	0.072418	0.29096	No
PDE4B	2808	0.069623	0.289683	No
ACVR2A	2836	0.068484	0.291498	No
ADRM1	2856	0.067442	0.293916	No
CMKLR1	2912	0.065556	0.293229	No
TNFAIP6	2956	0.064195	0.293459	No
P2RX7	3071	0.059359	0.2875	No
LY6E	3210	0.054324	0.279248	No
CXCL9	3284	0.051116	0.276209	No
CXCL10	3290	0.050857	0.278808	No
GABBR1	3581	0.040881	0.257123	No
MMP14	3701	0.036164	0.249373	No
GPR183	3986	0.026971	0.227362	No
TPBG	4158	0.021967	0.214449	No
LPAR1	4185	0.021263	0.213548	No
TIMP1	4254	0.019041	0.209023	No
RGS16	4376	0.015255	0.199868	No
ICAM1	4401	0.014576	0.198737	No
SCN1B	4433	0.013358	0.196952	No
PSEN1	4573	0.00934	0.18595	No
PLAUR	5005	-0.00427	0.150373	No
AHR	5010	-0.00441	0.150302	No
SLC7A1	5292	-0.01185	0.127644	No
FZD5	5427	-0.01518	0.117404	No
ABI1	5643	-0.02139	0.100798	No
STAB1	5805	-0.02536	0.088917	No
SGMS2	6234	-0.03676	0.055515	No
MET	6725	-0.05014	0.017752	No
SLC31A2	6733	-0.05038	0.020157	No
IFNGR2	6743	-0.05066	0.022411	No
KIF1B	6773	-0.05146	0.02305	No
DCBLD2	6786	-0.05168	0.025116	No
IFNAR1	6795	-0.05196	0.027531	No

TACR1	6934	-0.05514	0.019326	No
NMUR1	6936	-0.0553	0.022521	No
EMP3	7041	-0.05798	0.017312	No
CDKN1A	7289	-0.06459	6.07E-04	No
AXL	7425	-0.06813	-0.00658	No
SLC4A4	7451	-0.06868	-0.00459	No
P2RX4	7523	-0.07015	-0.00633	No
GNAI3	7543	-0.07065	-0.00372	No
MYC	7606	-0.07212	-0.0046	No
CYBB	7777	-0.07639	-0.01421	No
HRH1	7991	-0.08235	-0.02703	No
IL15	7993	-0.08239	-0.02223	No
PCDH7	8123	-0.08605	-0.02786	No
RIPK2	8192	-0.08773	-0.02831	No
SLC31A1	8202	-0.08803	-0.02384	No
PTGER2	8249	-0.0898	-0.02234	No
IL15RA	8270	-0.0906	-0.01863	No
BST2	8494	-0.09776	-0.03138	No
MSR1	8579	-0.10011	-0.03243	No
CSF1	8596	-0.10059	-0.0278	No
PTGER4	8655	-0.10248	-0.02654	No
OSMR	8710	-0.10427	-0.02485	No
CCL2	8870	-0.10908	-0.0316	No
GNA15	8917	-0.11066	-0.02887	No
IL1R1	8925	-0.1109	-0.02288	No
TLR3	9009	-0.11386	-0.02303	No
C3AR1	9063	-0.11551	-0.02059	No
MARCO	9186	-0.11915	-0.02367	No
CHST2	9436	-0.12786	-0.03679	No
PVR	9501	-0.13014	-0.0344	No
CD40	9710	-0.13828	-0.04349	No
ITGA5	9738	-0.13954	-0.03747	No
GPC3	9751	-0.14004	-0.03016	No
KLF6	9917	-0.14697	-0.03517	No
SERPINE1	10028	-0.15133	-0.03534	No
HAS2	10150	-0.15631	-0.03614	No
SRI	10229	-0.15974	-0.03315	No
EDN1	10297	-0.16336	-0.02904	No
SCARF1	10555	-0.17571	-0.03999	No
ATP2A2	10559	-0.1758	-0.02982	No
HBEGF	10658	-0.18115	-0.02723	No
SLC11A2	10721	-0.18467	-0.02144	No
APLNR	10823	-0.19011	-0.01857	No

CALCRL	10909	-0.1962	-0.014	No
SPHK1	11094	-0.20906	-0.01691	No
NFKB1	11234	-0.21946	-0.01546	No
LDLR	11658	-0.26305	-0.03503	No
ATP2C1	11707	-0.26932	-0.02306	No
CCRL2	11793	-0.28362	-0.01331	No
CX3CL1	12056	-0.35892	-0.01382	No
NFKBIA	12095	-0.38042	0.00557	No

OXIDATIVE PHOSPHORYLATION

PROBE	RANK IN GENE LIST	RANK METRIC SCORE	RUNNING ES	CORE ENRICHMENT
BCKDHA	510	0.206071	-0.03271	No
IDH3B	1339	0.14176	-0.09503	No
DLST	1836	0.113003	-0.13102	No
RHOT2	3006	0.062327	-0.2256	No
CPT1A	3250	0.052453	-0.24337	No
NDUFA5	3292	0.050849	-0.24436	No
ATP6V0C	3494	0.04425	-0.25902	No
UQCRFS1	3659	0.03768	-0.2709	No
MRPS12	3781	0.034167	-0.27937	No
PMPCA	3810	0.033022	-0.28012	No
MRPS30	3892	0.030418	-0.28543	No
MRPL11	3990	0.026741	-0.29225	No
PDK4	4089	0.023726	-0.29929	No
TIMM10	4097	0.023351	-0.29876	No
TCIRG1	4205	0.020563	-0.30671	No
ATP6V1G1	4256	0.018959	-0.30997	No
ETFB	4454	0.012729	-0.3258	No
ATP6V0B	4462	0.012646	-0.32578	No
TIMM50	4543	0.010234	-0.33197	No
IDH2	4638	0.007704	-0.33945	No
MTRF1	4644	0.007492	-0.3395	No
GRPEL1	4703	0.005416	-0.34409	No
GPI	4737	0.004133	-0.34664	No
ABCB7	4753	0.003614	-0.34772	No
NDUFS2	4758	0.003491	-0.34789	No
COX4I1	4823	0.001543	-0.35316	No
NDUFV1	5082	-0.0061	-0.37439	No
NDUFA6	5147	-0.00781	-0.37936	No
UQCRC1	5184	-0.00877	-0.38195	No
CASP7	5248	-0.01059	-0.3867	No

NDUFA2	5249	-0.0106	-0.38619	No
ATP6V1C1	5297	-0.0121	-0.38954	No
NQO2	5320	-0.01267	-0.39077	No
VDAC3	5336	-0.01308	-0.39139	No
NDUFS6	5528	-0.01793	-0.40647	No
MFN2	5618	-0.02048	-0.41292	No
HADHA	5730	-0.02346	-0.42106	No
NDUFC2	5759	-0.02421	-0.42224	No
NDUFS8	5771	-0.02452	-0.42199	No
SURF1	5775	-0.02464	-0.42106	No
SLC25A4	5810	-0.02544	-0.42268	No
AIFM1	6143	-0.03455	-0.44874	No
POR	6273	-0.03794	-0.45769	No
COX6B1	6278	-0.03816	-0.4562	No
COX10	6289	-0.03829	-0.4552	No
PDHA1	6360	-0.04001	-0.45913	No
UQCRQ	6513	-0.04402	-0.46971	No
UQCRC2	6666	-0.04811	-0.4801	No
UQCRB	6719	-0.04991	-0.48205	No
GLUD1	6738	-0.05057	-0.48114	No
ECHS1	6835	-0.05277	-0.48662	No
ACAA1	6885	-0.0539	-0.48814	No
RHOT1	6908	-0.05459	-0.48736	No
PDP1	6971	-0.05611	-0.48985	No
COX15	7052	-0.05821	-0.49375	No
NDUFA9	7137	-0.06061	-0.49786	No
PHYH	7251	-0.06375	-0.50424	No
HSPA9	7311	-0.06516	-0.50605	Yes
ATP6AP1	7337	-0.06588	-0.50499	Yes
NDUFV2	7356	-0.06628	-0.50332	Yes
LDHB	7428	-0.06816	-0.50599	Yes
PHB2	7437	-0.06836	-0.50339	Yes
OPA1	7506	-0.06987	-0.50572	Yes
TIMM9	7540	-0.07054	-0.50511	Yes
COX7C	7571	-0.0712	-0.50421	Yes
NDUFS4	7582	-0.07147	-0.50162	Yes
MPC1	7614	-0.07234	-0.50075	Yes
SUPV3L1	7674	-0.0738	-0.50215	Yes
ATP6V1E1	7685	-0.07417	-0.49944	Yes
OXA1L	7749	-0.07566	-0.50108	Yes
VDAC1	7754	-0.07586	-0.49779	Yes
PDHX	7778	-0.07647	-0.49605	Yes
NDUFS1	7794	-0.0769	-0.49363	Yes

CYB5R3	7798	-0.07705	-0.49019	Yes
ISCA1	7805	-0.07721	-0.487	Yes
ECI1	7823	-0.07766	-0.48471	Yes
AFG3L2	7961	-0.08149	-0.49225	Yes
IDH3G	8098	-0.08536	-0.49952	Yes
NDUFS7	8133	-0.08632	-0.49823	Yes
RETSAT	8138	-0.0864	-0.49443	Yes
ETFDH	8139	-0.08642	-0.4903	Yes
SUCLA2	8201	-0.088	-0.49118	Yes
COX6A1	8245	-0.08962	-0.49049	Yes
CS	8255	-0.09004	-0.48694	Yes
ACAA2	8263	-0.09029	-0.4832	Yes
MRPS15	8281	-0.0909	-0.48028	Yes
MRPL35	8356	-0.09332	-0.48199	Yes
FXN	8390	-0.09409	-0.48025	Yes
MDH1	8435	-0.09591	-0.47933	Yes
ECH1	8438	-0.09595	-0.47491	Yes
ATP6V0E1	8449	-0.09642	-0.47114	Yes
DECR1	8471	-0.09723	-0.46824	Yes
COX11	8488	-0.09766	-0.46491	Yes
SLC25A3	8532	-0.09872	-0.46378	Yes
NDUFB1	8629	-0.10172	-0.46693	Yes
NDUFB8	8731	-0.10497	-0.47034	Yes
VDAC2	8788	-0.10685	-0.46991	Yes
CYC1	8825	-0.1079	-0.46775	Yes
IDH1	8960	-0.11195	-0.47358	Yes
UQCR11	9044	-0.11485	-0.47502	Yes
ACADSB	9075	-0.11581	-0.47199	Yes
GPX4	9076	-0.11582	-0.46645	Yes
LRPPRC	9078	-0.11588	-0.46099	Yes
ISCU	9085	-0.11606	-0.45595	Yes
COX6C	9106	-0.11678	-0.45203	Yes
TIMM13	9174	-0.11877	-0.45195	Yes
LDHA	9177	-0.11887	-0.44643	Yes
COX7A2	9197	-0.11942	-0.44231	Yes
ACADM	9346	-0.12477	-0.4487	Yes
ATP6V1F	9375	-0.1259	-0.44501	Yes
SUCLG1	9539	-0.13158	-0.45233	Yes
DLAT	9562	-0.13257	-0.44783	Yes
COX5B	9577	-0.13308	-0.44263	Yes
NDUFB4	9601	-0.13403	-0.43815	Yes
UQCRH	9674	-0.13691	-0.43761	Yes
MDH2	9724	-0.13896	-0.43506	Yes

TIMM17A	9867	-0.14476	-0.43999	Yes
NDUFB7	9881	-0.14536	-0.43412	Yes
DLD	9891	-0.14593	-0.4279	Yes
NDUFA1	9897	-0.1461	-0.42133	Yes
SDHA	9904	-0.14642	-0.41483	Yes
IDH3A	9912	-0.1467	-0.4084	Yes
COX8A	9960	-0.14831	-0.40524	Yes
ATP6V1D	9967	-0.14861	-0.39863	Yes
OGDH	10033	-0.15161	-0.39681	Yes
NDUFB6	10057	-0.1525	-0.39144	Yes
PDHB	10095	-0.15385	-0.38717	Yes
ATP1B1	10098	-0.1539	-0.37998	Yes
MAOB	10103	-0.15421	-0.37295	Yes
COX5A	10197	-0.15862	-0.37313	Yes
NDUFC1	10221	-0.15958	-0.36742	Yes
IMMT	10248	-0.16064	-0.36191	Yes
SLC25A20	10280	-0.16246	-0.35673	Yes
ALDH6A1	10306	-0.1639	-0.35098	Yes
NDUFB2	10326	-0.16478	-0.34469	Yes
NDUFB3	10349	-0.16586	-0.3386	Yes
NDUFA7	10403	-0.16816	-0.33498	Yes
MRPS11	10417	-0.16885	-0.32799	Yes
ETFA	10501	-0.17281	-0.32666	Yes
NDUFS3	10561	-0.17596	-0.32317	Yes
SLC25A11	10588	-0.17722	-0.31687	Yes
NDUFA3	10601	-0.1782	-0.30935	Yes
ACADVL	10662	-0.18122	-0.3057	Yes
ALAS1	10663	-0.18129	-0.29703	Yes
HADHB	10692	-0.18299	-0.29062	Yes
TIMM8B	10796	-0.18799	-0.29023	Yes
SDHD	10800	-0.18824	-0.28148	Yes
BDH2	10819	-0.18978	-0.27391	Yes
CYB5A	10820	-0.1898	-0.26484	Yes
NDUFA8	10966	-0.20036	-0.26736	Yes
NDUFA4	10972	-0.20069	-0.25819	Yes
NDUFB5	11008	-0.20262	-0.25142	Yes
HSD17B10	11096	-0.2092	-0.24868	Yes
MTRR	11109	-0.21009	-0.23964	Yes
SDHC	11138	-0.21285	-0.2318	Yes
MRPL34	11236	-0.2196	-0.2294	Yes
UQCR10	11267	-0.22253	-0.22127	Yes
NDUFAB1	11347	-0.23029	-0.21685	Yes
TOMM22	11353	-0.23074	-0.20624	Yes

MRPL15	11378	-0.23229	-0.19714	Yes
ATP6V1H	11385	-0.23298	-0.1865	Yes
MRPS22	11417	-0.2352	-0.17784	Yes
POLR2F	11421	-0.23589	-0.16682	Yes
COX7B	11446	-0.23795	-0.15745	Yes
CYCS	11503	-0.24445	-0.15044	Yes
SLC25A12	11505	-0.24459	-0.13883	Yes
GOT2	11519	-0.24556	-0.12817	Yes
COX7A2L	11618	-0.25726	-0.12405	Yes
MGST3	11670	-0.2645	-0.11567	Yes
ACAT1	11676	-0.26546	-0.10339	Yes
HCCS	11684	-0.26675	-0.09123	Yes
FDX1	11690	-0.26718	-0.07887	Yes
NNT	11701	-0.26879	-0.06686	Yes
MTX2	11816	-0.28687	-0.06266	Yes
FH	11861	-0.29447	-0.05225	Yes
SDHB	11865	-0.29521	-0.03839	Yes
OAT	11907	-0.30608	-0.02718	Yes
SLC25A5	11938	-0.31175	-0.01478	Yes
COX17	12004	-0.33538	-0.00418	Yes
PRDX3	12062	-0.36146	0.008345	Yes

ADIPOGENESIS				
PROBE	RANK IN GENE LIST	RANK METRIC SCORE	RUNNING ES	CORE ENRICHMENT
ANGPTL4	11	0.442734	0.019645	No
RIOK3	66	0.322412	0.030112	No
BAZ2A	165	0.272676	0.034596	No
TOB1	313	0.2336	0.033175	No
BCKDHA	510	0.206071	0.026384	No
PPP1R15B	617	0.195642	0.026622	No
PIM3	706	0.188553	0.028034	No
PDCD4	988	0.166974	0.012331	No
TANK	1066	0.161049	0.013383	No
JAGN1	1162	0.154284	0.012619	No
UBC	1197	0.151903	0.016836	No
PHLDB1	1600	0.12563	-0.01089	No
CIDEA	1973	0.106146	-0.03701	No
PPM1B	2240	0.094044	-0.05485	No
NMT1	2241	0.09403	-0.05048	No
ABCA1	2341	0.089301	-0.0546	No
PFKFB3	2501	0.082248	-0.06405	No

G3BP2	2507	0.081926	-0.06066	No
SPARCL1	2710	0.073975	-0.07409	No
UCK1	2849	0.067731	-0.08247	No
ABCB8	3048	0.060543	-0.09618	No
NDUFA5	3292	0.050849	-0.11411	No
GADD45A	3309	0.0504	-0.1131	No
GPX3	3327	0.049877	-0.1122	No
SLC19A1	3345	0.049219	-0.11134	No
PEMT	3872	0.03095	-0.15381	No
DBT	3968	0.027696	-0.16045	No
LIFR	4162	0.021823	-0.17555	No
ACOX1	4223	0.020022	-0.17963	No
ACADS	4307	0.017029	-0.18577	No
ETFB	4454	0.012729	-0.19736	No
C3	4470	0.012314	-0.19804	No
ITSN1	4581	0.008993	-0.20681	No
APOE	4618	0.008222	-0.20943	No
PEX14	4701	0.005434	-0.21603	No
GRPEL1	4703	0.005416	-0.21586	No
APLP2	4873	-2.03E-04	-0.22996	No
LIPE	4881	-4.76E-04	-0.23052	No
ADCY6	4887	-6.17E-04	-0.23091	No
UCP2	5176	-0.00849	-0.25456	No
UQCRC1	5184	-0.00877	-0.25473	No
STOM	5231	-0.00998	-0.25811	No
ESYT1	5265	-0.01097	-0.26035	No
PTCD3	5315	-0.01261	-0.26386	No
TKT	5326	-0.01283	-0.2641	No
FZD4	5411	-0.01486	-0.27042	No
ARL4A	5513	-0.01749	-0.27804	No
ALDOA	5551	-0.01851	-0.28027	No
SCARB1	5757	-0.0242	-0.29626	No
CYP4B1	5766	-0.02442	-0.29579	No
SLC25A10	5838	-0.02628	-0.3005	No
ELOVL6	5908	-0.02827	-0.30494	No
TALDO1	6046	-0.03172	-0.31491	No
MGLL	6106	-0.03363	-0.31827	No
AIFM1	6143	-0.03455	-0.31967	No
REEP6	6228	-0.03668	-0.32498	No
POR	6273	-0.03794	-0.32689	No
ALDH2	6274	-0.03802	-0.32513	No
RREB1	6347	-0.03972	-0.32929	No
PFKL	6376	-0.04039	-0.32975	No

ENPP2	6491	-0.04351	-0.33725	No
UQCRQ	6513	-0.04402	-0.33696	No
VEGFB	6549	-0.04518	-0.33778	No
FAH	6646	-0.0477	-0.34358	No
SLC5A6	6662	-0.04797	-0.3426	No
MYLK	6713	-0.04978	-0.34446	No
ITGA7	6802	-0.05213	-0.34939	No
ECHS1	6835	-0.05277	-0.34961	No
CPT2	6910	-0.05468	-0.35325	No
AGPAT3	6960	-0.05593	-0.35474	No
SAMM50	6974	-0.05614	-0.35322	No
CD151	7152	-0.06103	-0.36516	No
ATP1B3	7230	-0.06322	-0.36865	No
PHYH	7251	-0.06375	-0.36736	No
DHRS7B	7346	-0.06604	-0.37214	No
GHITM	7373	-0.06674	-0.37121	No
ACLY	7488	-0.06961	-0.37749	No
STAT5A	7525	-0.0702	-0.37724	No
SULT1A1	7591	-0.07175	-0.37933	No
CHUK	7647	-0.07308	-0.38053	No
TST	7709	-0.0747	-0.38215	No
QDPR	7764	-0.07619	-0.38312	Yes
MCCC1	7779	-0.0765	-0.38074	Yes
DRAM2	7785	-0.07672	-0.37759	Yes
SLC25A1	7819	-0.0775	-0.37674	Yes
CHCHD10	7889	-0.07979	-0.3788	Yes
MAP4K3	7909	-0.08016	-0.37666	Yes
SORBS1	7925	-0.08052	-0.37417	Yes
REEP5	7967	-0.0817	-0.3738	Yes
DGAT1	7989	-0.08232	-0.37173	Yes
SLC1A5	8010	-0.0828	-0.36956	Yes
LPL	8035	-0.08346	-0.36768	Yes
IDH3G	8098	-0.08536	-0.36889	Yes
RETSAT	8138	-0.0864	-0.36814	Yes
UBQLN1	8239	-0.08942	-0.37233	Yes
COX6A1	8245	-0.08962	-0.36859	Yes
CS	8255	-0.09004	-0.36516	Yes
ACAA2	8263	-0.09029	-0.36155	Yes
RNF11	8338	-0.09287	-0.36341	Yes
RAB34	8437	-0.09594	-0.36714	Yes
ECH1	8438	-0.09595	-0.36268	Yes
DECR1	8471	-0.09723	-0.36083	Yes
SOD1	8574	-0.09991	-0.36471	Yes

CD36	8583	-0.10021	-0.36072	Yes
SSPN	8701	-0.10399	-0.36566	Yes
PLIN2	8702	-0.10408	-0.36083	Yes
ADIPOR2	8738	-0.10528	-0.35886	Yes
CYC1	8825	-0.1079	-0.36102	Yes
ME1	8858	-0.10879	-0.35864	Yes
DHRS7	8878	-0.10934	-0.35515	Yes
OMD	8906	-0.11032	-0.35228	Yes
IDH1	8960	-0.11195	-0.35151	Yes
CCNG2	8993	-0.11319	-0.34892	Yes
RTN3	9000	-0.11349	-0.34415	Yes
PREB	9013	-0.11395	-0.33986	Yes
YWHAG	9020	-0.11418	-0.33506	Yes
MTCH2	9036	-0.11455	-0.33099	Yes
DHCR7	9037	-0.11458	-0.32567	Yes
UQCR11	9044	-0.11485	-0.32083	Yes
ITIH5	9045	-0.11486	-0.3155	Yes
BCL2L13	9073	-0.11578	-0.31237	Yes
GPX4	9076	-0.11582	-0.30716	Yes
LEP	9164	-0.11839	-0.30893	Yes
AK2	9309	-0.12384	-0.31519	Yes
ACADM	9346	-0.12477	-0.3124	Yes
HSPB8	9428	-0.12752	-0.31324	Yes
SUCLG1	9539	-0.13158	-0.31631	Yes
DLAT	9562	-0.13257	-0.31199	Yes
PTGER3	9683	-0.13717	-0.31564	Yes
MDH2	9724	-0.13896	-0.31253	Yes
DNAJC15	9734	-0.13915	-0.30681	Yes
COQ9	9739	-0.13955	-0.30067	Yes
SNCG	9741	-0.13959	-0.29427	Yes
COL15A1	9780	-0.1415	-0.29087	Yes
GPAM	9781	-0.14152	-0.28429	Yes
RMDN3	9835	-0.14376	-0.28204	Yes
GBE1	9838	-0.14382	-0.27553	Yes
NABP1	9848	-0.14418	-0.26958	Yes
LPCAT3	9857	-0.14451	-0.26354	Yes
NDUFB7	9881	-0.14536	-0.25871	Yes
DLD	9891	-0.14593	-0.25268	Yes
IDH3A	9912	-0.1467	-0.24754	Yes
COX8A	9960	-0.14831	-0.24457	Yes
COQ3	9989	-0.14946	-0.23997	Yes
CDKN2C	10015	-0.15083	-0.23505	Yes
COL4A1	10108	-0.15451	-0.23555	Yes

PGM1	10175	-0.15761	-0.23374	Yes
CMBL	10216	-0.15945	-0.22967	Yes
IMMT	10248	-0.16064	-0.2248	Yes
SOWAHC	10330	-0.16528	-0.22389	Yes
ANGPT1	10337	-0.16542	-0.2167	Yes
SLC27A1	10339	-0.1656	-0.2091	Yes
IFNGR1	10342	-0.16569	-0.20157	Yes
PQLC3	10547	-0.17527	-0.21046	Yes
NDUFS3	10561	-0.17596	-0.20337	Yes
EPHX2	10574	-0.17646	-0.19617	Yes
NKIRAS1	10604	-0.17826	-0.19031	Yes
CMPK1	10899	-0.19555	-0.20578	Yes
HIBCH	11003	-0.20221	-0.20498	Yes
LAMA4	11048	-0.20559	-0.19911	Yes
SCP2	11101	-0.20959	-0.19371	Yes
GPHN	11117	-0.21071	-0.18518	Yes
ACADL	11132	-0.21256	-0.17647	Yes
SDHC	11138	-0.21285	-0.167	Yes
CAT	11187	-0.21618	-0.16097	Yes
UQCR10	11267	-0.22253	-0.15723	Yes
NDUFAB1	11347	-0.23029	-0.15313	Yes
MRPL15	11378	-0.23229	-0.14484	Yes
FABP4	11401	-0.23414	-0.13581	Yes
COX7B	11446	-0.23795	-0.12843	Yes
CRAT	11468	-0.24093	-0.11899	Yes
HADH	11469	-0.24138	-0.10778	Yes
ADIPOQ	11642	-0.26048	-0.11004	Yes
MGST3	11670	-0.2645	-0.10001	Yes
BCL6	11689	-0.26717	-0.0891	Yes
ARAF	11741	-0.27602	-0.08054	Yes
COQ5	11752	-0.27774	-0.06847	Yes
ELMOD3	11761	-0.27928	-0.05617	Yes
SDHB	11865	-0.29521	-0.05106	Yes
PPARG	11921	-0.30739	-0.04137	Yes
ATL2	11945	-0.31411	-0.0287	Yes
DNAJB9	11960	-0.31827	-0.01509	Yes
GPD2	11974	-0.32283	-0.00118	Yes
PRDX3	12062	-0.36146	0.008348	Yes

PEROXISOME

PROBE	RANK IN GENE LIST	RANK METRIC SCORE	RUNNING ES	CORE ENRICHMENT

HSD17B11	101	0.297262	0.023973	No
ABCB4	980	0.16753	-0.03048	No
SLC25A17	1375	0.13915	-0.04795	No
MLYCD	1651	0.122937	-0.05734	No
SLC23A2	1886	0.11036	-0.0647	No
VPS4B	2041	0.103112	-0.06624	No
ACSL5	2308	0.090852	-0.07837	No
ATXN1	2638	0.076581	-0.09727	No
PRDX5	2789	0.070637	-0.102	No
DHRS3	3176	0.055714	-0.12789	No
SOD2	3488	0.044359	-0.14881	No
RDH11	3587	0.040577	-0.1525	No
CNBP	3643	0.038375	-0.15288	No
EHHADH	4026	0.025569	-0.18172	No
ACOX1	4223	0.020022	-0.19576	No
BCL10	4294	0.017611	-0.19964	No
GSTK1	4358	0.015669	-0.20315	No
CADM1	4473	0.012234	-0.21126	No
IDH2	4638	0.007704	-0.22399	No
ABCB1	4667	0.006412	-0.22561	No
PEX11B	4680	0.006116	-0.22594	No
PEX14	4701	0.005434	-0.22701	No
SMARCC1	4779	0.002923	-0.23306	No
PEX5	5206	-0.00938	-0.2673	No
CTPS1	5651	-0.0215	-0.30171	No
MVP	5681	-0.02251	-0.30166	No
SLC25A4	5810	-0.02544	-0.30949	No
HMGCL	5866	-0.02693	-0.31111	No
SIAH1	6199	-0.0359	-0.33469	No
LONP2	6528	-0.04462	-0.35698	No
ERCC1	6562	-0.0455	-0.35476	No
CLN8	6631	-0.04729	-0.35525	No
DLG4	6655	-0.04783	-0.35195	No
ACAA1	6885	-0.0539	-0.36504	No
FIS1	6900	-0.05433	-0.36029	No
PABPC1	7179	-0.06185	-0.37657	No
STS	7270	-0.06404	-0.37706	No
NUDT19	7298	-0.06485	-0.37224	No
TSPO	7461	-0.06905	-0.37814	No
FADS1	7480	-0.06951	-0.37207	No
PEX11A	7625	-0.07246	-0.3761	No
PEX13	7627	-0.07253	-0.3683	No
HSD17B4	7681	-0.07408	-0.36462	No

PEX6	7950	-0.08128	-0.37797	No
HSD3B7	8102	-0.08552	-0.38116	No
RETSAT	8138	-0.0864	-0.37466	No
ECH1	8438	-0.09595	-0.38897	Yes
ISOC1	8469	-0.09718	-0.38089	Yes
SOD1	8574	-0.09991	-0.37863	Yes
HRAS	8673	-0.1032	-0.37551	Yes
ACSL4	8920	-0.11069	-0.38384	Yes
IDH1	8960	-0.11195	-0.37489	Yes
YWHAH	9114	-0.11707	-0.37482	Yes
ALDH9A1	9179	-0.1189	-0.36718	Yes
DHCR24	9250	-0.12144	-0.35977	Yes
TOP2A	9281	-0.12259	-0.34891	Yes
ACSL1	9394	-0.12655	-0.34442	Yes
ITGB1BP1	9667	-0.13667	-0.35207	Yes
ALDH1A1	9892	-0.146	-0.35473	Yes
CLN6	9985	-0.1493	-0.3461	Yes
ELOVL5	10099	-0.15398	-0.33871	Yes
SLC35B2	10126	-0.15532	-0.32397	Yes
IDI1	10529	-0.17442	-0.33827	Yes
EPHX2	10574	-0.17646	-0.32272	Yes
ERCC3	10640	-0.18019	-0.3085	Yes
GNPAT	10643	-0.18039	-0.28904	Yes
ABCD2	10694	-0.18305	-0.27327	Yes
ECI2	10905	-0.19581	-0.26935	Yes
SCP2	11101	-0.20959	-0.26269	Yes
SEMA3C	11123	-0.2116	-0.24142	Yes
PEX2	11158	-0.21453	-0.2209	Yes
CAT	11187	-0.21618	-0.1997	Yes
CRABP2	11230	-0.21939	-0.17932	Yes
CRAT	11468	-0.24093	-0.17273	Yes
MSH2	11633	-0.2585	-0.15818	Yes
CDK7	11648	-0.26134	-0.13092	Yes
PRDX1	11779	-0.28133	-0.11108	Yes
ABCD3	11796	-0.28401	-0.08151	Yes
IDE	11811	-0.28608	-0.05155	Yes
CTBP1	11956	-0.31685	-0.02901	Yes
ABCC5	12134	-0.42269	0.002317	Yes

Appendix D – Adipose Tissue SVC Isolation for Flow Cytometry and Flow Analysis

Note: Processing notes for human subcutaneous adipose tissue collected by aspiration

Reagents
Gibco Collagenase II, 15 mg/g tissue
HBSS+Ca/Mg
Buffer: 0.5% BSA/HBSS+Ca/Mg, 1-2 x 0.5 L ("FACS buffer")
RBC lysis buffer: 155mM NH_4Cl, 10mM $KHCO_3$, 1mM EDTA
(82.9 g Ammonium Chloride + 10.0g Potassium Bicarbonate + 0.37g EDTA, QS 1 liter with sterile water; pH will be 7.3, no need to test→ dilute to 1x with sterile water on experiment day, or keep 1X solution cold to use for a few days)
Trypan blue
Paraformaldehyde

Supplies
50 ml conical tubes
100 um cell strainers
Transfer pipettes
Small weigh boats
Forceps
Sharp scissors
Hemocytometer

RBC Lysis Recipe from O'Rourke Lab

Trial Day Prep

1. Perform all steps handling human tissue or cells in biosafety cabinet with BSL2 practice
2. Prep all reagents in sterile hood for FACS
3. First thing in AM
    a. Take 1X RBC lysis buffer to room temp
    b. Make 2X (6 mg/mL) collagenase solution in 0.5% BSA/HBSS and pre-warm at 37C
        i. 60mg/10mL for 2g sample; tweak volume from there and adjust to 6 mg/mL
        ii. Pre-warm equal volume of buffer to 37C
    c. Cool centrifuge to 4C

Notes

*Time of mincing is important, 8-10' rapid mincing for every 10g tissue is recommended, and no more than 20' total mincing time to retain viability of cells. Process in parallel if possible, with 1 person for every 10g (for large samples collected from surgery).

SVC Isolation

1. Tissue collected straight into ~10mL FACS buffer on ice (after cleaning in saline)
2. Weigh desired tissue amount (protocol tailored for 2g; 20g yields 1-20E6 cells)
    a. To weigh, waste infranatant with glass pipette and tip fat into weigh boat; if bloody sample, can rinse with PBS a few times in tube and gently rock by hand; can pick out visible clots from weigh boat
3. Mince pieces > ~3mm^3 with scissors quickly if needed (in weigh boat)
4. Divide into 50 ml conicals (2g/tube) with 10mL FACS buffer per tube
5. Add 10 ml pre-warmed 6 mg/mL collagenase solution per tube for **final concentration of 3 mg/mL**
6. Digest 30-45' on rocker at 37C, shaking by hand every 5-7' (tubes in box or tip box lids to contain leakage)
    a. Visually inspect tubes, solution should be cloudy, and if many pieces still visible digest max 10' more
7. During digest, prepare cell strainers
    a. Uncap new 50 ml conicals, one for every digest tube
    b. Pre-wet 100 um cell strainers by laying them in 50 ml conical caps, then adding and removing about 10 ml buffer
    c. Place strainers in the 50 ml conicals
8. Use transfer pipettes to collect pink aqueous layer under lipids and dispense over 100 um strainers into the conicals, then add lipid layer to avoid clogging filter (alternatively, pour)
    a. Gelatinous, fibrous aggregations are common, gently scrape the strainer surface with the transfer pipettes if needed
9. Wash buffer over strainer, bringing volume to 40 ml
10. Spin 300 x g for 7' at 4C (updated by L.G. 7-14-17 - slower and shorter spin than previous protocol yields more cells)
11. Aspirate adipocyte layer and supernatant, pouring buffer away from pellet during aspiration (use aspirator and glass pipet and can smoothly aspirate, tilting tube to parallel with ground as approaching pellet to collect all supernatant in lip at ~5mL mark)
12. Incubate in 3mL RBC lysis buffer for 6' at RT (pipet-mix).
13. If working with multiple 2g samples, transfer to new 50 ml conicals, pooling every 10 old tubes into 4 new (or 15 -> 6); working from aspirate, can pool all 2g samples together but usually only yield one 2g sample. Dilute lysis solution with buffer to 45 ml mark.
14. Spin 300 x g for 7' at 4C
15. Aspirate supernatant, pouring buffer away from pellet during aspiration (same technique); resuspend pellet in ~300-1000mL (depending on estimated cell yield) HBSS

without BSA if using a live/dead fixable stain and/or Arc reactive compensation beads because BSA interferes with the stain, measure final volume with pipette

16. Keep sample on ice in hood until use

17. Note: for rodent samples (with greater yield), there is an additional wash step through 70um filter + spin at 300G for 5 min (4C) at this stage; this reduces yield and is not usually recommended with human samples

18. Mix well and take 10 ul for counting, typical dilution is 10uL SVF prep with 20uL trypan blue (incorporate this e.g. 2-fold dilution into hemocytometer calculation). To minimize bias from chunks of cells, mix e.g. 10uL Trypan with 10uL cell solution; draw up 10uL and set aside inside wall of Trypan tube (chunks usually in first aspiration); take remaining 10uL for hemocytometer.

19. Count w/ hemocytometer, live & total in 4 quadrants (**count both round and irregularly shaped white or off-white/lighter blue cells; dead cells will appear very dark; RBC are noticeably smaller than SVC; exclude via a consistent size cut-off (by eye))**

#cells/mL = average of 4 quadrants·trypan dilution factor·hemocytometer factor 10^4

Flow staining SVCs

1. Thaw any antibodies in DMSO in advance
2. Label 5mL round-bottomed tubes for all controls and samples (unstained control, single stained controls, FMO's, full stain)
3. Keep samples on ice in hood when required
4. Divide 0.2E6 - 0.4E6 cells into control FACS tubes, divide remainder into sample FACS tubes: 0.4E6 - 6E6 cells per tube
    a. Can aliquot full stain sample and then volume up remaining sample with ice-cold PBS to dispense even amounts to control tubes (using one draw from serological)
    b. Can get away with 0.1E6 cells in unstained control
5. Volume all tubes to ~3mL; not to wash sample but to facilitate decanting after wash (this step is actually concentrating samples)
6. Spin 400 x g for 7' at 4C (with caps since human samples)
7. Decant supe by pouring 2 samples at a time: past 90 degrees, and firmly shake one time (pellet sticks well but will loose upon backwashing supernatant, so do not re-invert after decanting). Volume tubes to 200uL (shoot into each tube with P200) and resuspend pellets by flicking/roughing along flow tube rack
8. Add FC block to sample tubes (full stain and FMO's)
9. Pipet-mix in single/control stains first, then FMOs, then full stain for samples (see tables)
10. Stain 30' at 4C protected from light (wrap tube rack in foil and keep in fridge)
11. Wash: add 3 ml buffer, spin 400 x g for 7' at 4C, decant, and resuspend pellets in 500uL for Fortessa (or decant and volume to 200uL for fixing per below)
12. Fix if not sorting, by adding 100 ul 0.1% PFA to the vol after decanting, pulse vortex, and leave it in the sample until cytometer day

Flow Staining Panel

5mL tube #	Stain	Volume of Antibody
11-15	Trustain human FC block - BioLegend - cat 422301	1uL
1	Unstained	--
2	Live/Dead Fix Yellow single stain	0.8uL (0.5uL when first mixed fresh)
3	CD45-e450 single stain	1uL
4	CD64-APC single stain	1uL
5	CD11c-PE-Cy7 single stain	0.7uL
6	CD34-Percp-Cy5.5 single stain	1uL
7	CD31-APC-Cy7 single stain	1uL
8	CD29-PE single stain	1uL
9	CD3-FITC single stain	1uL
10	CD206-BV650 single stain	1uL
11	FMO**CD64-APC	Combined all but CD64-APC, volumes as above
12	FMO**CD11c-PE-Cy7	Combined all but CD11c-PE-Cy7, per above
13	FMO**CD29-PE	Combined all but CD29PE, volumes as above
14	FMO**CD206-FITC	Combined all but CD206-FITC, volumes as above
15	Full - standard	Combined all, volumes as above

** FMO = "Fluorescence Minus One," all stains are added except for the one listed

Flow Cytometry Analyzer Operation

Software Operation: LSR Fortessa

Sample Prep: Cells stained/fixed and resuspend cells in 300ul of FACS buffer, stored dark at 4C. Final volume can be adjusted before running on the cytometer:

a. If using a FACS Canto, 200ul is more appropriate.
b. I volume up to 500uL day of running on the Fortessa to give myself more wiggle room

Bring to Core: Protocol, color names for filter sets, flash drive, size M gloves, lab coat, samples (with foil cover in styrofoam box)

If First in AM:

1. Empty waste (with bleach)
2. Check that sheath fluid is full (add 1X if needed – can dilute from 10X in cabinet if needed)
3. Turn on main power (2xgreen lights – instructions on the cytometer)
4. Log on to computer (password = flowlab; software = BD FACS Diva; no password – at popup, hit Details→Use CST Settings)

BD FACS Diva Software Set-up

1. **Go to Horowitz folder → Experiment → New Experiment**
    a. Experiment templates pop up, select (General → blank experiment with sample tube, or choose an existing experiment from template)
    b. Name according to archiving system (F1JHFEB1418 for Fortessa1, PI initials, date), and change to 5 log decades
2. **Create experiment groups**
    Notes: Lindsey creates 2 groups here upon running for samples and controls. I have so far not separated tubes upon running.
    a. Select "Experiment" from tool bar → New Specimen
    b. Label tubes; F1JH021418_001, etc.
    c. Activate the Inspector window (click the green box to the left of the tube setup)
    d. Set up the parameters you will be using:
        i. Select FSC: (A(rea), H(eight), and W(idth)). FSC and SSC should be linear scale, not log scale!
        ii. Delete colors not being used in your panel
        iii. Label each color with its corresponding antigen (CD45, etc.) – use filter set list, or BD spectra viewer.

Note: could remove height information if this isn't used in analyses to reduce the number of options for axes and the size of data files.

3. **Set up a global worksheet** gating on cell populations of interest – note: plots on white space are recorded; plots on grey area are play space – see Flow Study plot setup. Create anticipated scatter gate at this time.
4. **Run unstained sample to adjust voltages** (steps below still occurring in Parameters tab in Inspector window):
    a. Set up FSC-A by count and SSC-A by count (mountain plots) in play area to look at alongside first scatter plot while adjusting FSC and SSC voltages to pull majority of cells into preemptive scatter gate (the only gate drawn in advance of running any samples; upon setting up the global workspace above)

Any time you add a tube: vortex your tube, flip the arm to the left while holding on to the existing tube (usually diH2O, but you can switch directly between samples if you don't need time to make adjustments in between), remove the existing tube, replace with your tube of interest, and slide the arm back to hold your tube of interest in place. **Note: for Fortessa, a decent bit of sample is sucked up right away, so you want to acquire/record quickly after tube is replaced provided you are *running* the sample throughout** (we are usually running sample or water, unless the instrument is in turned in to Standby if e.g. you are pausing within a particular sample; common with unstained – acquire, adjust voltages, acquire again)

    b. Add unstained sample→hit Acquire and run on LOW (at least to start, until you get a feel for how much sample/cells you have
    c. Gate off debris – on scatter plot in global worksheet (goal is to have most cells fall in the gate and exclude the small population of debris near the origin as well as some debris typically with very low FSC-A and very high SSC-A). This first adjustment may require large voltage changes! E.g. Cara typically sets voltages for adipose tissue FCS at 150 and SSC 210. Can also look at count plots to the right (play area)
    d. **Pay attention to sample yield during this time - if it is low, you can record a population of cells after gating off scatter and can create doublets gates on this population to give yourself more time to play with gates while machine is not recording (and importantly is in standby to preserve unstained sample - always want to save some for later in case you need to come back to unstained sample)** If sample yield is not limiting, keep acquiring unstained sample and go through subsequent steps:
    e. Gate off both doublet discriminators:
        i. Draw gate on FSC-A by FSC-H off of scatter gate (P1) by right clicking inside of the new graph→Go to Population→select P1; this is P2
        ii. Draw second doublet discriminator gate on SSC-A by SSC-H off of P2 and call this gate P3
        iii. Set up all subsequent graphs to be presented on P3 even before adjusting voltages or set up a live cell gate (P4) if doable (it looked tricky during our run). Could then collect 100k cells on live cell gate rather than 200k cells on singlets.
    f. Adjust voltages for individual fluorophores using this unstained sample:

i. Prepare mountain plot for first two fluorophores (fluorophore by count) and be ready to cycle through samples; can present plots as red dots on black background to help with visibility
ii. For each fluorophore, quickly adjust voltage so that the peak of the unstained population is around 10^2 and trailed off by 10^3 (prioritize the latter if).

5. **Area Scaling -** now go through all channels (FSC, SSC, all colors) and perform area scaling using each single stain control one by one. The goal here is to make sure voltage peaks are aligned for area and height for each channel. E.g. set up 2 mountain plots x count to display area (e.g. **FSC**-A on the x-axis on the one graph vertically centered above the other and **FSC**-H on the x-axis, centered below) - **These are obviously the same channel because this is what we are trying to scale** - the area for one channel with its height - will do this for all channels - steps:
    a. If the peak is right at the far right/end of the x-axis, bump down voltage (normal voltage adjustment, same as above - one adjustment per channel)
    b. If the two peaks are not centered over each other, in the laser tab (of the same window - the Parameter window - where voltage adjustments are being made), adjust the area scaling. This means adjust the number for whatever laser of interest to be lower if the area peak is to the right of the height peak (i.e. if it is higher, scale the laser lower). For the size lasers, the adjustment is in the drop down box below the table with the settings for all 4 excitation lasers where I will make the adjustments for colors. Note - I went through all single stain controls. Sometimes, I did not need to scale the excitation laser until the third fluorophore on that excitation laser
6. **Voltage Adjustments on FMOs** - two primary goals:
    a. Bring down voltage if an FMO has really high signal for the protein that is not supposed to be present (so there is actual space on the graph for the positive population to be gated);
    b. Adjust any voltages that have signal way against the axes

NOTE: DO NOT ADJUST VOLTAGES AFTER THIS STEP OR YOU WILL HAVE TO RERUN ALL SUBSEQUENT STEPS (COMPENSATION CONTROLS AND SAMPLES) WITH THESE ADJUSTED VOLTAGE SETTINGS

Make sure the sample doesn't have a plus sign next to the radio button. This will ensure that settings are kept constant for remaining samples (mostly relevant if compensating on the cytometer). For additional samples select "Next Tube".

7. **Run all samples! Unstained, single stain controls, FMOs, sample tubes. Set up the Acquisition dashboard:**

Note: a threshold rate above 12k is high! Lower the run speed if this happens. 10-12k is still high, but not concerning.

    a. Storage gate→Collect all events

b. Stopping gate→ P3: Collect 100 000 events on live cells (can set options that aren't displayed in the drop down menu by typing), medium rate
    i. Don't need as many cells in unstained control tube (10-20k should suffice) or in single stain control tubes - especially if using beads, which will be very bright (I collected 2k because had super low numbers because I didn't sufficiently vortex beads - again 10k would probably be sufficient)
    ii. Ideally want a similar number of cells in FMO as full stain tubes for ease of comparing between plots and having same amount of background/etc. 100-150k is a decent comparison to 200k. 200k would be the best if time is not an issue!
c. Events to display→5000 events

8. After data is recorded, click on the experiment in the left panel dashboard→ right click → **Export** → FCS files
    a. FCS3.1 file version, BD export/FCS → Save)
    b. Right click → close experiment
    c. Look for FCS files in the desktop FCS shortcut folder

Can also save an experiment template and open this at the start of the next data collection for the same experiment (will be found in Horowitz folder under New Experiment

If Last in PM: Follow the shutdown instructions clearly written on the cytometer (20-30 min)

LSR Fortessa Panel for Exercise Study

Protein	Excitation Laser: 488nm	
	Color	**Filter**
CD3	FITC	530/30
CD34	PerCPcy5.5	710/50
	Excitation Laser: 640nm	
	Color	**Filter**
CD64	APC	670/14
CD31	APCcy7	780/60
	Excitation Laser: 405nm	
	Color	**Filter**
L/D	L/D yellow	540/30
CD45	e450	450/50
CD16	BV	670/30
	Excitation Laser: 561nm	
	Color	**Filter**
CD29	PE	586/15
CD11c	PEcy7	780/60

In Order for Gating Strategy

Protein	**Color**	**Excitation**	**Emission**
L/D	L/D yellow	**405**	540/30
CD45	e450	**405**	450/50
CD64	APC	**640**	670/14
CD11c	PEcy7	**561**	780/60
CD34	PerCPcy5.5	**488**	710/50
CD31	APCcy7	**640**	780/60
CD29	PE	**561**	586/15
CD3	FITC	**488**	530/30
CD206	BV650	**405**	670/30

Appendix E – Adipose Tissue Cell Separation Protocol to Recover SVF and Adipocytes

Prep fresh in AM:

- Thaw Protease/Phosphatase Inhibitor Cocktails, HI-FBS (2 1mL aliquots)
- Make up 2% FBS/PBS (1mL FBS in 49mL PBS)
- Make up collagenase and warm

A. Adipose Tissue Digestion

1. Collect ~2g aspirate into cold PBS in 15mL conical tube and store on ice until processing
2. Mince large pieces (>3mm^3) with scissors
3. Incubate tissue in 2 mg/mL Collagenase Type 2 in HBSS, rocking gently @ 37°C for 30-50 min as needed (check for consistent slurry and don't over-digest)

NOTE: for Pre and Post samples, mix collagenase uniformly and distribute into 2 sample tubes - pre-warm before digestion

4. Strain digested tissue through 300 µm nylon mesh (affixed with rubber band to end of cut 10 mL syringe) in 50 mL conical tube – rinse mesh with 5 mL PBS.
5. Float adipocytes (5-10 min)
6. Carefully remove infranatant with glass pipette (try not to disturb floating adipocytes) into new 50 mL conical tube through a 70 µm cell strainer and rinse with FBS/PBS → **SVF isolation**; remaining adipocytes → **MA isolation**; in parallel.

B. Mature Adipocyte Isolation

1. Wash adipocytes by **gently** adding ~2 ml FBS/PBS Bx with a transfer pipette and **gently** mixing.
2. Transfer adipocytes and Bx to a 3ml Falcon tube
3. Float adipocytes and then carefully remove infranatant with a glass pipette and discard.
4. Repeat washing step twice, for a total of 3 washes.
5. Storage:

- 200uL MA in 1mL RNA-stat 60 - incubate @ RT for 10 minute, vortexing occasionally. Store @ -80°C.
- If more MA available: 200uL MA in 250uL fat cake lysis buffer (*add PICs*); or if more remaining, lyse 250-350uL in 500uL buffer; vortex well and store @ -80°C.

C. SVF Isolation

1. Move SVF mixture (after filtering through 70 μm cell strainer) into a clean 15 mL tube
2. Centrifuge @ 500xg, RT, for 7 minutes. Remove any remaining adipocytes or free lipid along with supernatant
3. Add 2 mL RBC lysis Bx, mix by pipetting, and incubate 5 min @ RT. Deactivate RBC lysis Bx with FBS/PBS.
4. Centrifuge @ 500xg, RT, for 7 minutes. Remove supernatant.
5. Resuspend pellet in FBS/PBS and move to polystyrene tube. Centrifuge @ 500xg, RT, for 7 minutes. Remove supernatant. (first wash)
6. Wash pellet two more times in in FBS/PBS (three washes total)
    a. Resuspend pellet in 1mL and take 10uL after second wash to plate in 10mL growth media in round dish if plating; volume up to 2mL and complete third wash
7. Resuspend pellet in 100uL FBS/PBS and label CD14+
8. Pipet-mix 10uL of Human CD14+ Selection Cocktail into SVF and incubate for 15 min on bench (cap on)
9. Pipet-mix 5uL CD14+ Magnetic Nanopartcles (mix well before use!) and incubate for 10 min on bench (cap on)
10. Volume sample to 3 mL and incubate in EasySep magnet for 5 min on bench (cap off)
11. In one movement, pick up magnet with tube and pour contents into a 5 mL tube labeled CD14+
    a. Add this tube to the magnet and incubate again for 5 min on bench (cap off); for second collection of CD14+ cells that may have been lost in first pour
    b. Volume first CD14+ selected tube back to 3mL
12. In one movement, pick up magnet with tube and pour contents into a 5 mL tube labeled CD14-; this is the final CD14– fraction
    a. Combine two CD14+ tubes into one
    b. There should now be one each of a CD14– and CD14+ tube
13. Pipet-mix both samples and centrifuge @ 500xg, RT, for 7 minutes.
14. Remove supernatant, resuspend pellets in 1mL RNA-Stat60 and transfer to 1.5mL eppendorf tubes. Vortex. Let tubes sit on bench for 5-10 min vortexing occasionally. Store at -80C.

Appendix F – RNA Isolation for qPCR

RNA Isolation from Whole Adipose Tissue

Note: this is the non-column isolation procedure used for Study 3. Modifications for RNA sequencing are shown in Appendix B.

1. Clean all supplies, gloves, and bench top with RNAse-away (repeat as needed throughout procedure→essential for RNA purity and yield)
2. Cool centrifuge and tissue lyser units to 4C
3. Chip 40-60mg adipose tissue using clean scalpel in mortar with liquid nitrogen (blood contamination becomes a problem with larger pieces)
4. Store samples in eppendorf tubes on dry ice until immediately before lysing in Cartee lab tissue lyser
5. Prep 2mL heavy-duty round-bottom eppendorf tubes with 2 steel ball bearings (RNAse-cleaned) and 1mL RNA-Stat 60 on RNAse-cleaned ice bucket
6. Add samples to RNA-Stat 60 quickly and lyse 60 seconds (max speed) on Cartee lab tissue lyser→check for homogenous slurry→repeat for 30-60 seconds as needed until sample is homogenous
7. Spin samples at 12 000G, 10 min, 4C to separate fat to top
8. Carefully waste top fat layer if too thick to access infranatant without contamination
9. Transfer infranatant (avoiding pelleted waste) into new 1.5mL eppendorf, entering through middle of sample to avoid lipid contamination
10. Add 200uL chloroform per 1mL RNA-Stat (starting volume), invert to mix, incubate 5min at room temp, spin at 12 000G, 15 min, 4C→this yields RNA fraction in clear top layer; be careful not to disturb
11. Carefully move upper phase only into new 1.5mL eppendorf tube (leave bottom ~1/3 of this layer to avoid protein and DNA contamination)
12. Add 0.5mL 2-propanol (GC grade), invert to mix, incubate 10min at room temp (or 20min to overnight at -20C; however, longer incubation may trade-off yield)
13. Pellet by centrifugation at 12 000G, 20 min, 4C
14. Pour off supernatant (invert tube and shake firmly one time – pellet sticks well) and wash pellet with 1mL 75% ethanol (mixed with RNAse-free H2O); vortex pellet each time to clean, and spin at 7500G, 5 min, 4C – 3 total washes
15. Pour off supernatant and remove residual with P200; let pellet dry (in chemical fume hood for air circulation) 10-15 min (careful not to over-dry)
16. Resuspend pellet in 25uL RNAse-free H2O, mixing vigorously
17. Spec concentration with nanodrop immediately before RT

RNA Isolation from Mature Adipocytes

Notes: samples collected directly into RNA-Stat 60. Procedure is identical except mechanical homogenization not required and lipid layer may be thicker; careful to avoid contamination of sample (step 8 above is particularly important)

RNA Isolation from SVF

Notes: samples collected directly into RNA-State 60. Procedure is identical except mechanical homogenization is not required and centrifugation to remove lipid layer is not required.

Appendix G – Protein Isolation and Western Blotting

SML Adipose Tissue Homogenization Protocol:

1. Cool tissue lyser blocks in freezer
2. Prep 2.0mL round-bottom Eppendorf tubes with steel ball bearing and 1.0mL ice-cold lysis buffer
3. Add 125-150mg adipose tissue to each tube (keep on ice)
4. Place samples in tissue lyser blocks (cold) and run at max for ~30sec to homogenize (confirm slurry)
5. Solubilize samples by placing in rotary wheel at 4˚C for 1 hour at 50rpm
6. Centrifuge samples for 15 min at 15 000G, 4˚C
7. Transfer supernatant to new tubes
8. Repeat steps 6 & 7 as necessary until all excess fat & debris clear (may take 4-5 spins)
9. Freeze lysates in -80˚C until BCA analysis

SML Tissue Lysis Buffer for Adipose Tissue:
****NOTE:** *This can be stored as "stock" buffer. Only add protease and phosphatase inhibitors to amount needed for samples when ready to use. DO NOT add inhibitors to entire stock of buffer***.****

50mM Tris-HCl pH=7.4
1mM EDTA
0.5% SDS
0.01% Triton X-100

Directions to make stock:
1. Add Tris base to water
2. pH to 7.4
3. add appropriate amount of EDTA, SDS, and Triton (depends on final volume)

Example for 100ml of stock buffer:
1. Add 0.605g Tris base to 70ml H_2O
2. pH to 7.4
3. Add 0.0292g EDTA
4. Add 0.5g SDS
5. Add 100ul Triton X-100

When ready to use buffer, aliquot the volume you need and add 1%volume/volume inhibitor cocktails

SML Western Protocol

Gel Preparation:

1. Clean glass plates with 70% ETOH, rinse with H_2O and dry
2. Place glass plates together (with spacers forming gap between plates) and slip into green clamp (large plate behind small plate).
3. Place grey rubber strip on base of gel casting stand and put green clamp-glass plate combo on top of the grey strip. Secure into place with the spring loaded lever on top of the casting stand
4. Press down firmly on both glass plates and lock plates into place using the levers on the green clamp assembly.
5. Place comb between glass plates. Mark 1 cm below where teeth are on outside of glass plate. Remove comb.
6. Make separating gel in a 50 ml beaker.

Reagent	7.5% gel	10% gel	15% gel
30% Acrylamide/ 0.8% Bis	5 ml	7 ml	10 ml
4X Separating buffer	5 ml	5 ml	5 ml
dH_2O	10 ml	8 ml	5 ml
10% APS	100 µl	100 µl	100 µl
Temed	20 µl	20 µl	20 µl

Percent Acrylamide	Separating resolution
15%	15-45kd
10%	18-75kd
7.5%	30-120kd

Add 10% APS and Temed last and in a relatively rapid sequence. The solution will begin to gel after these agents are added

7. Working quickly, pipette the gel solution between the plates using the automated pipette-man. Fill to the mark you made on the outside of the glass (1 cm below the comb)
8. Add 500 ul of dH2O to help form smooth top surface of gel. Let sit for 30-45 minutes.
9. When gel is polymerized, invert apparatus to empty H2O. Blot with filter paper to remove any excess water between the plates. Be careful not to "rough up" the gel.
10. Make stacking gel:

Reagent	Volume
30% Acrylamide/ 0.8% Bis	1.6 ml
Stacking Buffer	3 ml
dH_2O	7.2 ml
10% APS	60 µl
Temed	12 µl

Add 10% APS and Temed last and in a relatively rapid sequence. The solution will begin to gel after these agents are added

12. Working quickly, pipette the gel solution between the plates using the automated pipette-man, fill close to the top.
13. Insert comb between plates. Wipe-up over-flow. Let sit for 30-45 minutes.

Running Gel:

1. Once gel is polymerized, remove the gel and glass plates from casting stand and unlock the green clamps
2. Insert the plates and gel into inner core of "running rig" and lock into place.
3. Make ~800ml of 1X running buffer
4. Fill inner core with running buffer. Fill outer chamber with running buffer until glass plates are nearly submerged.
5. CAREFULLY remove comb from the gel
6. Blow out wells to eliminate air bubbles.
7. Load samples per antibody protocol
8. Place lid on running rig and set power-pac to 200 volts for ~45 min for cells; 100 volts for ~2 hours for adipose tissue.
9. When loading dye front gets the bottom of the plate, turn off power.

Setting up Transfer sandwich:

A. Before gel is done running, get 3 Pyrex dishes and fill with cold transfer buffer.
B. Put 2 filter papers and 2 fiber pads per gel in one dish. Ensure that they are soaking in the buffer
C. Cut membrane to proper size and place it in another Pyrex dish to soak in transfer buffer (5-10 min)
D. After gel is complete, remove glass plates and gel from rig. Carefully separate glass plates and cut off stacking gel with green tool or razor.
E. Put glass plate/gel into transfer buffer and carefully nudge gel off plate with spatula.
F. Soak gel in transfer buffer for 5-10 minutes.
G. Open transfer sandwich assembly and place things on it in the following order in this order:
- fiber pad
- filter paper
- gel
- nitrocellulose membrane
- filter paper
- fiber pad.

Make sure to roll out bubbles after each item (use test tube to help roll out bubbles).
H. Close the transfer assembly sandwich and slide into transfer chamber (Black to back).
I. Put in frozen block.
J. Fill chamber half-way with transfer buffer. Fill middle chamber all the way. (Get bubbles out of chamber by tilting)
K. Transfer at 100V for 1 hour for cells; .

Washes and Detection:

1. Take apart membrane assembly. Put membrane in clean container.
2. Rinse membrane with dH2O.
3. To assess quality of gel, pour small amount of ponceau S stain on gel (Ponceau S can be reused, so pour it back into storage vial/tube). After examining general gel quality, rinse with dH2O to remove excess Ponceau S and Rinse with TBS-T. Perform Memcode total protein stain at this stage if required.
4. Block with 50 ml for 1 hr on rocker (gentle swirl). (Blocking solution: 50 ml TBS-T + 5g dry milk or BSA)
5. Add primary antibody and incubate overnight at 4C on rocker. (POUR ANTIBODY BACK!)
6. Wash in TBS-T (1 x 15 min and 2 x 5 min) on rocker
7. Add secondary antibody and incubate for 1 hour on rocker. (1:3000 in TBS-T)
8. Wash in TBS-T (1x 15 min and 2 x 5 min) on rocker.
9. For ECL detection… Aliquot 3 mls of Reagent A and then 3 mls of Reagent B into tube. Invert to mix and pipette onto blot (ensure entire blot is covered. Incubate for 5 minutes.
10. Lift membrane up to pour off the ECL solution and remove excess ECL with Kim wipe.
11. Cover membrane with saran wrap.
12. Image on Bio-Rad imager.

Buffer Recipes:

<u>Separating Gel Bx (for 150 mL):</u>
1.5M Tris base (27.23 g)
pH to 8.8 with 6N HCl
store at 4C

<u>Stacking Gel Bx (for 100 mL):</u>
0.5M Tris base 6 g)
pH to 6.8 with 6N HCl
store at 4C

<u>10X Running Bx (for 1L)</u>
0.25M Tris base (30.3 g)
1.92M glycine (144 g)
1% SDS (10g)

<u>10X Transfer Bx (for 1L)</u>
0.25M Tris base (30.3 g)
1.92M glycine (144 g)

To make 2L of 1X Transfer Bx:
400 mL methanol
200 mL 10X Transfer Bx
1400 mL dH_2O

10X TBS (for 1L)
200mM Tris base (24 g)
1.5 M NaCl (88 g)

Dissolve in 900 mL dH_2O
pH to 7.6 with 12N HCl
Add dH_2O to final volume of 1 L

TBST (for 1 L)
100 mL 10X TBS
900 mL dH_2O
1 mL Tween 20